

1958

# A study of thermodynamic properties of electrolytic solutions of rare earths

David Judson Heiser  
*Iowa State College*

Follow this and additional works at: <https://lib.dr.iastate.edu/rtd>

 Part of the [Physical Chemistry Commons](#)

## Recommended Citation

Heiser, David Judson, "A study of thermodynamic properties of electrolytic solutions of rare earths " (1958). *Retrospective Theses and Dissertations*. 2251.  
<https://lib.dr.iastate.edu/rtd/2251>

This Dissertation is brought to you for free and open access by the Iowa State University Capstones, Theses and Dissertations at Iowa State University Digital Repository. It has been accepted for inclusion in Retrospective Theses and Dissertations by an authorized administrator of Iowa State University Digital Repository. For more information, please contact [digirep@iastate.edu](mailto:digirep@iastate.edu).

A STUDY OF THERMODYNAMIC PROPERTIES OF  
ELECTROLYTIC SOLUTIONS OF RARE EARTHS

by

David Judson Heiser

A Dissertation Submitted to the  
Graduate Faculty in Partial Fulfillment of  
The Requirements for the Degree of  
DOCTOR OF PHILOSOPHY

Major Subject: Physical Chemistry

Approved:

Signature was redacted for privacy.

In Charge of Major Work

Signature was redacted for privacy.

Head of Major Department

Signature was redacted for privacy.

Dean of Graduate College

Iowa State College

1958

## TABLE OF CONTENTS

	Page
I. INTRODUCTION . . . . .	1
II. GENERAL THEORY . . . . .	9
A. The Dissociation of Electrolytes . . . . .	10
B. Thermodynamics and the Concepts of Ideal and Non-ideal Solutions . . . . .	11
C. Inter-ionic Attraction Theory for Electrolytic Solutions . . . . .	14
III. ELECTROLYTIC CONDUCTANCE . . . . .	22
A. Theory . . . . .	23
1. The Force-Transfer Effect . . . . .	23
2. The Electrophoretic Effect . . . . .	26
3. Graphical Evaluation of the Electro- phoretic Term, Developed by J. L. Dye . . . . .	29
B. Historical Review of Experimental Techniques . . . . .	31
1. The Alternating Current Source . . . . .	31
2. The Conductivity Bridge . . . . .	33
3. The Amplifier . . . . .	35
4. The Detector . . . . .	35
5. Conductance Cells. Capacity Effects and Polarization . . . . .	36
6. The Constant Temperature Bath . . . . .	45
C. Preparation of Solutions . . . . .	45
D. Experimental Investigation . . . . .	50
1. Apparatus and Procedure . . . . .	50
2. Calculations and Results . . . . .	54
IV. TRANSFERENCE NUMBERS . . . . .	66
A. Theory . . . . .	68
1. The Onsager Theory Applied to Transference Numbers . . . . .	68
2. Theory of the Moving Boundary Method . . . . .	71
B. Historical Review of the Moving Boundary Method . . . . .	76
C. Experimental Investigation . . . . .	86
1. Apparatus and Procedure . . . . .	86
2. Calculations and Results . . . . .	94

## TABLE OF CONTENTS (Continued)

	Page
V. ACTIVITY COEFFICIENTS . . . . .	102
A. Theory of the Isopiestic Comparisons Method . . . . .	108
B. Historical Review of the Isopiestic Method . . . . .	112
C. Experimental Investigation . . . . .	117
1. Apparatus and Procedure . . . . .	117
2. Selection of Standard Data for Potassium Chloride . . . . .	125
3. Redetermination of Activity Coefficients for Lanthanum Chloride . . . . .	127
4. Calculations and Results for the Rare- earth Nitrates . . . . .	137
VI. GENERAL DISCUSSION AND CONCLUSIONS . . . . .	156
VII. BIBLIOGRAPHY . . . . .	170

## I. INTRODUCTION

To the electrolytic solutions domain of physical chemistry is relegated the study of the various equilibrium and non-equilibrium processes which can be made to occur in systems where ions are formed by the dissolution of electrolytes in a solvent. Such a study involves, after a qualitative description of observed phenomena, the evaluation, interpretation, and theoretical derivation of numerical quantities such as: the free energy of the solute in terms of its concentration and activity coefficient, enthalpies of solution and dilution, viscosities and diffusion constants, electrical conductances, ionic transference numbers, and partial molal quantities, each of which quantitatively describes the behavior of solutions under specified circumstances. As is usual with the scientific method, ideas for formal theoretical treatments for properties of electrolytic solutions grow out of empirical relationships observed from the experimental data. After the theories are formulated, experimental evidence is again needed to refute or substantiate their validity.

The practical objective of a theory about any chosen property of a solution is to express the required quantity as a function of the variables of the system, ideally in a closed equation if this is possible. Modern electrolytic solution theories have succeeded, to a limited extent, in formulating equations for the descriptive quantity, such as the activity coefficient, in terms of the concentration, temperature, dielectric properties of the solvent, valence type of the solute, and fundamental physical constants. Essentially for one solute in a given solvent at a specified temperature, they are concentration laws. At present the theories allow

adequate calculation of some properties for very dilute solutions. Outside the very dilute range, they do not predict the experimental data. Therefore, current work in the field is directed toward modifying the theory to account for these deviations.

Since many different properties may be observed in one and the same solution, depending on the circumstances of investigation, it is a welcome thought that these many properties should be able to be theoretically derived from the same basic model. At least this would save working out a separate theory for each property. The development of this basic model idea has been crystallized in the now classical inter-ionic attraction, ionic atmosphere theory of Debye and Hückel for very dilute solutions (1). Using Debye and Hückel's work as a basis, Onsager (2) developed the electrophoretic and time-of-relaxation effects in the calculation of the electrical conductance. Bjerrum's (3) "ion-pair" theory modifies the Debye-Hückel treatment to bring into account cases where ions may be close enough together on a statistical time average to be considered associated, and the mathematics is altered accordingly. Whereas the Debye-Hückel theory considers general interactions only between charged particles, Guggenheim (4) also brings specific ion-ion interactions to bear on the problem. In addition extensions to the mathematics of the original treatments have been proposed and worked out (5, 6, 7, 8). Theories purporting to calculate the extent of hydration of an ion have been proposed (9), and the results used to modify the basic Debye-Hückel formula for the activity coefficient.

Uni-univalent electrolytes in dilute solutions are most easily described by the Debye-Hückel and Onsager theories. Other valence types deviate more from the theories, and start to deviate at lower concentrations.

In addition it is found that the various properties start to deviate from the limiting laws of the theories at differing concentrations for the same electrolyte. Indeed a parallel study of several properties should give some insight into the validity of the various assumptions of the theories at various concentrations.

Of all the properties, application of the inter-ionic attraction theory to activity coefficients is most successful because of the existence of an adjustable parameter (the distance of closest approach) in the theoretical equation. With suitable values of the parameter excellent fits to the experimental data may be made up to 0.1 Normal concentration, although the assumptions of the theory do not necessarily hold this far. This is the case for solutions of such tri-univalent electrolytes as the rare-earth halides. In the case of the partial molal volumes and partial molal enthalpies, the theoretical equations require knowledge of the pressure and temperature dependence of the adjustable parameter. These cannot be known because of the parameter's complex character. Consequently one is restricted to the use of a limiting law, not depending on any adjustable parameter, and having only a very small range of agreement with experiment compared with that for activity coefficients. The extended Onsager theory for conductances has terms in the final equation which are very difficult to evaluate for concentrations beyond the very dilute range. The simpler linear limiting law coincides with the experimental conductance curve only below 0.001 Normal. Extrapolation to zero concentration of the available data for transference numbers does not have the theoretical limiting slope, but this discrepancy is probably due to the lack of data in the very dilute region where the theory might be applicable.

Since the equations of the Debye-Hückel and Onsager theories are highly sensitive to the valencies of the ions, studies of polyvalent electrolytes should indicate directions of improvement in the theories. But because polyvalent ions generally undergo hydrolysis and undesirable complexing reactions, solutions of the pure simple ions are difficult to prepare. A moderate amount of work has been done on electrolytes with divalent ions. But for trivalent salts, because of their complex chemistry, comparatively little data has appeared in the literature with the exception of the rare-earth salts. Typical examples of work with polyvalent ions in solution are conductance studies of aluminum and gallium halides in non-aqueous solvents (10, 11, 12) and conductance and e.m.f. studies of ferric chloride in HCl and non-aqueous solvents (13, 14). In aqueous solutions, conductances have been measured for potassium ferricyanide (15) and for potassium ferrocyanide (16). Transference numbers by the moving boundary method have been measured for potassium ferricyanide and hexaminecobalt-III chloride (17). Activity coefficients have been derived from vapor pressure measurements on solutions of aluminum nitrate (18), and the isopiestic comparisons method has been applied with success to determine the activity coefficients of aqueous potassium ferricyanide and thorium nitrate (19). Most recently the activity coefficients of gallium perchlorate have been determined by isopiestic comparisons (20).

For reasons to be discussed below, by far the bulk of the work with trivalent salts has employed ions of the rare-earth elements. Conductance measurements have been made on aqueous and mixed solvent solutions of lanthanum ferricyanide (21, 22), and on aqueous lanthanum sulfate, nitrate, and chloride (23, 24). Isopiestic comparisons have yielded activity



coefficient data for many rare-earth halides (25, 26, 27, 28). Electrical conductances, transference numbers, activity coefficients, heats of solution and dilution, and partial molal volumes of rare-earth halides, perchlorates, and nitrates have been determined by F. H. Spedding and his group here at Iowa State College.

Of all trivalent electrolytes, natural choices for electrolytic solution studies are the rare-earth ions. Relative to other salts of Groups III and IV and transition-group elements, the rare-earths show only a slight tendency to hydrolyze by reason of their relatively greater basicity, and they have a smaller complexing tendency.

In the theoretical section it will be shown that the properties of a solution depend on the radius of the solute ion (in terms of the distance-of-closest-approach parameter). In the rare-earth series one element differs from another only in the number of electrons in the inner  $4f$  shell, and in an increasing nuclear charge with increasing atomic number. From one rare-earth to the next, the increasing nuclear charge produces a greater force field on the  $5s$  and  $5p$  electrons which predominantly determine the ionic size. The increasing force field through the series pulls these electrons closer to the nucleus and shrinks the radius of the atom, one from another. This is the "Lanthanide Contraction." Thus, although the hydrated rare-earth ions in aqueous solution all have very similar chemical properties, there is a gradual change in atomic radius which accompanies the increase in atomic number through the series. Accordingly, the rare-earth salts form a particularly ideal group for studying the variation of physical chemical properties as a function of the radius of the ion (or ionic unit, which may be hydrated).

Heretofore individual pure rare-earth salts were comparatively unavailable for extended research because only tedious fractional crystallization procedures were available to produce them. Currently, however, the ion-exchange techniques developed at Iowa State College have made kilogram quantities of spectrographically pure rare-earth oxides available for research. With certain precautions, solutions of the rare-earth salts are easy to prepare from these pure oxides, and the solutions may be analyzed accurately by well established gravimetric procedures.

As soon as some of the lighter rare-earths began accumulating from the ion-exchange columns, an extensive program was begun at Iowa State College to investigate a variety of electrolytic solution properties with the advantages offered by using the rare-earth salts. The broad purpose of such a program is this: As various theories and empirical equations have developed, it is usually found that the experimental data can be represented by smooth curves which can be fitted by equations with but one or two adjustable parameters. If one has complete freedom to adjust these parameters, even in the theoretical equations, at least partial fits to the experimental curve can most generally be obtained. With the exception of the uni-univalent electrolytes, no extensive data exist in the literature where the adjustable parameters can be cross-checked for various cations, various anions, and for the various properties of the same solution. Unless the values used for the parameters can be made consistent for all combinations of cations, anions, and properties, one can glamorize the equations with empirical factors and delude oneself with fancy, but meaningless, curve fitting. Therefore complete sets of data are needed, which can be cross-checked in many ways. For this reason the program was undertaken.

P. E. Porter and J. M. Wright started the experimental investigations on rare-earths with some of the chlorides in solution. They measured the conductances, transference numbers, and activity coefficients by means of emf's of concentration cells with transference for the chlorides of lanthanum, cerium, praseodymium, neodymium, samarium, europium, and ytterbium (29, 30, 31). The same three properties were measured by I. S. Yaffe (32) for the bromides of lanthanum, praseodymium, neodymium, gadolinium, and erbium; and by J. L. Dye (33) for the chlorides of dysprosium, holmium, erbium, thulium, and ytterbium. S. Jaffe determined the solubilities, conductances, and densities for solutions of the sulfates of nine of the rare-earths plus yttrium (34), and determined the conductances and transference numbers for the perchlorates of eight of the rare-earths and the nitrates of lanthanum, neodymium, and gadolinium (35). As part of this program, the partial molal volumes were obtained from density measurements by the magnetic float method for the chlorides and nitrates of lanthanum, neodymium, erbium, and ytterbium by B. O. Ayers (36), and the partial molal compressibilities for the same salts were derived from ultrasonic wave velocity measurements by G. Atkinson (37).

In the area of calorimetry, C. F. Miller measured the heats of solution of cerium and neodymium metals in hydrochloric acid, and the heats of solution in water of both anhydrous and hydrated crystals of  $\text{CeCl}_3$  and  $\text{NdCl}_3$  (38, 39). From the experimental work, heat capacities and other thermochemical quantities were calculated. This work was continued by J. P. Flynn (40, 41) who measured the heats of solution in HCl of the metals and chlorides of lanthanum, praseodymium, gadolinium, erbium, and yttrium, and the heats of solution in water of anhydrous and hydrated

chlorides of these same rare-earths plus samarium and ytterbium. Heats of dilution have been measured for solutions of  $\text{NdCl}_3$  and  $\text{ErCl}_3$  by A. W. Naumann (42) and for solutions of the chlorides and nitrates of lanthanum and ytterbium by R. E. Eberts (43).

J. L. Dye (8), in addition to his experimental work listed above, succeeded in developing an extension to the application of the Onsager theory of conductances for calculating theoretical conductance and transference number values which are in much better agreement with the experimental results than was possible previously.

Enough variations have been found in the above-mentioned work to point out that the phenomena are complex, and that it is dangerous to draw conclusions from insufficient data. In particular, studies of the nitrates in solution are very incomplete, so that further work on this series of salts would be very worth while.

This thesis, then, represents a continuation of the comprehensive investigation of rare-earth electrolytic solutions at Iowa State College. Herein will be reported the conductances, transference numbers, and activity coefficients of the nitrates of samarium, holmium, erbium, and ytterbium, with the object of extending the knowledge of the electrochemical properties of polyvalent electrolytes in solution. The properties mentioned were chosen because there are well established limiting laws for them whose extension into the range of higher concentrations would be highly desirable.

## II. GENERAL THEORY

The first successful theoretical treatment of electrolytes in solution which provided easily applicable equations for the equilibrium properties was presented in 1923 by Debye and Hückel (1). The basic assumption for their work had been previously proposed by Bjerrum in 1909 (44). He suggested then that the typical strong electrolytes are completely dissociated in dilute aqueous solutions and that the deviations of such solutions from ideality are due to the electrostatic field of force of the ionic charges. He also pointed out that the magnitude of these deviations is determined primarily by the concentrations and charges of the various ions, and only to a less extent by their individual specific properties.

Since the Debye-Hückel theory validly predicts at least the limiting behavior of very dilute solutions, much subsequent effort has been directed toward extending the theory to apply to less dilute solutions by taking into account effects which were neglected by Debye and Hückel. Consequently, in order to assure a firm theoretical foundation for these later endeavors, their original presentation has been extensively analysed from the viewpoint of statistical mechanics, and many features of the original treatment have been corrected and modified. Some of those responsible for the critical examination of the Debye-Hückel theory, and discussing the statistical basis for it, are Kramers (46), Fowler (47), Fowler and Guggenheim (48), Onsager (49), Kirkwood (50), and Halpern (51). The purpose of this section is to present a brief and qualitative discussion of modern electrolytic

solution theory.

### A. The Dissociation of Electrolytes

Electrolytes are substances which, when dissolved in water (or other polar solvent), form electrically charged ions. These exhibit themselves by the comparatively high electrolytic conductivity, and increased magnitude of the changes in colligative properties, which electrolytic solutions possess relative to solutions of molecular solutes. Some of these compounds may only partially dissociate into ions when dissolved, and are termed "weak electrolytes." They may be roughly identified as those which conform to the Arrhenius law, which equates the degree of dissociation of a weak electrolyte in a solution to the ratio of the equivalent conductance of the solution to that at infinite dilution. "Strong electrolytes" dissociate more or less completely in solution.

While frequently the solid salts, having a crystalline lattice composed of units of M and of A, vaporize to form molecules MA, they will dissolve in water to form the ions  $M^+$  and  $A^-$ . It may therefore be concluded that the solvent itself must be responsible for the separation of the charged particles. This is accomplished by two means. The first is the apparent behavior of the solvent as if it were a continuous medium of dielectric constant D. In any medium, energy is required to separate the ionic units from their close proximity in the crystal lattice to their extension in the solution. Any effect which minimizes this energy requirement will assist in the formation of ions. For water having a large dielectric constant, the Coulomb force between the ions,  $F = e_M e_A / D r^2$ , is lower than would be

the case in vacuo or in gases. Thus formation of ions is favored in water (or other media of high dielectric constant) over media in which the energy of separation would be greater. The second effect is that of hydration. Since the hydration of an ion is associated with a decrease in energy, there is immediately available an energy source for the dissociation of the ions from their lattice.

### B. Thermodynamics and the Concepts of Ideal and Non-ideal Solutions

To characterize a completely homogeneous part of some physical material, called a phase, one must specify the composition in terms of the number of moles  $N$  of various types of molecules that it contains, the values of the geometrical parameters such as the volume  $V$ , and one other degree of freedom, such as the entropy  $S$ . Then for any variation in the state or nature of the phase, the variation in the total internal energy  $E$ , of the phase is

$$dE = \frac{\partial E}{\partial S} dS + \frac{\partial E}{\partial V} dV + \sum_i \frac{\partial E}{\partial N_i} dN_i$$

Through the application of the First and Second Laws of Thermodynamics, the variation in the internal energy becomes

$$dE = TdS - PdV + \sum_i \mu_i dN_i$$

where  $\mu_i = \left(\frac{\partial E}{\partial N_i}\right)_{V,S}$  is the partial chemical potential of the component "i" in the phase.

The Gibbs free energy is defined as

$$F = E - TS + PV.$$

Its variation is

$$dF = -SdT + VdP + \sum_i \mu_i dN_i ,$$

in which  $\mu_i = \left(\frac{\partial F}{\partial N}\right)_{P,T}$  .

Since the Gibbs free energy is that thermodynamic potential which defines the condition for stable equilibrium in a reversible process at constant temperature and pressure,

$(\Delta F)_{P,T} = 0$  (for zero work other than mechanical work of expansion), and indicates which direction chemical reactions will spontaneously take,

$(\Delta F)_{P,T} < 0$  (for zero work other than mechanical work), the calculation of this function is of primary importance in physical science. For this reason the determination of  $F$ , or of the partial chemical potential of an ionic species in solution, is one of the objects of any electrolytic solution theory.

The partial chemical potential of any component "i" may be defined for an Ideal Solution as

$$\mu_i = \mu_i^{\circ} + RT \ln(x_i)$$

in which  $x_i$  is the mole-fraction of "i", and  $\mu_i^{\circ}$  is a constant. The concept of a solution which obeys the above equation is a hypothetical one, or at best only a limiting case for the nearly unit mole-fraction range of volatile component "i" in an actual solution.

Actual solutions are assemblies of molecules and ions between which there are interactions which disturb the internal rotational and vibrational modes of motion of each particle. As a consequence, each particle



cannot act as an independent unit, as is implicitly assumed for ideal solutions. Since the effects of these interactions are concentration dependent, real solutions cannot conform to the defining equation above for ideal solutions, and hence are classed as Non-ideal solutions. For an actual solution, the deviation from ideality may be indicated by the magnitude of a factor multiplied on the term variable in the concentration. Thus the partial chemical potential of the solvent in a real solution may be written

$$\mu_{\text{H}_2\text{O}} = \mu_{\text{H}_2\text{O}}^{\circ} + g RT \ln(x_{\text{H}_2\text{O}}),$$

in which  $g$  is termed the rational osmotic coefficient, and has the property

$$g \longrightarrow 1 \quad \text{as} \quad x_{\text{H}_2\text{O}} \longrightarrow 1.$$

By substituting for the solvent concentration the solute mole-fraction of ion type "i",  $x_i$ , we have

$$\mu_{\text{H}_2\text{O}} = \mu_{\text{H}_2\text{O}}^{\circ} + g RT \ln(1 - \sum_i x_i),$$

in which  $g$  again has the property

$$g \longrightarrow 1 \quad \text{as} \quad x_i \longrightarrow 0.$$

The osmotic coefficient  $g$  is obtainable from direct measurements of any of the colligative properties.

The deviation from ideality for the solute is indicated by the value of the rational activity coefficient  $f_i$ . In place of the equation for the ideal solution, the partial chemical potential of the solute "i" in an actual solution is

$$\mu_i = \mu_i^{\circ} + RT \ln(f_i x_i),$$

where  $f_1 \rightarrow 1$  as  $x_1 \rightarrow 0$ .

It is convenient to conceive of a separation of  $\mu_1$  into three contributing terms: a term  $\mu_1^\circ$  constant for the particular solute in the particular solvent at given temperature and pressure, differing from the molal Gibbs free energy of the pure solute by a characteristic amount; a general term  $RT \ln(x_1)$ , representing the ideal effect of the solute's concentration; and a term of the form  $RT \ln(f_1)$ , representing specifically the effect of deviation from the ideal dilute-solution laws.

### C. Inter-Ionic Attraction Theory for Electrolytic Solutions

In Section A, the distinction was made between weak electrolytes and strong electrolytes which dissociate more or less completely in solution. This leads to the first assumption in the development of a theory for Dilute solutions of strong electrolytes:

Assumption I: The solute is completely dissociated into its ions upon dissolving in water.

A second assumption follows.

Assumption II: The deviation in the behavior of an actual dilute electrolytic solution from an ideal aqueous solution is due entirely to the electrostatic interactions between the ions.

Thus the van der Waals forces between the solute and solvent particles which cause the non-ideality in solutions of non-electrolytes, are considered to be of minor (indeed of neglected) importance compared to the electrostatic forces causing deviations from ideality in electrolytic solutions.

Now an assembly of  $N$  ions moving freely in a volume  $V$  of continuous

incompressible medium of dielectric constant  $D$ , is formally the same as that for an imperfect gas, and modern electrolytic solution theory developed from statistical mechanics uses this analogy for the statistical treatment of electrolytes in solution. By considering the configuration potential energy contribution to the total Gibbs free energy for the solution, and analyzing its various parts, the free energy of electrostatic mutual interactions between the ions  $F_e$ , can be found to be

$$dF_e = \psi_\lambda |e| dz_\lambda + \psi_\mu |e| dz_\mu + \psi_\nu |e| dz_\nu + \dots$$

in which  $\psi_\lambda$  is the average electrostatic potential at the place of an ion  $\lambda$  due to all the other ions,  $e$  is the electronic charge, and  $z_\lambda$  is the valence or multiples of electronic charge on the  $\lambda$  ion. The free energy of the electrostatic interactions  $F_e$ , is the quality to which Assumption II attributes the complete deviation from ideality.

To evaluate the potential  $\psi_\lambda$ , so that  $F_e$  can be obtained, further assumptions in the theory must be considered.

Assumption III: The ions are spherically symmetrical. Let there be considered a particular ion  $\lambda$  in the solution to be fixed. The radial distance out from the center of the ion  $\lambda$  may be denoted by  $r$ . Then, due to all the ions, including  $\lambda$ , there will be an electrostatic potential

$\psi(r)$  which will be a function of the radial distance  $r$ .

Assumption IV: The Linear Superposition of Fields. One assumes that  $\psi(r)$  is determined by adding the contributions from ion  $\lambda$  and from all the other ions  $\mu, \nu, \dots$  at positions of distances  $r_\mu, r_\nu, \dots$  out from  $\lambda$ . The field contribution of an ion  $\lambda$  to the total resultant electric field in a particular elemental region of space is assumed to be not affected or changed

by the presence of other field contributions in the same region from other ions.

Assumption V: A smoothed electrostatic charge density  $\rho(r)$  exists in the medium, which is a function of  $r$ . Assume that the charges of the ions may be smeared out into continuous distributions throughout the volume of the solution. At some instantaneous time there may be an ion in the element of volume  $dV_\lambda$  giving a large electrostatic potential fluctuation in this region, but on a statistical time average  $dV_\lambda$  will generally not be occupied, so that the charge smear assumption through this region is a fairly good one.

The electrostatic potential  $\overline{\psi(r_\lambda)}$  and smoothed charge density  $\overline{\rho(r_\lambda)}$  as functions of the radial distance  $r$  out from the  $\lambda$  ion, with values averaged over all configurations of ions other than  $\lambda$ , are related by Poisson's Equation:

$$\nabla^2 [\overline{\psi(r_\lambda)}] = - \frac{4\pi}{D} [\overline{\rho(r_\lambda)}]$$

The potential function can be found from Poisson's equation if the charge density can be formulated. The charge density is the summation of the charge on each ion times the number of ions per unit volume. Instead of a static number of ions per volume, one must use a time-average frequency of occurrence of an ion  $\mu$  in an element of volume  $dV_\mu$  specified to be at a distance  $r$  from a given ion  $\lambda$  in  $dV_\lambda$ . Such a frequency of occurrence is given by the statistical Boltzmann distribution law. When this is used to calculate the charge density, Poisson's Equation becomes

$$\nabla^2 [\overline{\psi(r_\lambda)}] = - \frac{4\pi}{D} \sum_{\mu} \frac{q_\mu z_\mu}{V} e^{-W_{\lambda\mu}/kT}$$

in which  $\sum_{\mu}$  is the summation operator over all ions about the central ion  $\lambda$ , and  $W_{\lambda\mu}$  is the potential energy whose gradient gives the average force acting on the  $\mu$  ion in  $dV_{\mu}$  a distance  $r$  from a fixed ion  $\lambda$ . That is,  $W_{\lambda\mu}$  is the work required to bring an ion  $\mu$  from infinity to a distance  $r$  from an ion  $\lambda$ , the process averaged over all configurations of the other ions. The volume of the solution is  $V$ .

It is at this stage of the theory that Debye introduces his fundamental assumption to evaluate  $W_{\lambda\mu}$ :

Assumption VI: Using the definition of electrostatic potential as energy per charge, Debye assumes the linear superposition of fields, and suggests that the time-average potential energy of interaction between the  $\lambda$  and  $\mu$  ions depends on the charge on one ion and on the potential in the vicinity of the other:

$$W_{\lambda\mu} = z_{\mu} |e| \overline{\psi(r_{\lambda})}.$$

This assumption leads directly to the Poisson-Boltzmann Equation:

$$\nabla^2 [\overline{\psi(r_{\lambda})}] = -\frac{4\pi}{DV} \sum_i N_i z_i |e| e^{-\frac{z_i |e| \overline{\psi(r_{\lambda})}}{kT}}$$

in which  $N_i$  is the number of ions of kind "i" in the volume  $V$ , and  $\sum_i$  is the summation operator over all types of ions.

By making two final assumptions, the Poisson-Boltzmann Equation may be solved for the potential  $\overline{\psi(r_{\lambda})}$ .

Assumption VII:

$$\frac{z_i |e| \overline{\psi(r_{\lambda})}}{kT} \ll 1.$$

This allows the exponential to be expanded in a power series, and the first

two terms only retained for a first approximation.

Assumption VIII: Assume the ions to be rigid spheres with "closest distance of approach"  $= \overset{\circ}{a}$ . This allows certain boundary conditions to be defined in solving the Poisson-Boltzmann Equation for ions of finite size. The solution is

$$\overline{\psi(r_\lambda)} = \frac{z_\lambda |e|}{Dr} \frac{e^{-\kappa(r-\overset{\circ}{a})}}{1 + \kappa \overset{\circ}{a}}$$

in which  $\overline{\psi(r_\lambda)}$  is the average electrostatic potential at distance  $r$  from the  $\lambda$  ion,  $\overset{\circ}{a}$  is its distance of closest approach, and  $\kappa$  is defined by

$$\kappa^2 = \frac{4\pi \sum_i N_i z_i^2 |e|^2}{VDkT},$$

where  $N_i$  is the number of ions of type "i" in the volume  $V$ .

At  $r_\lambda = \overset{\circ}{a}$ ,

$$\psi(\overset{\circ}{a}) = \frac{z_\lambda |e|}{D\overset{\circ}{a}} \frac{1}{1 + \kappa \overset{\circ}{a}}.$$

Here  $\psi(\overset{\circ}{a})$  includes both the self-potential of the ion  $\lambda$ , and the resultant electrostatic potential due to the remaining ions at the position  $\lambda$ , namely  $\psi_\lambda$ .

Hence

$$\psi_\lambda = \frac{z_\lambda |e|}{D\overset{\circ}{a}} \frac{1}{1 + \kappa \overset{\circ}{a}} - \frac{z_\lambda |e|}{D\overset{\circ}{a}} = \frac{-z_\lambda |e| \kappa}{D(1 + \kappa \overset{\circ}{a})}.$$

To solve for  $F_\phi$  from its total differential given on page fifteen, one must carry out the mathematical process of integration, which in this case corresponds to the physical process of charging each ion from zero charge up to its normal charge  $z_\lambda |e|$ . According to the charging process

of Debye, the charges on all the ions are increased in the same ratio, so that if  $\alpha$  is the fraction of their final charges which each ion will have at any stage of integration, then  $\alpha z_i |e|$  is the instantaneous charge, and

$$F_e = \int_{\alpha=0}^{\alpha=1} \sum_i N_i \psi_i(\alpha) z_i |e| d\alpha$$

The completely integrated form is

$$F_e = -\sum_i \frac{N_i z_i^2 |e|^2 \kappa}{D} \frac{1}{(\kappa a)^3} \left[ \ln(1 + \kappa a) - \kappa a + \frac{1}{2}(\kappa a)^2 \right]$$

This is the complete Debye-Hückel formula for the contribution to the Gibbs free energy of the electrostatic interactions between the ions in an electrolytic solution. If  $\kappa a$  is small, as in the case of highly dilute solutions, then

$$F_e \approx \frac{-\sum_i N_i z_i^2 |e|^2 \kappa}{3D}$$

The contribution of the electrostatic interionic forces to the partial chemical potential of an ion is

$$(\mu_e)_i = \left[ \frac{\partial F_e}{\partial N_i} \right]_{P,T} = \left( \frac{\partial F_e}{\partial N_i} \right)_\kappa + \frac{\partial F_e}{\partial \kappa} \frac{\partial \kappa}{\partial N_i} + \frac{\partial F_e}{\partial \kappa} \frac{\partial \kappa}{\partial V} \frac{\partial V}{\partial N_i}$$

$$(\mu_e)_i = \frac{-z_i^2 |e|^2 \kappa}{2D} \frac{1}{1 + \kappa a} + \frac{\sum_i N_i z_i^2 |e|^2}{D} \frac{\kappa}{2V} \bar{V}_i \frac{1}{(\kappa a)^3} \left[ \frac{\kappa a}{1 + \kappa a} + \kappa a - 2 \ln(1 + \kappa a) \right]$$

in which  $\bar{V}_i$  is the molecular volume of an ion of type "i".

From the discussion on page 14 concerning the separability of different

terms in the partial chemical potential, we may assign the electrostatic interactions contribution to the partial chemical potential entirely to the activity coefficient terms:

$$(\mu_e)_i = kT \ln(f_i),$$

so that

$$\ln(f_i) = \frac{-z_i^2 |\epsilon|^2 \kappa}{2DkT} \frac{1}{1 + \kappa a} + \frac{\kappa^3 \bar{v}_i}{8\pi (\kappa a)^3} \left[ \frac{\kappa a^3}{1 + \kappa a^3} + \kappa a^3 - 2 \ln(1 + \kappa a^3) \right]$$

This is the complete Debye-Huckel form for the rational activity coefficient of an ion of type "i". The whole second term in this formula is usually dropped by most authors to obtain the approximation

$$\ln(f_i) \approx \frac{-z_i^2 |\epsilon|^2}{2DkT} \frac{\kappa}{1 + \kappa a} .$$

Now the mean ionic rational activity coefficient is defined by

$$f_{\pm} = \left[ \prod_i f_i^{\nu_i} \right]^{1/\nu}$$

in which  $\nu_i$  is the number of moles of type "i" formed from one mole of the completely dissociated electrolyte, and  $\nu = \sum_i \nu_i$ .

The Ionic Strength is defined as

$$s = \frac{\sum_i N_i z_i^2 (10)^3}{2N\nu} = \frac{1}{2} \sum_i c_i z_i^2$$

so that by using the definition of  $\kappa$  on page 18, the mean ionic rational



activity coefficient becomes

$$\ln(f_{\pm}) = \frac{-\left[\frac{1}{\nu} \sum_i \nu_i z_i^2\right] \sqrt{\frac{2\pi N}{(10)^3} \frac{|\epsilon|^6}{(DKT)^3}} \sqrt{S}}{1 + 2|\epsilon| \sqrt{\frac{2\pi N}{(10)^3} \frac{1}{DKT}} \overset{\circ}{a} \sqrt{S}}$$

The above equation is the most useful form of the Debye-Hückel mean ionic rational activity coefficient. In application the values of  $\overset{\circ}{a}$  fitting the experimental data are sometimes reasonable, but sometimes impossibly small. It must be admitted then, that the parameter  $\overset{\circ}{a}$  is not a real mean ionic diameter, but rather a parameter correcting for a whole variety of theoretical imperfections. Nevertheless for low concentrations, small charges, and large ionic diameters, the assumptions postulated for the theory are very nearly fulfilled, and the Debye theory is reasonably accepted as a valid limiting law.

### III. ELECTROLYTIC CONDUCTANCE

In an electric field every charged particle of an electrolytic solution will sustain a net linear motion in the same or opposite direction of the field, depending on the sign of the ionic charge. As the ions move, they carry or "conduct" their charges with them; hence the name "conductance" for this phenomenon.

The presence of charge carrying ions gives a solution an electrical resistance lower than that of the pure solvent. Providing an alternating current is used to avoid accumulative electrolysis, it is the property of resistance which can be experimentally measured in the laboratory. Since the first accurate measurements by Kohlrausch (53) in 1869, the apparatus and experimental technique for studying electrolytic conductances have been highly refined and developed, so that very precise measurements have become possible. The existence of good experimental data arouses interest in theoretical treatments, and with the advent of the inter-ionic attraction theory by Debye and Hückel the basis was laid for the development of a theory of conductance.

Debye (54) himself tackled the theory of conductance by making preliminary estimates of the time-of-relaxation and electrophoretic effects, which are to be discussed below. It was left for Onsager (2) to give a more extensive treatment of these effects and to derive a valid limiting law. Recently Dye (8) has made a mathematical extension to the electrophoretic effect given in Onsager's original treatment. It is the author's understanding that extensive additions to the theory of conductance have been prepared by Onsager and Fuoss, but publication of this work had not

been made at the time this thesis was written.

## A. Theory

The theory of conductance is based on the notion that ions in an electric field will have a velocity of migration characteristic of their natures and that of the solvent, and dependent on the concentration and temperature. The velocity of an ion in solution will be affected in two different ways by its ionic atmosphere, the time-average array of ions about a central one. Firstly, as the ion moves, the concentration disturbance arising in its neighbourhood must be forced to move with the same velocity. Thus the moving ions will be exposed to electric forces from the surrounding ones. This is the "force-transfer" or "time-of-relaxation" effect. Secondly, the surrounding ions, by the action of the external electric field, will cause an additional movement of the solvent, essentially in the reverse direction from the one in which the central ion is migrating. This second phenomenon is generally known as "electrophoresis."

### 1. The Force-Transfer Effect

In the atmosphere of a positive central ion, there are on the average more negatively charged ions than positive ones, and vice-versa. This gives the atmosphere a charge opposite to that of the central ion. Therefore with the application of an external electric field, the spherical symmetry of the atmosphere about an ion is destroyed. That is, the center of charge of the atmosphere becomes displaced from the moving ion. Then additional electrical forces between the ion and its atmosphere arise, and the velocity of the central ion is consequently decreased. If the external

electric field were suddenly removed, the symmetry of the ionic atmosphere would be restored, but only after a finite time, called the Time of Relaxation. It is because Debye used the time-of-relaxation concept in his estimate of the force-transfer effect that the name "time-of-relaxation" effect generally is used. Debye's calculations of the velocity of an ion corrected for the time-of-relaxation effect were made with the assumption that the ions move at constant velocity in a straight line. Onsager (2) presented a more general treatment which automatically accounts for the Brownian or thermal motion of the ions.

By considering time-average distribution functions of the ions, by formulating the hydrodynamic equations of continuity, and constructing equations of motion for the ions in a medium, Onsager calculated a series of partial differential equations for the potential  $\psi_j'$  at the place of a "j" ion due to the asymmetry or perturbation of its ionic atmosphere in an external electric field impressed on the solution. In his original presentation Onsager limited his treatment to the case for electrolytes which dissociate into but two kinds of ions. With this restriction, Onsager's solution for the atmosphere asymmetry potential in the element of volume containing an ion of kind "1" is

$$\psi_1' = \frac{z_1 z_2 |\epsilon|^2 \vec{E} k_1^2 x}{DKT (k^2 - k_1^2)} \left[ - \left( \frac{k - k_1}{3} \right) + \left( \frac{k^2 - k_1^2}{8} \right) r - \dots \right]$$

in which  $z_1$  and  $z_2$  are the valences of the ion types "1" and "2",  $\epsilon$  is the electronic charge,  $D$  is the dielectric constant of the solvent,  $k$  is the Boltzmann constant,  $T$  is the absolute temperature,  $\vec{E}$  is the external electric field vector,  $x$  is the coordinate in the direction of the external

electric field,  $r$  is the radial distance out from the "1" ion,

$$K_1^2 = qK^2,$$

$$K^2 = \frac{4\pi |\epsilon|^2}{DKT} \sum_{i=1}^2 n_i z_i^2$$

and

$$q = \frac{z_1 \omega_1 - z_2 \omega_2}{(z_1 - z_2)(\omega_1 + \omega_2)}$$

where  $n_i$  is the number of ions per cubic centimeter of volume, and  $\omega_i$  is the mobility of the "i" ion, that is, the velocity per ionic charge per unit of force acting.

The perturbation potential  $\psi'_1$  gives rise to a new electric field resulting from the asymmetric distribution of ions about the ion of kind "1". This is the "force-transfer" effect. The new field is

$$\Delta \vec{E}_1 = -\nabla \psi'_1 = -\frac{\partial \psi'_1}{\partial x}$$

or

$$\Delta \vec{E}_1 = \frac{z_1 z_2 |\epsilon|^2 \vec{E}}{3DKT(1 + \sqrt{q})} - \frac{z_1 z_2 |\epsilon|^2 \vec{E} q K^2 r}{8DKT}$$

The velocity of an ion "1" corrected for the force-transfer effect will then be

$$(\vec{v}_1)_{\text{corrected for force transfer}} = \omega_1 z_1 |\epsilon| (\vec{E} - \Delta \vec{E}_1)$$

where  $\omega_1$  is the mobility, or velocity per unit of force acting, and  $\vec{E}$  is the force per charge of the electric field.

## 2. The Electrophoretic Effect

Electrophoresis describes the necessity of an ion having to swim upstream against a solvent current carried along by the ions of opposite charge in the central ion's atmosphere. Onsager's treatment of electrophoresis is based on the assumption that Stokes' Law for the movement of a particle through a viscous medium is valid. Stokes' Law states that the resultant force of all the components in an element of volume will give a particle a velocity such that

$$d\vec{v} = \frac{dF}{6\pi\eta r}$$

where  $dF$  is the force in the element of volume, or "volume-force",  $\eta$  is the viscosity of the medium, and  $r$  is the radius of the spherical particle. Once  $\vec{v}$  is calculated from Stokes' Law, it can be combined with the velocity corrected for force transfer to obtain the net velocity of an ion moving in an external electric field.

By considering the balance of forces on the various particles of the solution, and evaluating the distribution functions with the aid of the Boltzmann distribution law and results of Debye and Hückel's inter-ionic attraction theory, one can calculate the volume-force  $dF$ , and from this the Stokes Law velocity  $d\vec{v}$ :

$$d\vec{v}_j = \frac{4\pi r^2}{6\pi\eta r} \sum_i \left[ \left( n_i e^{\frac{-z_i z_j |\epsilon|^2 e^{-\kappa(r-a)}}{DkT(1 + \kappa a)}} - n_i \right) z_i |\epsilon| \vec{E} \right] dr$$

which is a function of the distance of closest approach parameter,  $a$ .

Onsager makes a power series expansion of the exponential term in the above equation, and integrates, to obtain for the electrophoretic velocity con-

tribution the following:

$$(\Delta \vec{v}_j)_{\text{Electrophoretic}} = \sum_i \left[ -\frac{2}{3\eta} \frac{z_i^2 z_j |\epsilon|^3 n_i \vec{E}}{DkT \kappa (1 + \kappa a)} \right. \\ \left. + \frac{1}{3\eta} \left( \frac{z_i z_j |\epsilon|^2 e^{\kappa a}}{DkT (1 + \kappa a)} \right)^2 z_i |\epsilon| \vec{E} n_i \int_{2\kappa a}^{\infty} \frac{e^{-t}}{t} dt \right]$$

This formula for the electrophoretic velocity may be simplified by dropping the second term which has a squared factor, making it small compared with the first term. Also if  $\kappa a$  is considered small compared with unity for very dilute solutions, we have the electrophoretic velocity for use in a limiting law for conductances:

$$(\Delta \vec{v}_j)_{\text{Electrophoretic}} \text{ Limiting Law} = -\sum_i \frac{z_j |\epsilon| \vec{E} \kappa}{6 \pi \eta}$$

Now the net velocity of an ion is the sum of the velocities against the current of the atmosphere (electrophoresis) and the forward migration modified by the dissymmetry of the atmosphere:

$$\vec{v}_j = \omega_j z_j |\epsilon| (\vec{E} - \Delta \vec{E}_j) + \Delta \vec{v}_j \text{ Electrophoretic}$$

whence by making the substitutions,

$$\vec{v}_1 = \vec{E} \left( \omega_1 z_1 |\epsilon| - \frac{\omega_1^2 z_1^2 |\epsilon|^3 q \kappa}{3DkT(1 + \sqrt{q})} - \frac{z_1 |\epsilon| \kappa}{6 \pi \eta} \right).$$

The ionic mobility is defined as the velocity of an ion per unit

potential gradient. In practical units,

$$\vec{\mu}_1 = \frac{\vec{v}_1 \text{ cm/sec}}{\vec{E} \text{ volts/cm}} = \frac{\vec{v}_1}{299.8 E'} \quad (E' \text{ in } \frac{\text{statvolts}}{\text{cm}})$$

The first term in the velocity expression is the simple forward migration of the ion under unit potential gradient at infinite dilution:

$$\frac{1}{299.8} \omega_1 |z_1| |E| = \vec{\mu}_1^{\circ}$$

Now the Ionic Equivalent Conductance is defined as the charge carried a centimeter per second by one equivalent of the ionic species under a potential gradient of one volt per centimeter:

$$\lambda_1 = \frac{\text{coulombs}}{\text{equivalent}} \cdot \frac{\text{cm/sec}}{\text{volt/cm}} = \mathcal{F} \vec{\mu}_1,$$

and

$$\lambda_1 = \mathcal{F} \vec{\mu}_1^{\circ}$$

where  $\mathcal{F}$  is the Faraday of charge.

Therefore, from the velocity expression, the ionic equivalent conductance for the ionic species "1" is

$$\lambda_1 = \lambda_1^{\circ} \left( \frac{|z_1 z_2| |E|^2 q \kappa}{3DKT (1 + \sqrt{q})} \right) - \frac{\mathcal{F} z_1 |E| \kappa}{299.8 \cdot 6\pi \eta}$$

By writing the equation for  $\lambda_2$  and evaluating  $\kappa$  in terms of the Ionic Strength  $S$ , as on page 20, the equivalent conductance for a salt yielding two kinds of ions in solution may be found:

$$\Lambda = \lambda_1 + \lambda_2$$



and

$$\Lambda = \Lambda_0 - \Lambda_0 \left[ \frac{2 |\epsilon|^{3/2} \sqrt{2\pi N}}{3\sqrt{1000} (DKT)^{3/2}} \frac{q}{1 + \sqrt{q}} |z_1 z_2| \sqrt{S} \right] - \frac{\mathcal{F} |\epsilon|^{2\sqrt{2N}} (z_1 + z_2) \sqrt{S}}{899.4 \eta \sqrt{1000 \pi DKT}}$$

which is the Onsager Limiting Law for Conductances.

### 3. Graphical Evaluation of the Electrophoretic Term, Developed by

J. L. Dye

It will be observed that the electrophoretic velocity in the Onsager theory was approximated in such a way as to neglect any dependence on the distance of closest approach parameter  $\bar{a}$ . Dye calculated the electrophoretic velocity with a graphical integration which retains the dependence on the  $\bar{a}$  parameter. The resulting theoretical conductance law gives a good fit to the experimental data up to about 0.006 Normal for rare-earth salts, compared with 0.001 Normal with the Onsager limiting law. Dye essentially started with the formulation for the Stokes Law velocity  $d\vec{v}$  given on page 26 before expansion of the exponential. It was this expansion and loss of higher terms which Dye avoided. His final result for the electrophoretic contributions to conductance is

$$\Delta \lambda_+ = \eta \int_{\infty}^0 \left[ \frac{-z_+^2 Pe^{-e}}{e} - e \frac{+ |z_+ z_-| Pe^{-e}}{e} \right] d\varrho$$

$$\Delta \lambda_- = \eta \int_{\infty}^0 \left[ \frac{-z_-^2 Pe^{-e}}{e} - e \frac{+ |z_+ z_-| Pe^{-e}}{e} \right] d\varrho$$

$$\Delta \Lambda_{\text{Electrophoretic}} = \Delta \lambda_+ + \Delta \lambda_-$$

in which

$$\eta = \frac{\sum v_j c_N |e| Z_j}{449.7(10)^3 \eta \kappa^2}$$

$$P = \frac{\kappa |e|^2 e^x}{DkT(1+x)}$$

$$x = \kappa \overset{\circ}{a}$$

$$\rho = \kappa r$$

The integrals in Dye's equations are determined graphically.

$\Delta \wedge_{\text{Electrophoretic}}$  is a function of concentration  $C$ , and  $\overset{\circ}{a}$ , and replaces the term

$$\frac{\sum |e|^2 \sqrt{2N} (z_1 + z_2) \sqrt{S}}{899.4 \eta \sqrt{1000 \pi DkT}}$$

in the Onsager Limiting Law.

Dye's equations will be used in the section on Activity Coefficients to estimate values of  $\overset{\circ}{a}$  for rare-earth nitrates from conductance data.

## B. Historical Review of Experimental Techniques

The elements of an apparatus to measure the resistance of electrolytic solutions include a source of alternating current, a modified Wheatstone bridge having the conductance cell in one of its arms, a detector to indicate the current minimum across the mid-points of the bridge, and a constant temperature bath for the cell. The first to make accurate measurements with such an assembly was Kohlrausch (53) as early as 1869. He used an alternating current of 1000 cycles per second generated by an induction coil, and a telephone earpiece as the detector. Kohlrausch modified his Wheatstone bridge by connecting a variable capacitance in parallel with the variable resistance arm. Since the total impedance of the alternating current must be balanced on the bridge, the use of a parallel resistance and condenser allowed the capacitative reactance of the cell to be balanced as well as its resistance. The electrodes of his cell were of platinized platinum. To express his experimental measurements in terms of the specific resistance of the solution, Kohlrausch actually measured the geometry of his cell. Later investigators found their cell characteristics indirectly by taking readings on materials of known specific resistance.

The history of the experimental method simply follows the development and improvements of the various elements of the conductivity apparatus. Each of the components will now be considered in sequence.

### 1. The Alternating Current Source

Washburn and Bell (55) in 1913 replaced Kohlrausch's induction coil with a high frequency generator. This was a mechanical device mounted in a

room some distance from the conductivity laboratory and enclosed in a box to shut in the screeching noise emitted by the rapidly moving toothed wheel. Although only one frequency was available from the generator, that frequency may have varied during a conductivity measurement, since it depended on the rate at which the wheel was driven by an electric motor depending in turn on the constancy of the 110 volt supply. The advantage of the high frequency generator lay in the nature of the alternating current it produced. This was nearly one of single frequency, practically free from the overtones present in the complex wave system developed by the induction coil.

A comprehensive study of the best type of alternating current source was made by Taylor and Acree (56) in 1916. They pointed out that a current of pure sine wave should be required to prevent unsymmetrical electrolysis at the electrodes and to annul the influence of harmonics in the detector. By making oscillograms of the currents produced by an induction coil, a Holzer-Cabot wireless alternating current generator, the city of Madison, Wisconsin, and by various makes of the Vreeland oscillator, they easily made visual comparisons of the purity of sine waves obtained. The Vreeland oscillator works by the action of an oscillating electric circuit upon a double mercury vapor arc. Their choice went to a type B Vreeland oscillator because it produced a practically pure sine wave of constant frequency, free from harmonics. It was noiseless, could be started and stopped conveniently, and could be adjusted to give any voltage desired. The variable voltage feature was useful to Taylor and Acree in their studies of the effect of voltage changes on the apparent resistance of solutions, i.e., the validity of Ohm's Law for a. c. conductivity measurements. They found that the resistance of solutions are independent of the voltage

providing the cells are scrupulously clean, and low voltages are used to avoid heating effects in the cell.

Hall and Adams (57) in 1919 were the first to adopt the electronic oscillator to supply alternating current for some of their electrolytic conductance measurements. The electronic oscillator has been increasingly popular as the current source since then. It provides a range of constant frequencies in pure sine wave form.

## 2. The Conductivity Bridge

In place of ordinary resistance boxes in the ratio arms of the bridge, Washburn and Bell (55) used "film" resistance units. These were made by sealing two platinum wires into the ends of a glass rod, and then connecting the wires by a thin film of platinum deposited upon the glass. Such resistance elements were found practically free from either inductance or capacitance. Taylor and Acree (56) on the other hand used Curtis-type ratio and dial coils in their bridge. The Curtis coil has the wire wound on porcelain spools in such a way as to be essentially free of inductance and capacitance. Non-inductive coils are the type of resistance units used on modern bridges. Taylor and Acree had both variable inductances and variable capacitances in the measuring arm of the bridge.

Jones and Josephs (58) in 1928 wrote the classic paper on Wheatstone bridge design for electrolytic solution conductivity measurements. Their emphasis was on proper shielding, grounding, and arrangement of parts in the bridge assembly. From an extended analysis of alternating current theory, they conclude that if electrical leaks are to be avoided, any grounding must be done at the end-points of the bridge, at opposite corners

from the detector connections. This places the ground in parallel with the bridge proper and the oscillator. This method of grounding eliminated a bridge reading difference when the current through the bridge was "reversed", an effect noticed with the earlier unsatisfactory method of grounding.

Jones and Josephs advise that the connections and switches be so made that one of the leads to the detector, from the mid-point of the bridge, can be disconnected, and this end of the detector connected to the ground instead. Then variable resistances and capacitances in the ground circuit in parallel with the bridge can be adjusted so that the midpoints of the bridge are brought to ground potential. Whereupon the detector can be reconnected, and the resistance of the cell balanced.

These authors caution that the oscillator and any electric motors be kept away from the vicinity of the bridge to avoid stray magnetic fields which may induce currents in the bridge.

As for electrostatic shielding, Jones and Josephs advise that any grounded metallic shield about the bridge should be far enough away from its parts that any capacitance between the bridge and the shield should be negligible. Their timidity in using a shield very close to the bridge was tantamount to advising against its use at all. Shedlovsky (59) in 1930 objected to this point of view. After a theoretical analysis of his own, he concluded that an electrostatic shield was perfectly safe to use without fear of capacitance effects, if it is but  $2\frac{1}{2}$  inches away from the critical parts of the bridge. This made enclosure of the shield in the bridge cabinet possible. Shedlovsky points out that a properly shielded bridge allows sensitive balances to be made without the changing capacities of the moving hands of the observer changing the reading. In addition, a shielded

bridge allows other electrical work to be in progress in the laboratory without affecting the bridge accuracy.

Dike (60) has described the construction of a modern Leeds and Northrup conductivity bridge based on the recommendations of both Shedlovsky, and Jones and Josephs.

### 3. The Amplifier

The use of a thermionic amplifier between the bridge and the detector was not introduced until 1919 when Hall and Adams (57) discovered that the sensitivity of the detector could be enhanced from  $\pm 5$  scale divisions on the variable resistance dial to  $\pm 0.05$  with amplification. They cautioned that leads to the amplifier should be grounded and shielded.

In 1929 Jones and Bollinger (61) improved their amplifier by the addition of a wave filter to cut out the 60 cycle hum and tube noises. They found, however, that a mutual inductance between the oscillator and the amplifier may induce an alternating e.m.f. at the ends of the lead wires from the amplifier to the bridge, thus causing an error in bridge setting. The only remedy they found was to remove both the oscillator and the amplifier as far away as possible from each other and from the bridge. They say that even a 35 foot separation may be needed.

### 4. The Detector

Kohlrausch used a simple telephone earpiece as the detector. With the bridge in balance, the potentials at the mid-points would be the same, resulting in a minimum hum in the telephone. Washburn and Bell (55) used a telephone tuned to respond to the frequency of the current employed.

A tuned telephone is one which is substantially free from reactance for the frequency employed and whose diaphragm has a natural period of vibration for its fundamental, which is the same as that for the current. Such a telephone is more sensitive than the simple earpiece of Kohlrausch. Taylor and Acree (56) used a stethoscope with their tuned telephones! Washburn and Parker (62) in 1917 made various studies on the audibility current and sensitivity of the telephone receiver.

The telephone has been the standard detecting instrument until recently when Spedding, Porter, and Wright (29) replaced it with a cathode-ray oscilloscope in 1952. The use of the eye rather than the ear allows much more sensitive estimations of the null point. The oscilloscope is much handier to use since it avoids telephone wires dangling about the head of the operator.

#### 5. Conductance Cells. Capacitance Effects and Polarization

Taylor and Acree (56) considered a conductance cell in the circuit in the following way: "A cell behaves toward an alternating current as if it were made up of a resistance in series with a condenser with a small leak. It offers an impedance to the harmonically varying current, changes the phase in its bridge arm, and gives an unbalance in the detector." This cell capacitance may be balanced out with a condenser either in parallel or in series with the variable resistance arm of the bridge, or with an inductance in series with the cell. Taylor and Acree used each of these methods to balance the cell capacitance, and observed that the resistance of solution in a cell remains the same within experimental error for each method.



Among others, Taylor and Acree found that the resistance of solutions decreased slightly with an increase in frequency of the current used. This effect was most pronounced with cells having small bright electrodes. When the electrodes were made large, and were platinized, however, the variation of resistance with frequency could be made practically negligible. Here then was a very practical reason for the platinization of electrodes. During these studies Taylor and Acree found that some criterion was needed for deciding whether a true resistance was being measured. They reasoned that the ratio of resistances for any given solution in two cells, or of two solutions in any cell, must be constant. Experimentally they observed that the ratio of resistances from cells with platinized electrodes was indeed constant. But the ratio of resistances of two solutions in a cell with platinized electrodes differed by about 2% at 60 cycles from the ratio of resistances of the same two solutions in a cell with bright electrodes. However this difference in ratios between such two cells decreased as the frequency was increased, and became minimal (0.004%) when the results were extrapolated to infinite frequency. Thus Taylor and Acree experimentally established the rule that a group of cells will give resistance readings consistent among themselves if the results are extrapolated to infinite frequency. They used the extrapolation formula

$$R_{\text{infinite frequency}} = R_f - \frac{K'}{f}$$

in which  $R_f$  is the measured resistance at the frequency  $f$ , and  $K'$  is a constant.

In 1916 Washburn (63) presented an extensive study on the theory and design of conductivity cells. Washburn considered the cell to be a resistance

and a capacity in series, shunted by a capacity. He ascribed the series capacitance to polarization, a composite of various electrode effects including ionic discharging, adsorption, and concentration gradients near the electrode. The use of platinized electrodes and a high frequency minimize this polarization, however, so that the cell can easily be reduced to a resistance and capacitance in parallel.

To find the optimum geometrical characteristics of a cell, Washburn applied alternating current theory to the different elements in the bridge, and derived the distribution of the current in the bridge network. From this he was able to obtain formulas for the best area of the electrodes and their optimum separation in the cell as functions of resistances of various components in the bridge, the specific conductance of the solution being measured, the percentage accuracy desired, and other factors. In general, he found that the lower the specific conductance being measured, the larger should be the electrode areas for greatest accuracy.

Before the remainder of the work on cells is presented, the concept of the "cell constant" should be introduced. The total resistance (in ohms) of a body is proportional to its geometry:

$$R = k \frac{d}{A}$$

where  $d$  is the body's length,  $A$  its cross-sectional area, and  $k$  is the specific resistance. The specific conductance,  $L$ , is the reciprocal of the specific resistance  $k$ , or

$$L = \frac{1}{k} = \frac{d}{A} \frac{1}{R} = \frac{K}{R} \cdot$$

When the body whose resistance is being measured is an electrolytic solution in a cell,  $K$  is the "cell constant" and is a function of the area of the electrodes and their separation. In principle,  $K$  can be determined by directly measuring the geometrical characteristics of the cell, as Kohlrausch did. It is more accurate, however, to measure the resistance of a substance of known specific conductance in the cell, since very elaborate procedures are required to determine the cell geometry.

In 1923 Parker (64) found that the determination of the cell constant is not so simple as outlined above. He found, while calibrating some cells, that the cell constant changes with different concentrations of KCl solutions used as the standardizing media. That is, the experimental resistance readings gave a small but uniform change in the cell constant with a change in the measured resistance. This same effect was reported by Randall and Scott (65) in 1927. They noticed a change in cell constants with resistance by intercomparing cells. Smith (66) confirmed these results in the same year. He found that as the resistance changes, there is a change not only in the cell constants of two cells, but also in the ratio which they bear to one another. The criterion of reliability imposed by Taylor and Acree was found to be complied with by two cells in the region of concentration in which they were calibrated, but not in regions which vary greatly from that in which the cell constants were determined.

In his work with electrolytic conductance Shedlovsky (67) in 1930 tried to design a cell with a constant "cell constant." He ascribed Parker's effect, which the change in cell constant has come to be called, to polarization, and so designed his cell to eliminate the contributions of the electrode processes from the resistance measurements. Shedlovsky's cell

had multiple electrodes - two platinum cones at each end, and several platinum rings spaced along the body of the cell. Then the cell could be connected to the bridge and to the detector in a variety of ways. By measuring resistance values for various combinations of connections, and by writing algebraic equations for the resistance contributions of the several components of the cell, the effects of the electrodes could be subtracted out. In this way the effective resistance of that portion of the solution between two ring electrodes could be obtained, without any contributions from processes at the end electrodes at which the electric field was applied. Values thus obtained showed no variation of resistance with the frequency, nor dependence of the cell constant on the resistance being measured. Hence the Parker and frequency effects seemed to be exclusively due to electrode polarizations, although later investigators arrived at conclusions different from these of Shedlovsky.

The classic paper on the design of conductivity cells is that of Jones and Bollinger (68) in 1931. Their study involved polarization, capacitance, and Parker effects in cells. The authors began by investigating the alternating current phase displacement in a cell. They plotted the tangent of the phase angle,

$$\tan \theta = C(2\pi f)R$$

versus the resistance measured for various frequencies  $f$ , and degrees of platinization of their electrodes. The capacitance  $C$ , was measured on a calibrated condenser in parallel with the variable resistance in the bridge. The  $\tan \theta$  vs.  $(\log)R$  curves were found to have a minimum which occurred at lower resistances for increasing frequency or platinization. That part of

the curve on the low resistance side of the minimum could be made to have smaller and more constant values of  $\tan \theta$  with increasing frequency and platinization, qualities which directly affect the electrodes themselves. That part of the curve on the high resistance side of the minimum was not affected much by change in frequency or platinization. Therefore Jones and Bollinger separated cell behavior into two parts: Data taken at low resistances (high solution concentrations) were affected mainly by polarization phenomena. In this region resistance readings were most constant with change in frequency when the phase angle and cell capacitance were low, and these were low for large frequencies and heavy platinization. Data taken at high resistances (low solution concentrations) were affected mainly by what Jones identified as the Parker effect.

As an extension to Washburn's ideas on the part played by a cell in the circuit, Jones and Bollinger considered polarization to play the part of both a capacitance and an additional resistance in series with the resistance of the solution. The polarization resistance must be independent of the distance between the electrodes, and therefore the percentage error caused by polarization could be decreased by using cells of high cell constant. Thus the authors point out that a shorter cell will have a relatively greater polarization error with the same solution than a longer one. As pointed out previously, the polarization capacitance is minimized by increasing the electrode areas (with the diameter and platinization) and increasing the frequency.

The capacitance in parallel with the cell resistance, in Washburn's analysis, is now identified as the cause of the Parker effect by Jones and Bollinger. The old-fashioned pipette cells then in use (1931) were

suspended vertically in the bath, with one electrode above the other, and filling tubes bent close to and parallel with the body of the cell. Thus a capacitor in parallel (with the cell proper as one "plate", and the filling tubes as the other) was inherent in the very design of the old cells. This capacitative shunt causes more current leakage past the cell at high resistances than at low, and this is the very region of the Parker Effect. This interpretation is found to be in complete opposition to the conclusions of Shedlovsky (67) a year previously.

Next Jones and Bollinger carried out a mathematical analysis of errors due to the capacitative shunt. If  $\Delta R$  is the error due to the Parker Effect shunt, they derived the approximate relationship,

$$\Delta R \cong -R_p \tan^2 \theta .$$

in which  $R_p$  is the resistance through the vertical filling tubes, and  $\theta$  is the phase angle. Since the measured resistance is

$$R = R_t - R_p \tan^2 \theta,$$

where  $R_t$  is the true resistance, and  $\tan \theta = C(2\pi f)R$ , their theory could be experimentally verified if the parallel capacitance  $C$  could be measured. This they did by inserting a variable air condenser in one of the leads between the cell and the bridge. Then the combination of the parallel capacitance  $C$  and that of the air condenser could be measured in the usual way with the variable calibrated condenser in the bridge. They plotted the measured resistance  $R$  vs.  $C^2$  and also vs.  $f^2$ , and found in both cases straight lines with negative slope, and intercepts presumably at  $R_t$ .

Jones and Bollinger next demonstrated mathematically that the measured

resistance ratio of two cells,  $R_A/R_B$  -- which is also the cell constant ratio  $K_A/K_B$  for the cells containing the same solution -- depends upon the parallel capacitances of each cell,  $C_A$  and  $C_B$ , on the frequency  $f$ , and on the specific conductance of the solution:

$$\frac{R_A}{R_B} = \frac{K_A}{K_B} = \frac{R_{tA}}{R_{tB}} \left[ 1 - (kC_A^2 - kC_B^2) \frac{(2\pi f)^2}{L^2} \right]$$

This equation shows that if  $C_A = C_B$ , the cell constant ratio should be independent of the specific conductance  $L$ . Furthermore if  $L$  is small (high resistance range) the variation in the resistance or cell constant ratios from  $R_{tA}/R_{tB}$  is large. This variation of the cell constant ratio with changing specific conductance (or measured resistance) for two types of cells is precisely the form of the Parker Effect observed by Smith (66). Jones and Bollinger then verified the above equation experimentally, which firmly established the identity of the capacitative shunt effect with the Parker Effect.

Since a set of cells for a wide range of solution concentrations may have various parallel capacitances, the only way to eliminate the Parker Effect would be to design cells such that each parallel capacitance is as low as possible. To avoid capacitance between cell parts, Jones designed cells to be suspended horizontally in the bath, with vertical filling and electrical connecting tubes placed as far apart from each other as possible. The electrodes of his cells were heavily platinized. Jones' cells had negligible capacitance between the parts, constant cell-constant ratios among the cells, and less than 0.01% change of resistance with change in

frequency. It is generally agreed that Jones and Bollinger's work is monumental in the experimental conductance field, and their types of cells are extensively used in current researches.

In 1935 Jones and Christian (69) returned to the problem of polarization. They used a cell with variably separable electrodes, so designed that electrodes of different metals could be used. They reasoned, as did Jones and Bollinger, that if polarization causes an extra resistance  $R_s$  in series with the cell and having its seat at the electrodes, then  $R_s$  should be independent of the separation  $d$  of the electrodes, and one should expect the following relationship to hold:

$$R = R_t + R_s = \frac{d}{AL} + R_s$$

where  $R$  is the measured resistance,  $R_t$  is the true resistance of the solution,  $d$  is the electrode separation,  $L$  is the specific conductance, and  $R_s$  is the series resistance due to polarization at the electrodes. With their special cell, Jones and Christian obtained data which gave a straight line on an ( $R$  vs.  $d$ ) plot, with presumably  $R_s$  as the intercept. Data at different frequencies gave parallel lines. These results confirmed their surmise that the polarization  $R_s$  is not located in the body of the solution. The authors then repeated their measurements for other electrode metals and for different salts and concentrations. They concluded that the least polarization resistance occurred for platinized platinum electrodes and for high frequencies of alternating current.

Jones and Bollinger (70) in 1935 undertook a practical study to develop a reliable quantitative test of the quality and sufficiency of platinization



for electrodes. They adopted Warburg's Law as their criterion, which is

$$R_f = R_{\text{infinite frequency}} + k/\sqrt{2\pi f}$$

Thus for optimum platinization, a plot of the resistance, at a variety of frequencies  $f$ , vs.  $1/\sqrt{2\pi f}$  should give a straight horizontal line, showing no dependence of the resistance on frequency. For platinizing electrodes they suggest using a 0.01 ampere current with polarity reversal every 10 seconds. The platinizing solution is 0.025 N HCl with 0.3% PtCl<sub>4</sub> and 0.025% (CH<sub>3</sub>COO)<sub>2</sub>Pb. Best results were obtained when 6 coulombs of charge had been passed per square centimeter of electrode surface.

#### 6. The Constant Temperature Bath

Most investigators found any arrangement suitable which would hold the temperature constant within  $\pm 0.01^\circ\text{C}$ . Jones and Josephs (58) point out that in comparison with mineral oil, water is a conductor, and as the walls of the glass cell may act as a dielectric in a condenser, alternating current may thereby be permitted to flow in the water outside the cell, with resultant error in the measurements. Hence mineral oil is recommended as the bath medium.

#### C. Preparation of Solutions

Solutions of the nitrates of samarium, holmium, erbium, and ytterbium were essentially obtained by reacting the appropriate oxide with nitric acid. The Iowa State College Institute for Atomic Research provided the pure rare-earth oxides which were separated from the other rare-earths in

in the ore concentrates by ion-exchange techniques. The degree of purity of the rare-earth oxides was determined with emission spectroscopy by the spectrographic group of the Institute for Atomic Research. Table I presents a summary of the analyses on the oxides.

Upon delivery of the oxides by the ion-exchange group, each pure sample of about 50 grams was reprecipitated as the oxalate three times to insure removal of any traces of calcium or iron that may have been present. The oxide sample was completely dissolved in an equivalent amount of nitric acid, and the solution filtered through sintered glass to remove any foreign matter. Then the filtrate was diluted to a handy volume, heated almost to boiling, and a hot solution of twice recrystallized "Baker's Analyzed" oxalic acid was added to the rare-earth filtrate with vigorous stirring. Since the solutions were hot, and the final acid concentration was about 1 Normal, any calcium oxalate would presumably stay in solution. By filtering the precipitated rare-earth oxalate on sintered glass, and igniting at about 900°C. in a muffle furnace, the rare-earth oxide could be recovered. This reprecipitating procedure was then repeated twice.

To prepare a nitrate in solution, the desired reprecipitated oxide was dissolved with heating in an insufficiency of C. P. nitric acid so that a small amount of undissolved oxide remained. The clear solution from a filtration had a pH of about 6. It is easily surmised that such a solution would contain a moderate amount of unneutralized hydrous rare-earth oxide and such ionic species as  $R.E.(OH)^{++}$ . The solution desired is one that would result if a pure sample of the anhydrous salt  $R.E.(NO_3)_3$  were placed

Table I. Spectrographic analyses of rare-earth oxides

Oxide	Analysis
$\text{Sm}_2\text{O}_3$	Ca: less than 0.02% Fe: less than 0.005% Nd: less than 0.05% Eu: less than 0.025% Gd: less than 0.04% Ho: none
$\text{Ho}_2\text{O}_3$	Ca: less than 0.1% Fe: less than 0.03% Dy: less than 0.04% Er: less than 0.02% Tm: less than 0.01% Y : less than 0.01%
$\text{Er}_2\text{O}_3$	Ca: less than 0.02% Dy: less than 0.005% Ho: less than 0.01% Tm: less than 0.02% Yb: less than 0.01% Y : less than 0.01%
$\text{Yb}_2\text{O}_3$	Ca: less than 0.05% Er: less than 0.01% Lu: less than 0.09%

in water and allowed to come to hydrolysis equilibrium:



Since for this equilibrium the concentrations of  $\text{H}^+$  and of  $\text{R.E.}(\text{OH})^{++}$ -type ions would be equal (neglecting the ion-product of water for moderate concentrations of  $\text{R.E.}^{+++}$ ), the pH of such a solution could be designated as the "stoichiometric point." To find the stoichiometric point of the filtrate described above, a titration with 0.1 Normal  $\text{HNO}_3$  was made on an aliquot. The course of the titration was followed with a Beckman Model G pH-meter. A plot of pH vs. added volume of  $\text{HNO}_3$  gave a typical strong acid - weak base titration curve for each of the four rare-earths studied in this research. A differential plot  $\Delta\text{pH}/\Delta\text{ml}_{\text{HNO}_3}$  vs. ml  $\text{HNO}_3$  was made for each titration to find the stoichiometric pH at which the acid ( $\text{H}^+$ ) and base ( $\text{R.E.}(\text{OH})^{++}$ ) concentrations for the reaction would be equal and minimal. Stoichiometric pH's were found to be in the range 3-5, depending on the individual rare-earth and the concentration of the solution. Sufficient  $\text{HNO}_3$  was then added to the bulk of the filtrate to bring its pH to the stoichiometric value.

To break up any colloidal complexes of hydrous oxide which may not have been neutralized, the pH-adjusted solution was boiled for about 15 minutes. The titration of an aliquot and pH adjustment of the bulk of the solution were then repeated. Generally a second boiling and third pH measurement were necessary to verify that the solution had a constant pH at the stoichiometric value. By diluting this preparation to a convenient volume, one had a "stock solution" which was ready for use. Such solutions were optically clear, and would remain so indefinitely.

To find the concentration of the stock solution, analyses in triplicate were made for the rare-earth cation by precipitating the oxalate and igniting to the oxide. Portions of the stock solution were weighed directly into constant weight porcelain crucibles. Hot oxalic acid solution was then poured slowly into the crucibles. The precipitating mixture was stirred vigorously while the oxalic acid was added to avoid trapping liquid in large coagulations of precipitate which might rapidly form otherwise. The supernatant liquid was evaporated slowly by leaving the crucibles under an infra-red lamp. When the precipitate was dry, it was ignited at 900°C. in a muffle furnace, and final weighings made to determine the amount of oxide. A precision of 0.1% was easily obtained with this method.

A series of solutions in the concentration range from 0.0001 Normal to 0.1 Normal was prepared from the stock solution by volume dilution with conductivity water. Calibrated glassware was used. The conductivity water was prepared by redistilling ordinary distilled water as an alkaline potassium permanganate solution in a Barnsted conductivity still with block tin condensers. The pure water produced had a specific conductance of  $8(10)^{-7}$  mhos/cm, and a pH of the order of 5.8. The acidic pH of water is due exclusively to the fact that it is a saturated solution of carbonic acid, as pointed out by Kendall in 1916 (71).

Potassium chloride solutions for the calibration of the conductance cells were prepared by weighing out an appropriate amount of C.P. KCl which had been fused to insure removal of water from the crystals. The weighed KCl crystals were dissolved in conductivity water and diluted to the proper volumes.

## D. Experimental Investigation

### 1. Apparatus and Procedure

The experimental resistance measurements were made with a Leeds and Northrup research model conductivity bridge, catalogue #4666. This bridge is designed in accordance with the recommendations of Jones and Josephs (58), and its construction and operation are completely described by P. H. Dike (60). Alternating current of frequencies 500, 1000, and 2000 cycles per second was provided by a Leeds and Northrup audio frequency electronic oscillator, catalogue #9842. For greater sensitivity the signal from the bridge was amplified with a Leeds and Northrup audio frequency amplifier, catalogue #9847, which could be tuned to the same frequency as the oscillator. A cathode-ray oscillograph, type 274-A, manufactured by the Allen B. DuMont Laboratories, Inc., was used as the detector. The use of this instrument provided not only a precise visual indication of the bridge balance, but gave a continuous verification of the pure sine wave nature of the alternating current in the bridge and cell circuit. Any trouble with the assembled apparatus would be accompanied by harmonics in the current wave pattern, which would become immediately obvious to the operator as he glanced at the oscillograph screen. The constant temperature bath was heated with an infra-red lamp, and controlled with a thermoregulator of the type having an expanding mercury column contacting the point of a platinum wire to activate the relay. The temperature of the mineral oil medium in the bath could be controlled to  $\pm 0.01^{\circ}\text{C}$ .

The conductance cells used for this research were of the general form recommended by Jones and Bollinger (58) from their extensive study of cell

design. A set of four cells of widely varying cell constants were used so that the specific conductance of a solution could be cross checked with two or three cells, and so that appropriate cells could be used to keep the measured resistance within the optimum range of the Jones conductivity bridge. The cells were of Leeds and Northrup make, catalogue numbers 4911, 4914, 4915, and a special type A Jones cell rigidly tailored to the Jones and Bollinger models. The electrodes of these cells were platinized in accordance with the recommendations of Jones and Bollinger (70). That the platinization was adequate was shown by the agreement of resistance measurements at 2000 and at 1000 cycles, which was better than 0.01% for all cells.

To maintain the continuity of conductance measurements in the Ames Laboratory (29, 32, 33, 35) in which the aqueous potassium chloride conductance data of Shedlovsky (72) has been used as the standard, Shedlovsky's data was also used to calibrate the conductance cells employed in this research. To take account of any Parker effect present in the cells, a calibration curve of "cell constant" vs. resistance was plotted for each cell from measurements on a series of potassium chloride solutions prepared by weight dilution. To illustrate the consistency of results given by any pair of cells, the criterion of Taylor and Acree (56) may be used. This provides that the ratio of resistances of two solutions in any cell must equal the ratio for those solutions in any other cell. In order to show the magnitude of the Parker effect for each cell, and to show compliance with the Taylor and Acree criterion, the calibration data for the four cells are summarized in Table II.

Table II. Calibration of conductance cells

Normality of KCl	L-cell, #4911		M-cell, #4914		H-cell, #4915		Jones Cell, type A	
	Resistance	Cell constant	Resistance	Cell constant	Resistance	Cell constant	Resistance	Cell constant
0.0008420	1765.38	0.22001					1985.15	0.24740
0.001			7681.2	1.1344				
0.0025	604.24	0.22004						
0.0032827	463.11	0.22019	2385.21	1.1341			520.98	0.24771
0.005	306.29	0.22021	1577.22	1.1340	47270.	33.985		
0.01	155.83	0.22034	802.39	1.1346	24048	34.003	175.37	0.24795
0.05			170.08	1.1340	5097.4	33.986		
0.10			87.96	1.1339	2635.31	33.971		

Parker effect for L-cell: Overall cell-constant change  
in range 1800 - 150 ohms. . . . 0.14%

Parker effect for M-cell: Overall cell-constant change  
in range 8000 - 80 ohms . . . . 0.07%

Parker effect for H-cell: Overall cell-constant change  
in range 50,000 - 2000 ohms . . 0.09%

Parker effect for Jones  
Cell, type A: Overall cell-constant change  
in range 2000 - 170 ohms. . . . 0.2%



From the measured resistances shown in Table II, examples of Taylor and Acree ratios are given below which show the degree of consistency within pairs of cells:

For the L and Jones Cells:

$$\frac{1765.38}{463.11} : \frac{1985.15}{520.98} = 3.8120 : 3.8104 \text{ (0.04\% difference)}$$

For the L and M Cells:

$$\frac{463.11}{306.29} : \frac{2385.21}{1577.22} = 1.5120 : 1.5123 \text{ (0.02\% difference)}$$

For the Jones and M Cells:

$$\frac{520.98}{175.37} : \frac{2385.21}{802.39} = 2.9707 : 2.9726 \text{ (0.06\% difference)}$$

For the M and H Cells:

$$\frac{1577.22}{170.08} : \frac{47270.}{5097.4} = 9.2734 : 9.2734 \text{ (0.0\% difference).}$$

These percentage agreements were quite satisfactory considering that the concentrations of the solutions to be measured were not known with better than 0.1% accuracy.

To measure the resistances of rare-earth nitrate solutions, the following general laboratory procedure was used. A series of 14 solutions in the concentration range from 0.0001 Normal to 0.1 Normal was prepared from a stock solution by volume dilution with calibrated glassware using conductivity water of previously measured specific conductance. To avoid errors due to soaking out salt absorbed at the electrodes, the solution of lowest concentration was measured first, followed by ones of increasing concentration. For each measurement the cell was thoroughly rinsed three times, and then allowed to soak for an hour with the solution to be studied.

Fresh solution was replaced in the cell which was then suspended in the bath for temperature equilibration. With the cell connected into the circuit, resistance measurements were made with the Jones conductivity bridge at intervals over a two hour period. Generally at the end of half an hour, or forty-five minutes, the readings would become constant for the remainder of the equilibration period. Then the readings were repeated on a new sample of the same solution. Resistance measurements were made at both 2000 and 1000 cycles; the differences in such readings were generally of the order of 0.01%.

## 2. Calculations and Results

In accordance with the suggestions of Taylor and Acree (56) and of Jones and Bollinger (70) that the most consistent sets of data are those taken at infinite frequency of the alternating current, all the resistance data of this research were reduced to values at infinite frequency. The extrapolation formula (known as Warburg's Law),

$$R_{\text{at frequency } f} = R_{\text{infinite frequency}} + \frac{k}{\sqrt{f}},$$

was used in an algebraic form,

$$R_{\infty} = \frac{\sqrt{2} R_{2000} - R_{1000}}{\sqrt{2} - 1} = 3.414217 R_{2000} - 2.414217 R_{1000} .$$

This formula for the resistance at infinite frequency  $R_{\infty}$ , was obtained by writing Warburg's Law twice, once for  $f = 2000$ , and once for  $f = 1000$ , and solving the two equations simultaneously to eliminate the constant  $k$ . Values of  $R_{\infty}$  generally differed from those of  $R_{2000}$  by around 0.03%.

The proper value of the "cell constant"  $K$  was found from the calibration curve for each cell. Then the measured specific conductance of the solution was found from

$$L_m = \frac{K}{R_{\infty}}$$

The specific conductance due to the solute alone was found by subtracting the contribution of the solvent,

$$L_{R.E.(NO_3)_3} = L_m - L_{H_2O}$$

and the equivalent conductance was calculated from the relation

$$\Lambda = \frac{1000 L_{R.E.(NO_3)_3}}{C_n} \quad \frac{\text{coulombs}}{\text{equivalent}} \cdot \frac{\text{cm/sec}}{\text{volt/cm}}$$

in which  $C_n$  is the normal concentration (equivalents per liter).

By using the Onsager Limiting Law for conductances, given on page 29, Shedlovsky (73) has suggested an extrapolation method to evaluate the equivalent conductance at infinite dilution,  $\Lambda_0$ . His method, with a slight modification, was adopted for this research. Essentially the Onsager Limiting Law was solved for  $\Lambda_0$ , and at each experimental concentration, measured values of  $\Lambda$  were used to calculate  $\Lambda_0$ , the calculated values given the symbol  $\Lambda'_0$ . Then the series of  $\Lambda'_0$ -numbers were plotted vs.  $\sqrt{C_n}$ . The resulting curve was practically horizontal in the dilute range, and could be extrapolated with confidence to the ordinate of the graph. The value at the intercept was taken to be  $\Lambda_0$ , the equivalent conductance at infinite dilution.

The various factors in the Onsager limiting law were evaluated as follows:

The valence factor

$$q = \frac{z_1 \omega_1 - z_2 \omega_2}{(z_1 - z_2)(\omega_1 + \omega_2)}$$

is a function of  $\omega$ , the mobility per unit charge of an ion, which is related to the ionic equivalent conductance through the definition of the practical mobility at infinite dilution given on page 28:

$$\frac{1}{299.8} \omega_1 |z_1| \epsilon = \bar{\mu}_1^\circ = \frac{\lambda_1^\circ}{\mathcal{F}}$$

Then, since  $z_- = -|z_-|$ ,

$$q = \frac{| \epsilon | z_+ \left( \frac{299.8 \lambda_+^\circ}{z_+ | \epsilon | \mathcal{F}} \right) + | \epsilon | |z_-| \left( \frac{299.8 \lambda_-^\circ}{|z_-| \epsilon \mathcal{F}} \right)}{| \epsilon | (|z_+| + |z_-|) \left( \frac{299.8 \lambda_+^\circ}{z_+ | \epsilon | \mathcal{F}} + \frac{299.8 \lambda_-^\circ}{|z_-| \epsilon \mathcal{F}} \right)}$$

or

$$q = \frac{|z_+ z_-| (\lambda_+^\circ + \lambda_-^\circ)}{(|z_+| + |z_-|) (|z_-| \lambda_+^\circ + |z_+| \lambda_-^\circ)} = \frac{|z_+ z_-| \Lambda_0}{(|z_+| + |z_-|) (|z_-| [\lambda_+^\circ] + |z_+| \lambda_-^\circ)}$$

The ionic strength  $S$ , is related to the molar concentration of the cation  $c_+$  and of the anion  $c_-$ , and to the Normality  $C_N$  of the solution by

$$S = \frac{1}{2} (c_+ z_+^2 + c_- z_-^2) = \frac{1}{2} C_N (z_+ + z_-).$$

The values used for the fundamental physical constants (74) were

$$e, \text{ the electronic charge} = 4.80223(10)^{-10} \text{ statcoulombs}$$

$$\pi = 3.14159$$

$$N, \text{ Avogadro's Number} = 6.02380(10)^{23} \text{ mole}^{-1}$$

$$k, \text{ Boltzmann's constant} = 1.380257(10)^{-16} \text{ erg/degree}$$

$$F, \text{ the Faraday constant} = 96,493.1 \text{ coulombs/equivalent}$$

For solutions of R.E.(NO<sub>3</sub>)<sub>3</sub> in water at 25.00°C.,

$$T, \text{ the absolute temperature} = 298.16 \text{ degrees}$$

$$D, \text{ the dielectric constant of water} = 78.54 \text{ (reference 75)}$$

$$\eta, \text{ the viscosity of water} = 0.008949 \text{ poise (reference 76)}$$

$$\lambda_{\text{NO}_3^-}^{\circ} \text{ the ionic equivalent conductance of the nitrate ion at infinite dilution} = 71.42 \text{ (reference 77)}$$

The working form of the Onsager limiting law used to calculate  $\Lambda'_o$  was then

$$\Lambda'_o = \frac{\Lambda + 170.241 \sqrt{C_n}}{1 - \left[ \frac{2.48719 \Lambda'_o}{(\Lambda'_o + 142.84) \left( 1 + \frac{3/4 \Lambda'_o}{\sqrt{\Lambda'_o + 142.84}} \right)} \right] \sqrt{C_n}}$$

Since this expression cannot be explicitly solved for  $\Lambda'_o$ , values for this quantity at each concentration  $C_n$  had to be obtained by successive approximations. The intercept on a  $\Lambda'_o$  vs.  $\sqrt{C_n}$  plot was then taken as  $\Lambda_o$ .

The Kohlrausch law for the additivity of equivalent conductances of ions may be expressed for a binary electrolyte at infinite dilution by the

Table IV. Conductances of holmium nitrate

Normality	Specific conductance	Equivalent conductance	Calculated $\Lambda^{\circ}$
0.19091	0.016304	85.401	
0.095454	0.0088485	92.699	
0.066813	0.0064403	96.392	
0.047724	0.0047616	99.775	
0.038197	0.0038906	101.86	
0.019075	0.0020777	108.92	
0.0095440	0.0010977	115.01	
0.0076288	0.00089190	116.91	
0.0047697	0.00057465	120.48	139.60
0.0019064	0.00024106	126.45	138.49
0.00095384	0.00012354	129.52	138.02
0.00076243	0.000099393	130.36	137.96
0.00047669	0.000062889	131.93	137.94
0.0		137.92	

Table V. Conductances of erbium nitrate

Normality	Specific conductance	Equivalent conductance	Calculated $\Lambda^{\circ}$
0.094717	0.0087565	92.449	
0.063106	0.0061165	96.924	
0.047327	0.0047056	99.427	
0.031559	0.0032604	103.31	
0.015766	0.0017349	110.04	
0.0063126	0.00074182	117.51	139.50
0.0031559	0.00038592	122.29	137.73
0.0015766	0.00019930	126.41	137.31
0.00063126	0.000082128	130.10	136.99
0.00031559	0.000041720	132.20	137.07
0.0		137.0	

20. Patterson, C. S., Tyree, S. Y., and Knox, K., J. Am. Chem. Soc. 77, 2195-2197 (1955)
21. Davies, C. W., and James, J. C., Proc. Roy. Soc. London A195, 116-123 (1948)
22. James, J. C., J. Chem. Soc. London 1950, 1094-1098
23. Jenkins, I. L., and Monk, C. B., J. Am. Chem. Soc. 72, 2695-2698 (1950)
24. <sup>H</sup>Ohlm, L. W., Soc. Sci. Fennica Commentationes Phys.-Math. 9, No. 2, 2-14 (1936)
25. Robinson, R. A., Trans. Faraday Soc. 35, 1229-1233 (1939)
26. Mason, C. M., and Ernst, G. L., J. Am. Chem. Soc. 58, 2032 (1936)
27. \_\_\_\_\_, J. Am. Chem. Soc. 60, 1638-1647 (1938)
28. \_\_\_\_\_, J. Am. Chem. Soc. 63, 220 (1942)
29. Spedding, F. H., Porter, P. E., and Wright, J. M., J. Am. Chem. Soc. 74, 2055 (1952)
30. \_\_\_\_\_, \_\_\_\_\_, and \_\_\_\_\_ J. Am. Chem. Soc. 74, 2778 (1952)
31. \_\_\_\_\_, \_\_\_\_\_, and \_\_\_\_\_ J. Am. Chem. Soc. 74, 2781 (1952)
32. \_\_\_\_\_ and Yaffe, I. S., J. Am. Chem. Soc. 74, 4751 (1952)
33. \_\_\_\_\_ and Dye, J. L., J. Am. Chem. Soc. 76, 879 (1954)
34. \_\_\_\_\_ and Jaffe, S., J. Am. Chem. Soc. 76, 882 (1954)
35. \_\_\_\_\_ and \_\_\_\_\_ J. Am. Chem. Soc. 76, 884 (1954)
36. Ayers, B. O., "Apparent and Partial Molal Volumes of Some Rare-Earth Salts in Aqueous Solutions", Unpublished Ph.D. Thesis, Iowa State College Library, Ames, Iowa (1954)
37. Atkinson, G., "Compressibilities of Some Rare-Earth Nitrates and Chlorides in Aqueous Solution", Unpublished Ph.D. Thesis, Iowa State College Library, Ames, Iowa (1956)
38. Spedding, F. H., and Miller, C. F., J. Am. Chem. Soc. 74, 3158 (1952)
39. \_\_\_\_\_ and \_\_\_\_\_ J. Am. Chem. Soc. 74, 4195 (1952)
40. \_\_\_\_\_ and Flynn, J. P., J. Am. Chem. Soc. 76, 1474 (1954)

Table VI. Conductances of ytterbium nitrate

Normality	Specific conductance	Equivalent conductance	Calculated $\Lambda'_0$
0.21563	0.018306	84.89	
0.10777	0.0099156	92.01	
0.075400	0.0072105	95.63	
0.053882	0.0053327	98.97	
0.032333	0.0033574	103.84	
0.021551	0.0023220	107.75	
0.010775	0.0012271	113.88	
0.0086166	0.00099780	115.80	
0.0053851	0.00064270	119.35	139.68
0.0032315	0.00039666	122.75	138.42
0.0021539	0.00026954	125.14	137.91
0.0010769	0.00013823	128.36	137.37
0.00086116	0.00011123	129.16	137.21
0.00053820	0.000070294	130.61	136.97
0.00032296	0.000042540	131.72	136.64
0.00021526	0.000028555	132.65	136.67
0.0		136.6	

Values of  $\lambda_{R.E.}^{\circ}$  from the nitrate data are given in Table VII along with results obtained by other investigators for other salts of the same cations.

The equivalent conductances for  $\text{Sm}(\text{NO}_3)_3$  and  $\text{Ho}(\text{NO}_3)_3$  have been plotted versus the square root of the normality in Figure 1 so that the two curves may be compared. In Figure 2 are the conductance curves for  $\text{Er}(\text{NO}_3)_3$  and  $\text{Yb}(\text{NO}_3)_3$ . The curves in Figure 2 are practically identical to the one for  $\text{Ho}(\text{NO}_3)_3$  with regard to curvature and position relative to the axes. Figure 3 shows the curves for  $\Lambda'_0$  versus the square root of the normality, which were extrapolated to the ordinate to find  $\Lambda_0$ .



Table VII. Ionic equivalent conductances at infinite dilution of rare-earth cations

Salt	$\lambda_{\text{R.E.}^{+++}}^{\circ}$	Investigator
$\text{Sm}(\text{NO}_3)_3$	68.64	this research
$\text{SmCl}_3$	68.56	Wright (29)
$\text{Sm}(\text{ClO}_4)_3$	68.5	Jaffe (35)
$\text{Sm}_2(\text{SO}_4)_3$	68.6	Jaffe (34)
$\text{Ho}(\text{NO}_3)_3$	66.5	this research
$\text{HoCl}_3$	66.3	Dye (33)
$\text{Ho}(\text{ClO}_4)_3$	66.5	Jaffe (35)
$\text{Ho}(\text{SO}_4)_3$	66.5	Jaffe (34)
$\text{Yb}(\text{NO}_3)_3$	65.2	this research
$\text{YbCl}_3$	65.2	Wright (29)
$\text{YbCl}_3$	65.7	Dye (33)
$\text{YbBr}_3$	65.1	Atkinson
$\text{Yb}(\text{ClO}_4)_3$	66.1	Jaffe (35)
$\text{Yb}_2(\text{SO}_4)_3$	65.5	Jaffe (34)
$\text{Er}(\text{NO}_3)_3$	65.6	this research
$\text{ErCl}_3$	66.0	Dye (33)
$\text{ErBr}_3$	65.9	Jaffe (32)
$\text{Er}(\text{ClO}_4)_3$	66.2	Jaffe (35)
$\text{Er}_2(\text{SO}_4)_3$	66.0	Jaffe (34)

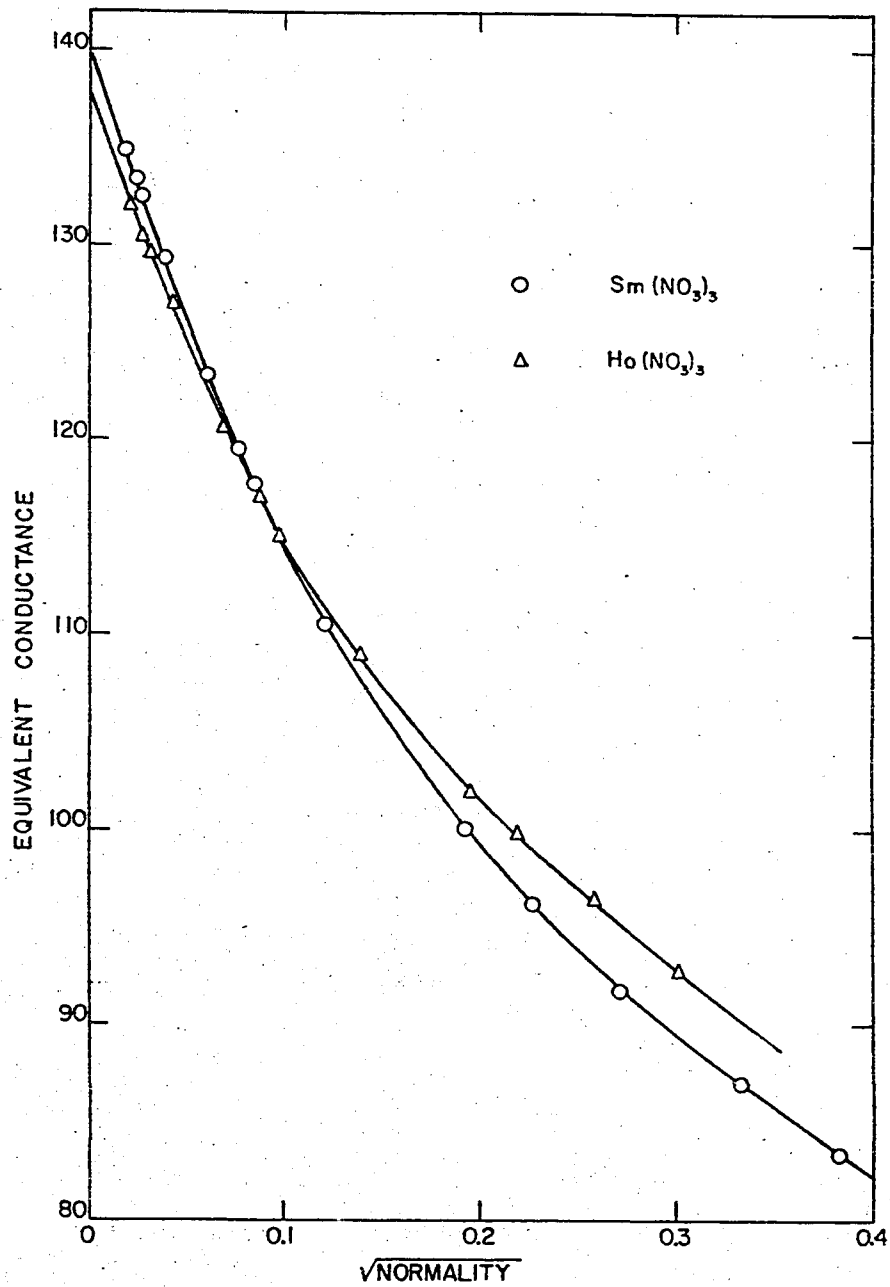


Figure 1. Equivalent conductances of samarium and holmium nitrates at 25.00°C.

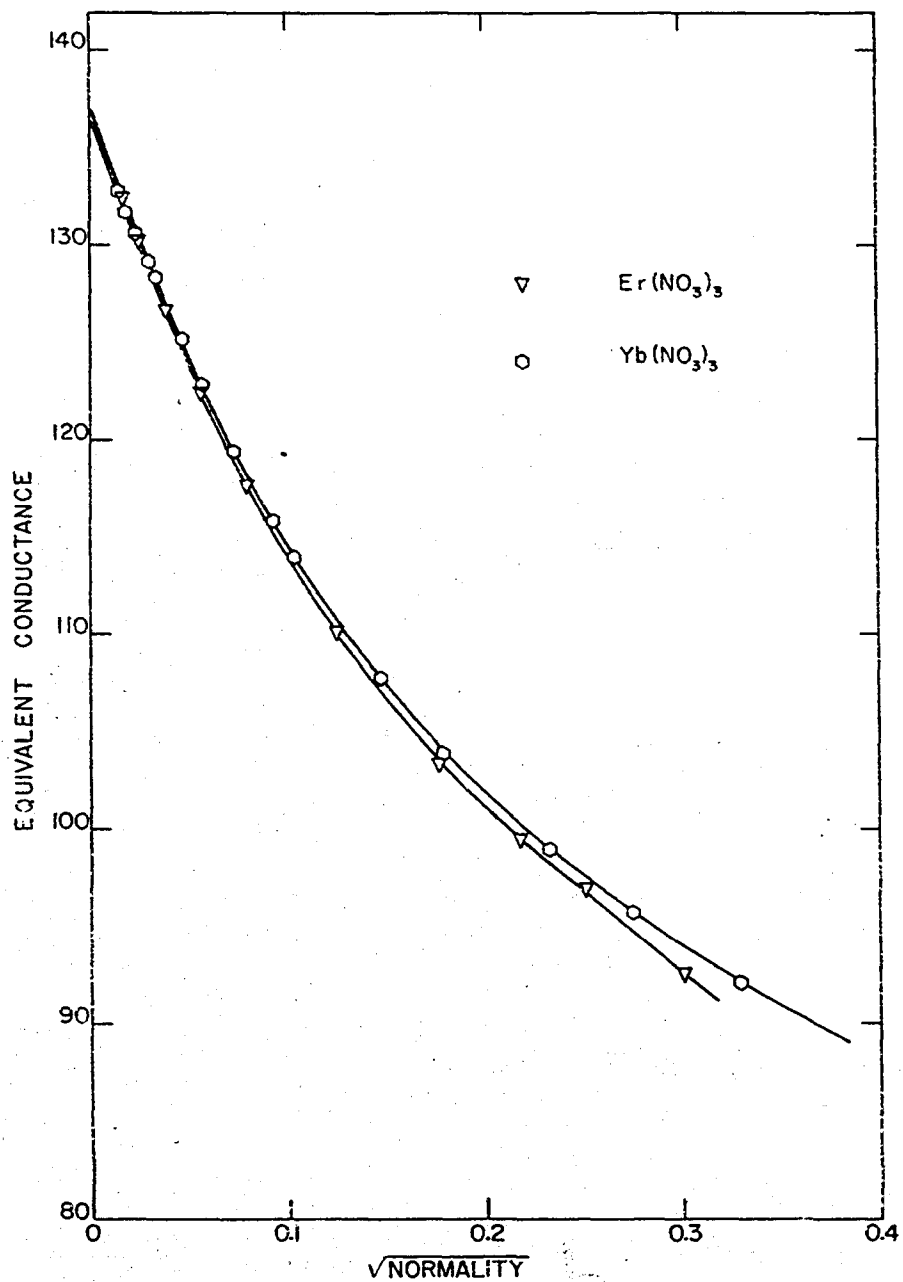


Figure 2. Equivalent conductances of erbium and ytterbium nitrates at 25.00°C.

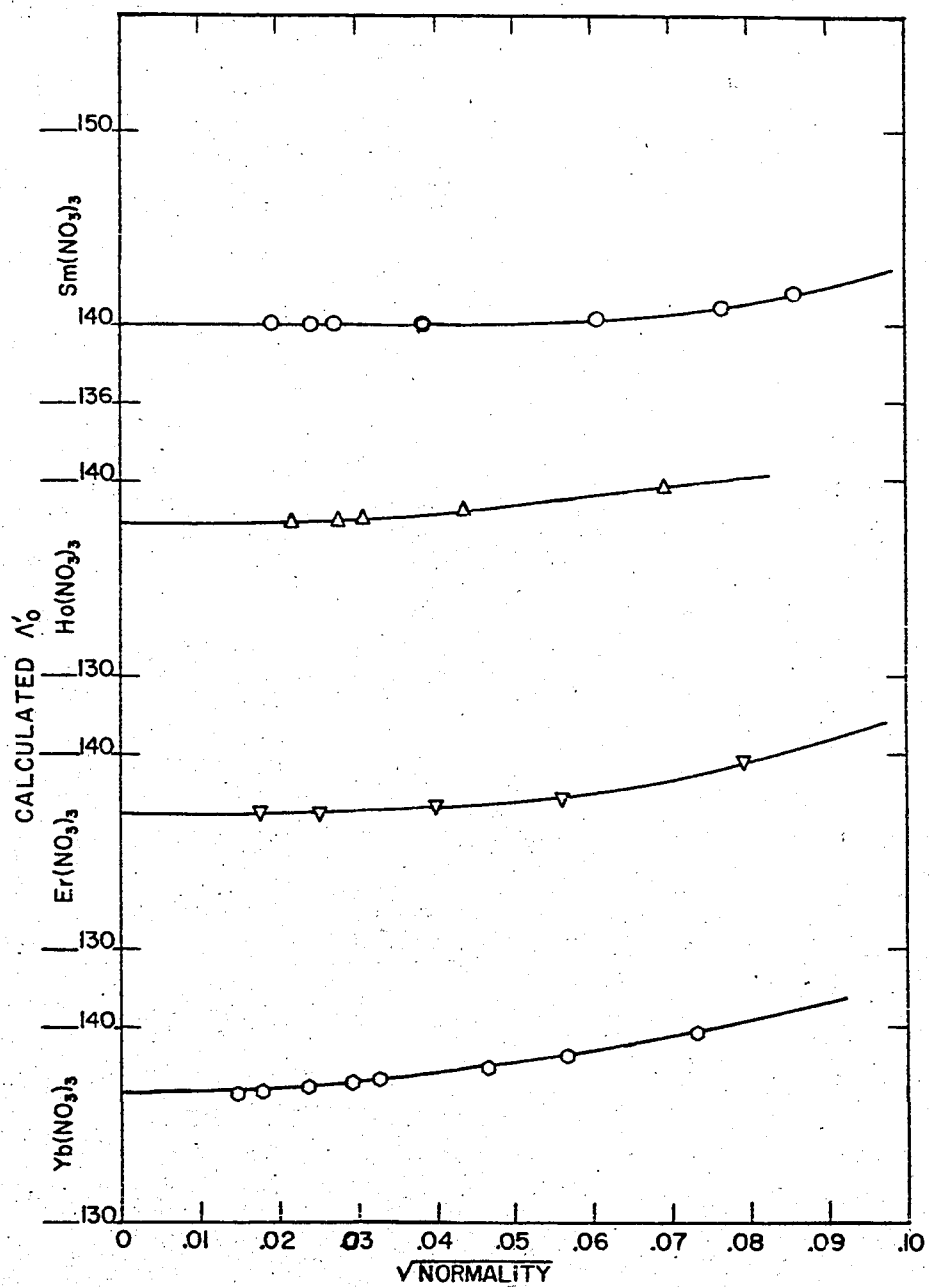


Figure 3. Extrapolation of equivalent conductances.

Discussion of the conductance data will be reserved for the final section of the thesis after results of the transference numbers and activity coefficients measurements have been presented.

## IV. TRANSFERENCE NUMBERS

In the phenomenon of conductance, the migrating ions in the solution are responsible for transferring electrical charge from one electrode to the other. Because each kind of ion has its own characteristic mobility, no two species will ordinarily carry the same fraction of the total charge passed through the solution. Consequently each ionic species "i" will have a particular Transference Number  $T_i$  (at a given temperature and concentration) defined as the fraction of the total charge passed that is transported by the ions of kind "i". Thus if  $q_i$  is the charge carried by ions "i", and  $\bar{\mu}_i$  is their mobility, then

$$T_i = \frac{q_i}{Q} = \frac{c_i z_i \bar{\mu}_i}{\sum_j c_j z_j \bar{\mu}_j}$$

where  $c_i$  is the molar concentration,  $z_i$  the valence or multiples of electronic charge on the ion, and  $Q$  is the total charge passed through the solution.

Since the transference number is a function of the mobility of ions, it is alternatively a function of the conductances. Although the Onsager theory for conductances may therefore be readily extended to transference numbers, the concentration range of applicability of the theory is below that of most of the experimental data. Where it does apply, the simple Onsager theory seems to predict the limiting slopes of experimental  $T_i$  vs.  $C_n$  curves for uni-univalent electrolytes. The Dye extension, however, with dependence on the  $\bar{a}^0$  parameter, is needed to bring the theory

into a concentration range permitting application to ions of higher charge type.

The original method for measuring transference numbers was developed by Hittorf (78) in 1853. The investigator uses an electrolytic cell with electrodes in individual compartments. The cell is so designed that, after a period of electrolysis, the solutions in each of the electrode compartments may be removed and analyzed. With allowance for chemical changes at the electrodes, the transference number of a cation follows from its definition as the ratio of the change in equivalents of electrolyte in the anode compartment to the total equivalents of charge passed. The total electrical charge may be measured with a coulometer in the cell circuit. Although simple in principle, the method is difficult in application. The current used must be small enough to avoid heating in the cell and consequent mixing of solutions between different compartments by convection. Too long a time must not be used, to avoid diffusion between different regions of solution. On the other hand sufficient charge must be passed to give a significant change in the solution concentrations in the electrode compartments.

A second experimental method uses the measurement of the electromotive forces of concentration cells with and without transference. Estimation of the transference number is made from the relation

$$T_i = \frac{dE_t/d \log a}{dE/d \log a}$$

in which  $E_t$  is the emf of a cell with transference, and  $E$  that of the cell without. Since  $T_i$  depends on the activity,  $a$ , of the electrolyte in

solution, the activity coefficients must be known. The calculations involve determination of the slopes of the  $E$  vs.  $\log(a)$  curves, so the method is not particularly accurate or precise.

The most successful experimental procedure for studying transference numbers has been the observation of a moving boundary between solutions of different electrolytes. The moving boundary cell consists of anode and cathode compartments connected in some manner by a vertical graduated tube of known volume calibration. Some provision is made for establishing a boundary between the solution of one electrolyte placed in the cathode compartment, and the second solution of different electrolyte in the anode side of the cell. The boundary is formed in or near the measuring tube, so that as electrolysis proceeds, the boundary progresses along the tube by virtue of the migrating ions. From measurements of the time required for the boundary to sweep out a known volume while a known constant current is passing through the cell, the transference number of the ions on a given side of the boundary may be calculated. This method, which was used in the present research, will be discussed further in the sections that follow.

## A. Theory

### 1. The Onsager Theory Applied to Transference Numbers

From the definition of  $T_i$  given on page 66, the cation transference number for an electrolyte dissociating into but two kinds of ions is

$$T_+ = \frac{c_+ z_+ \bar{\mu}_+}{c_+ z_+ \bar{\mu}_+ + c_- z_- \bar{\mu}_-}$$



Since  $c_+z_+ = c_-z_-$ , the transference number may be expressed in terms of the mobilities alone:

$$T_+ = \frac{\vec{\mu}_+}{\vec{\mu}_+ + \vec{\mu}_-} .$$

The definition of the ionic equivalent conductance from page 28 allows the transference number to be expressed in terms of conductances:

$$T_+ = \frac{\lambda_+ / \mathcal{F}}{\lambda_+ / \mathcal{F} + \lambda_- / \mathcal{F}} = \frac{\lambda_+}{\lambda_+ + \lambda_-} = \frac{\lambda_+}{\Lambda} .$$

Also

$$T_+^0 = \frac{\lambda_+^0}{\Lambda_0} \quad \text{at infinite dilution.}$$

Now the Onsager limiting law for the ionic equivalent conductance is, from page 29,

$$\lambda_+ = \lambda_+^0 - \lambda_+^0 \left[ \frac{2 |\epsilon|^3 \sqrt{2\pi N}}{3\sqrt{1000} (DkT)^{3/2}} \frac{q}{1 + \sqrt{q}} |z_+ z_-| \sqrt{S} \right] - \frac{\mathcal{F} |\epsilon|^2 \sqrt{2N} z_+}{899.4 \eta \sqrt{1000 \pi DkT}} \sqrt{S} ,$$

where  $S$  is the ionic strength.

For convenience, let

$$\frac{2 |\epsilon|^3 \sqrt{2\pi N}}{3\sqrt{1000} (DkT)^{3/2}} \frac{q}{1 + \sqrt{q}} |z_+ z_-| = A ,$$

and

$$\frac{\mathcal{F} |\epsilon|^2 \sqrt{2N}}{899.4 \eta \sqrt{1000 \pi D k T}} = \frac{B}{z_+ + z_-}$$

Then

$$\lambda_+ = \lambda_+^0 - A \lambda_+^0 \sqrt{S} - \frac{B z_+}{z_+ + z_-} \sqrt{S}$$

and

$$\lambda_- = \lambda_-^0 - A \lambda_-^0 \sqrt{S} - \frac{B z_-}{z_+ + z_-} \sqrt{S}$$

The calculated equivalent conductance from the Onsager law is now

$$\Lambda' = \Lambda_0 - \Lambda_0 A \sqrt{S} - B \frac{z_+ + z_-}{z_+ + z_-} \sqrt{S}$$

whence the theoretical transference number becomes

$$T_+ = \frac{\lambda_+}{\Lambda'} = \frac{\lambda_+^0 - \lambda_+^0 A \sqrt{S} - \frac{B z_+}{z_+ + z_-} \sqrt{S}}{\Lambda_0 - \Lambda_0 A \sqrt{S} - B \sqrt{S}}$$

Now observe that

$$\lambda_+ = \frac{\lambda_+^0}{\Lambda_0} (\Lambda_0 - \Lambda_0 A \sqrt{S} - B \sqrt{S}) + \left[ \frac{\lambda_+^0 (z_+ + z_-) - z_+}{z_+ + z_-} \right] B \sqrt{S}$$

Therefore

$$T_+ = \frac{\lambda_+}{\Lambda'} = \frac{\lambda_+^0}{\Lambda_0} + \left[ \frac{\lambda_+^0 (z_+ + z_-) - z_+}{z_+ + z_-} \right] \frac{B \sqrt{S}}{\Lambda'}$$

or

$$T_+ = T_+^0 + \left[ \frac{T_+^0 (z_+ + z_-) - z_+}{\Lambda_0 (z_+ + z_-)} \right] \left( \frac{\Lambda_0}{\Lambda'} \right) B \sqrt{S} .$$

which is the Onsager limiting law for transference numbers. Note that there is no dependence on the constant "A" in this equation. The constant "B" arises from the electrophoretic effect in the conductance theory, and is more accurately evaluated by using the graphical integrations of the Dye extension. ✓

## 2. Theory of the Moving Boundary Method

In the moving boundary method a plane boundary between two solutions of different electrolytes is forced to move through the volume of a calibrated measuring tube by the application of a constant steady electric field. Suppose a solution of electrolyte MA were placed in one compartment of a moving boundary cell so that its surface lies somewhere in the measuring tube. Then let a solution of another electrolyte RX be carefully placed or laid on top of the first solution so that a boundary is formed, and the second solution fills the remainder of the cell. The experimental means for accomplishing this is of no interest now, but will be discussed later. Also, the solutions used must fulfill certain conditions for the boundary to be stable during electrolysis. These conditions will be discussed in the next section which reviews the historical development of the experimental method.

When the cell is connected into a circuit of constant direct current, two boundaries, in principle, emerge from the original one, and move in

opposite directions along the tube. On either side of the cation boundary, moving toward the cathode, are the ions  $M^+$  and  $R^+$ . On either side of the anion boundary, moving toward the anode, are the ions  $A^-$  and  $X^-$ . In the region between the boundaries as they move apart is a solution of the hybrid electrolyte,  $RA$ . In practice, only one boundary, often the cation one, is observed, and the volume it sweeps out is experimentally measured.

Now the cation transference number is that fraction of the current carried by the cation. Therefore the number of faradays of charge carried by the cation past a reference plane in the measuring tube when one faraday is exchanged between electrodes is the transference number of the cation. The number of faradays carried by the cation is the number of equivalents of the cation that pass the reference plane. Let  $v$  be the volume in milliliters swept out by the boundary during time  $t$  when current of  $I$  amperes is passing, and let  $C_n$  be the concentration of the cation in equivalents per liter. Then

$$T_+ = \frac{\text{number of faradays carried by cation}}{\text{number of faradays passed through cell}}$$

$$T_+ = \frac{\text{number of equivalents of cation passing reference plane}}{\frac{I t}{F}}$$

$$T_+ = \frac{v C_n F}{1000 I t} .$$

In general practice one electrode compartment of the moving boundary cell is completely filled with solution and closed to the atmosphere so that no bubbles of air remain in the cell. The other side of the cell is

arranged to be left open to the atmosphere so that the system may be at constant pressure. Under these circumstances the measured volume will be masked by volume changes due to reaction at the closed electrode and transfer of matter in the tube. Thus the experimental volume  $V_{\text{exp}}$  includes the true  $v$  for the transference number, plus a  $\Delta V$  of reaction and material transfer:

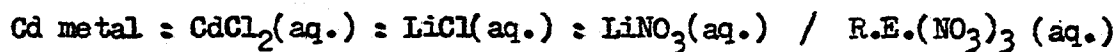
$$V_{\text{exp}} = v + \Delta V$$

Therefore the transference number corrected for the volume effect is

$$T_{+} = \frac{(V_{\text{exp}} - \Delta V) C_n F}{1000 I t} = T_{+}(\text{observed}) - \frac{\Delta V C_n}{1000}$$

where  $\Delta V$  must be calculated on the basis of one faraday passed through the cell.

In this research, boundaries between solutions of the rare-earth nitrates and of lithium chloride were observed in cells employing a closed cadmium electrode. As electrolysis proceeded, cadmium from the metal anode would be oxidized to form  $\text{Cd}^{++}$  ions in the region near the electrode. Also as the cation boundary moved toward the cathode, the region through which the boundary passed would effectively become a solution of  $\text{LiNO}_3$ . Thus the sequence of chemical regions on the closed side of the cell was as follows:



where / denotes the position of the boundary. The  $\Delta V$  of reaction and material transfer for the passage of one faraday through the cell is

calculated as follows, where the  $\bar{V}$ 's are partial molal volumes:

1. Loss of one-half mole of Cd metal:  $\Delta V_1 = -\frac{\bar{V}_{Cd}}{2}$
2. Gain of one-half mole of  $Cd^{++}$  ions in  $CdCl_2$ :  $\Delta V_2 = +\frac{\bar{V}_{Cd^{++}}(CdCl_2)}{2}$
3. Gain of one mole of  $Cl^-$  ions from  $LiCl$  to  $CdCl_2$ :  $\Delta V_3 = +\bar{V}_{Cl^-}(CdCl_2)$
4. Loss of one mole of  $Cl^-$  ions to  $CdCl_2$  from  $LiCl$ :  $\Delta V_4 = -\bar{V}_{Cl^-}(LiCl)$
5. Gain of one mole of  $NO_3^-$  ions into the Li region to replace lost  $Cl^-$  ions:  $\Delta V_5 = +\bar{V}_{NO_3^-}(LiNO_3)$

This mole comes from  $T_-$  moles by migration towards the positive electrode, and from  $T_+$  moles due to the downward motion of the boundary.

6. Loss of  $T_-$  moles of  $NO_3^-$  ions from  $R.E.(NO_3)_3$  to  $LiNO_3$  due to downward motion of the boundary:  $\Delta V_6 = -T_- \bar{V}_{NO_3^-}(R.E.(NO_3)_3)$
7. Loss of  $T_+/3$  moles of  $R.E.+++$  by migration toward the cathode:  $\Delta V_7 = -\frac{T_+}{3} \bar{V}_{R.E.+++}(R.E.(NO_3)_3)$

Consequently the total  $\Delta V$  is

$$\Delta V = \sum_i \Delta V_i = -\frac{\bar{V}_{Cd}}{2} + \frac{\bar{V}_{CdCl_2}}{2} - \bar{V}_{Cl^-}(LiCl) + \bar{V}_{NO_3^-}(LiNO_3) - \frac{T_-}{3} \bar{V}_{R.E.(NO_3)_3}$$

Providing  $\bar{V}_{\text{Li}^+(\text{LiCl})} = \bar{V}_{\text{Li}^+(\text{LiNO}_3)}$ , the ionic partial molal volumes in the above relation may be evaluated by writing

$$\bar{V}_{\text{NO}_3^-(\text{LiNO}_3)} - \bar{V}_{\text{Cl}^-(\text{LiCl})} = \bar{V}_{\text{LiNO}_3} - \bar{V}_{\text{LiCl}}$$

The method of evaluating the partial molal volumes, so that  $\Delta V$  may be calculated, will be outlined in the experimental section.

It was pointed out by Longworth (79) that a correction to the experimental transference number should be made for the conductance of the solvent, since conducting impurities in the solvent may carry a small, but not negligible, fraction of the total current. The correction formula derived by Longworth is a function of the specific conductances,  $L$ , of the solvent and of the solution being studied:

$$T_+ = T_+(\text{observed}) + T_+ \left[ \frac{L_{\text{solvent}}}{L_{\text{solution}}} \right]$$

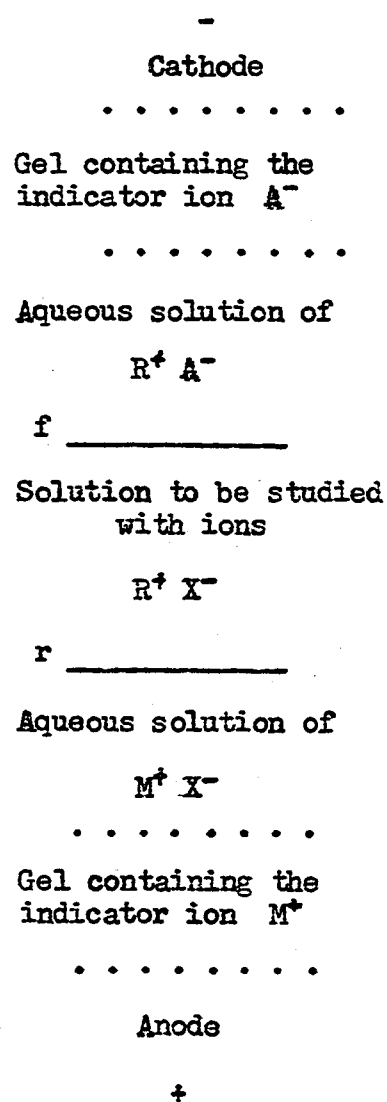
In summary, we write the total equation to correct the observed transference number for the volume and solvent-conductance effects:

$$T_+(\text{true}) = T_+(\text{observed}) - \frac{\Delta V C_n}{1000} + T_+(\text{observed}) \left[ \frac{L_{\text{solvent}}}{L_{\text{solution}}} \right].$$

B. Historical Review of the Moving Boundary Method

The moving boundary method was originated in 1886 by Lodge (80) who attempted a study of absolute ionic velocities using a gelatin gel medium through which the ions migrated. The gel was saturated with suitable colored indicators to show the progress of the ions. In the following years various experimenters worked on moving boundary techniques for measuring ionic velocities in aqueous solutions instead of in a semi-solid gel. One of the successful procedures was that of B. D. Steele (81) developed in 1901. His method consisted in the imprisonment of the aqueous solution to be measured between two partitions of gelatin containing certain "indicator" ions in solution. The indicator ions were chosen to have specifically slower velocity than the ions to be measured, and to form solutions of refractive index different from that of the solution to be measured. As electrolysis proceeded, Steele's cell would have had the sequence of regions as in the arrangement shown at the right of the page. Boundary "f" is a falling boundary which has emerged from the surface of the gel containing  $A^-$ .

Boundary "r" is a rising boundary which has emerged from the surface of the





gel containing  $M^+$ . By virtue of the difference in refractive index between the leading and following solutions, the interfaces were observed with the aid of a telescope cathetometer. By measuring both the distances covered by the anion and cation boundary through the tube of uniform cross section, the relative velocities and the transference numbers of the ions could be calculated. Steele found that there was a definite range of potential gradient to be used which produced a sharp boundary without the production of too great a current density and consequent heating effect.

Steele's use of a gel in his cell was the first method for forming a boundary between the indicator solution and the solution under study. (The later is generally called the "leading solution" since it usually occupies the region into which the boundary passes.) Attention will now be focused on succeeding methods for forming the boundary as they developed historically. The simplest means was to allow the dissolving ions from a metal anode form the indicator solution as electrolysis proceeded. The boundary emerging from the surface of the electrode and progressing toward the cathode is termed an "autogenic" boundary. This procedure was employed by Franklin and Cady (82) in 1904 who used a mercury anode to form a mercuric salt solution as the indicator. The high density of the mercuric salt indicator minimized any diffusion of  $Hg^{++}$  ions ahead of the rising boundary, so that a fairly sharp boundary could be maintained.

The indicator and leading solutions were separated in the cells of Denison and Steele (83) by a membrane diaphragm. The membrane, stretched over the end of a movable tube, was placed on the shoulder at the entrance to the calibrated measuring tube in the cell while the cell was being filled. When the current was turned on, leakage around the membrane was

sufficient to allow the boundary to form. After the boundary was well established, the diaphragm was removed, and the boundary followed by making conductivity measurements of the solutions in the cell during electrolysis. MacInnes and Smith (84) in 1923 formed their boundary with a variation of the 1906 Denison and Steele membrane diaphragm. Instead of a membrane plunger, a ground glass disk at the end of a movable rod was seated at the entrance to the measuring tube in the cell. After electrolysis was started, it could be pulled away to allow the indicator solution above the disk to join the leading solution below it.

A boundary formed by action of a shearing disk was introduced by MacInnes and Brighton (85) in 1925. In their apparatus, a drop of indicator solution hung from the open end of a filled electrode tube which was fitted into an upper disk. The graduated measuring tube, fitted into the lower disk, was filled with a slight excess of the leading solution so that a drop protruded. When the disks were slid together so as to join the tubes, the excess amounts of both solutions were sheared away and a sharp boundary between the solution in the two tubes was made. Their arrangement had double hole disks so that two boundaries could be made to follow the anion and cation migrations simultaneously. MacInnes and Brighton at first had difficulty with current leaks through the grease between the disks, which gave  $T_+$  values too low. A redesign of the disks to provide air spaces for insulation between the tubes circumvented the difficulty. In the 15 years following MacInnes and Brighton's work, most investigators used the shearing disk to form boundaries between indicator and leading solutions for experiments in which the boundary progressed down the tube, i.e., falling boundaries. For rising boundaries, generally

the autogenic method was used to generate the indicator solution as electrolysis progressed.

In 1940 Allgood, LeRoy, and Gordon (86) introduced a modified sheared boundary in which a four-way stop-cock was employed. By simply turning a glass stop-cock in the apparatus, two tubes containing the appropriate solutions could easily be connected. Later in 1952 Spedding, Porter, and Wright (30) used an even simpler hollow bore stop-cock with a single hole in the barrel. A quarter turn of the stop-cock served to lay the indicator solution in the barrel onto the leading solution in the measuring tube below with a sharp boundary between solutions.

In order to calculate the transference number from the time required for the boundary to sweep out a certain volume, the current through the cell must be kept constant, and the current or total charge must be measured. MacInnes and Smith (84) hand regulated their current by periodically checking the potential drop across a standard resistor. They actually determined their current from knowledge of the specific conductance  $L$  of the solution used, the area  $A$  of the tube, and the potential gradient  $E$  through the cell:

$$I = ELA \text{ volt/cm ohm}^{-1}\text{cm}^{-1} \text{ cm}^2 = \text{amperes}$$

Hand regulated current was used by all investigators until 1929 when Longworth and MacInnes (87) invented a mechanical constant current regulator for moving boundary experiments. Their arrangement included an optical system acting on a galvanometer-potentiometer system which measured the potential drop across a standard resistor. The optical system activated a photocell which by action of relays caused a motor to adjust a variable

resistance coil. A change in this resistance coil altered the current in the cell supply. The direction of adjustment was reversible. LeRoy and Gordon (88) in 1938 introduced a crude electronic constant current regulator into their apparatus. They measured the total charge passed with a microcoulometer. Bender and Lewis (89) in 1947 described an improved electronic current controller. Their controller kept the current within 0.8% of the initial value as the resistance of the moving boundary cell increased from 5300 ohms to 50,000 ohms during an experiment.

Before passing to a discussion of the properties of the boundary, we will review a couple other facets of experimental technique. Since the time of Steele's use of refractive index difference to observe boundaries, the use of suitable lighting arrangements and the telescope cathetometer to observe the boundary has been standard procedure. A few investigators followed Denison and Steele's (83) example and fitted their cells with electrode probes so that the boundary could be followed by conductance measurements. When only one boundary is observed, the time of its travel must be measured, for which a stopwatch has usually been employed. However MacInnes, Cowperthwaite, and Huang (90) replaced the stopwatch with a Veeder magnetic counter. These authors also pointed out that a measuring tube of very small diameter should be used so that the ratio of external surface to tube diameter is small to conduct away heat generated by the passing current. E. R. Smith (91) experimented with a novel type cell in which volume calibration of the measuring tube was not necessary. His cell was arranged so that a sample of mercury could be withdrawn which volume equaled that swept out by the boundary. By weighing the mercury, and finding the total charge passed with a silver coulometer, Smith calcu-

lated his transference numbers. The ingenious design of the cell allowed the whole body of solution in the cell to be moved as the mercury was withdrawn, so that the boundary could be returned to the starting point for a rerun of the experiment.

Properties of the boundary and of the indicator solution will now be considered. Since the boundary is common to both the indicator and leading solutions, the equation for the cation transference number derived on page 72 must hold for both cations on either side of the boundary:

$$T_1 = \frac{vC_1 F}{1000 I t} \quad \text{and} \quad T_2 = \frac{vC_2 F}{1000 I t}$$

or

$$\frac{T_1}{C_1} = \frac{T_2}{C_2}$$

where the subscript "1" applies to the leading solution, and the subscript "2" applies to the indicator or following solution. The above ratio was originally derived by Kohlrausch (92) in 1897. The Kohlrausch ratio describes the conditions for a stable boundary with constant velocity. Although Kohlrausch assumed that automatic concentration adjustment took place in any moving boundary system, later work has shown that the concentrations used in the cell must be within 3 - 5 percent of the proper values if the Kohlrausch ratio is to represent the correct transference number values.

Since the leading solution initially occupies the region into which the boundary moves, it has the power to regulate the concentration of the

indicator solution which replaces it. This accounts for the fact that a moving boundary gives information directly for only the leading solution.

In 1923 MacInnes and Smith (84) set out to determine whether the boundary moves at the theoretical velocity if the Kohlrausch condition is fulfilled at the boundary, and whether any automatic concentration actually does take place. They studied the apparent cation transference number in 0.1 Normal KCl with varying concentration of LiCl indicator solution, and with varying potential gradient  $E$  through the cell. When the observed  $T_{K^+}$  was plotted vs. the concentration of LiCl used for a number of different experiments, they found  $T_{K^+}$  to increase with increasing  $C_{LiCl}$ , with a plateau region in the curve. The shape of the curve was thus much like that of a cubic equation with a horizontal plateau at the place of a single inflection point. The center of the plateau was always found around  $T_{K^+}(0.1 N) = 0.492$ ,  $C_{LiCl} = 0.065$  Normal regardless of the potential gradient used through the cell. The width of the plateau giving constant values of  $T_{K^+}$  was about 5% of the LiCl concentration. MacInnes and Smith concluded that automatic concentration adjustment to satisfy the Kohlrausch ratio apparently takes place in the plateau range. Smith and MacInnes (93) found similar Kohlrausch plateau curves in 1924, and in 1925 they (94) verified the Kohlrausch ratio to be valid in typical 5% ranges of the indicator concentration for leading solutions of HCl and NaCl.

In 1929 MacInnes and Cowpertwaite (95) began a study of the effects tending to sharpen the boundary between two solutions of electrolytes, and of effects causing diffusion of the boundary. During experiments to see whether the movement of the boundary is affected by diffusion of one electrolyte into the solution of the other, the current was stopped so

that the motion of the boundary was halted. Gradually the boundary became more diffuse, until the current was restored. Thereupon the boundary slowly reformed as the experiment was continued. MacInnes and Cowperthwaite found that the boundary region, either diffuse or sharp, moved down the measuring tube at a constant velocity when the current was on, regardless of its previous history. Consequently observed values of  $T_+$  were not affected by the interruption of the current. The authors explain the mechanism of restoration of the boundary between a leading solution of  $\text{AgNO}_3$  and a following solution of  $\text{LiNO}_3$  in the following way: "Due to the passage of current there is a drop of potential in both solutions. The potential gradient in the leading solution is, however, lower than in the following solution which contains ions of lower mobility and is also more dilute. If, under these conditions, the relatively fast  $\text{Ag}^+$  ions diffuse back into the  $\text{LiNO}_3$  solution they encounter a high potential gradient and are rapidly sent forward to the boundary. On the other hand, if  $\text{Li}^+$  ions diffuse into the  $\text{AgNO}_3$  region they move slower than the  $\text{Ag}^+$  ions and will be finally overtaken by the moving boundary."

The difference in potential gradient between regions of leading and following solutions leads to a side-effect which makes rising boundaries less useful than falling ones. MacInnes, Cowperthwaite, and Huang (90) in 1927 studied rising boundaries with 0.1 N  $\text{KCl}$  as the leading solution and more dense 0.07 N  $\text{KMnO}_4$  as the indicating following solution below the boundary. Considerable diffusion of the boundary was observed, with the following explanation. Since the indicator solution contains ions which have lower mobility than the ions of corresponding charge in the leading solution, and since the indicator solution is more dilute, the

conductance of the  $\text{KMnO}_4$  must be lower than that of the leading solution. The result is therefore that due to the higher potential gradient, more heat is generated in the indicator solution than in the  $\text{KCl}$  above the boundary. The warmer  $\text{KMnO}_4$  would then mix with the solution above it by convection. This same effect would serve to prevent diffusion in the case of falling boundaries where the following-solution region of higher potential gradient is on top.

Cady and Longworth (96) in 1929 used an ascending autogenic boundary to measure the  $T_+$  in  $\text{KNO}_3$ . During electrolysis a silver anode oxidized to form  $\text{Ag}^+$  ions which served as the indicator for the autogenic boundary. However, they too had difficulty with heat convection currents distorting the rising boundary.

Longworth (97) by 1930, however, had a kinder word for the usefulness of rising boundaries. By replacing the  $\text{KMnO}_4$  indicator in MacInnes, Cowperthwaite, and Huang's experiments with more dense solutions of  $\text{KIO}_3$ , sharper boundaries were experienced. Longworth found a wider range of automatic concentration adjustment of the indicator solution when ascending boundaries were used, particularly if the initial concentration of indicator was larger than that required by the Kohlrausch ratio. In this case, the correct concentration of indicator, being lighter, stayed on top of the more dense initial concentration in a rising boundary system. On the other hand for falling boundaries, the same advantage could be gained by using an indicator concentration less than that demanded by the Kohlrausch ratio.

All these disturbing and restoring effects at the boundary have been summarized by Longworth (79) and by MacInnes and Longworth (98) in a review paper. The effects of diffusion and of heat convection tend to



disturb the boundary, particularly if the indicator solution is on the bottom. The abrupt change of potential gradient at the boundary, and an advantageous difference in density of solutions tend to keep the boundary sharp. MacInnes and Longworth (98) also summarized the properties an indicator solution must have for a successful moving boundary system:

1. For falling boundaries the indicator solution should be less dense than the leading solution, and vice-versa for ascending boundaries.
2. The mobility of the indicator ion constituent must be lower than that of the leading ion. Useful indicator ions are  $\text{Li}^+$  for descending boundaries, and  $\text{Cd}^{++}$  for ascending ones.
3. The indicator solution must "indicate" the boundary, i.e., its color or refractive index must be different from that of the leading solution.
4. The indicator solution must not react chemically with the solution with which it is in contact.
5. The concentration of the indicator must be such that the Kohlrausch ratio will be fulfilled.

The theoretical and practical differences in transference numbers obtained by the Hittorf and moving boundary methods have been discussed by W. L. Miller (99) in 1909 and by G. N. Lewis (100) in 1910. They point out that the Hittorf transference number is a function of the velocities of the solute ions relative to the solvent particles. The moving boundary number, however, refers to ionic velocities relative to a plane stationary with regard to the walls of the measuring tube. The basic distinction lies, then, in the net displacement sustained by the solvent in the cell.

Moving boundary transference numbers may, therefore, be reduced to Hittorf numbers by making the volume correction discussed in section A on the theory of the moving boundary method:

$$T_{\text{Hittorf}} = T_{\text{moving boundary}} - \frac{\Delta V C_n}{1000}$$

where  $\Delta V$  is the net volume displacement of the solution as a whole from cathode to anode when one faraday passes.

MacInnes and Dole (101) in 1931 measured the transference numbers in solutions of KCl by both the Hittorf and moving boundary methods, and applied the volume correction to the latter. Their results showed excellent agreement between the two methods. The validity of the volume correction equation above was further demonstrated by two other methods. E. R. Smith (102) in 1932 used an apparatus in which one electrode chamber could be disconnected and used as a pycnometer. The experimental change in solution density after a transference experiment agreed with the calculated  $\Delta V$ . Finally, MacInnes and Longworth (98) measured  $T_{K^+}$ 's using first a Ag anode and then a Cd anode. The corrected transference numbers agreed within 0.1% when the corrections with the appropriate respective  $\Delta V$  equations were made.

### C. Experimental Investigation

#### 1. Apparatus and Procedure

The apparatus used to determine transference numbers included the moving boundary cell, the lighting system and telescope cathetometer for observing the boundary, an electronic current controller, a circuit to

measure the current through the cell, the constant temperature bath, and a holder for mounting and operating two stop watches.

The moving boundary system was contained in a U-shaped glass cell, 50 centimeters high, and 10 centimeters wide. The upper end of one side of the cell consisted of the anode compartment. This was fitted at the top with a standard taper ground glass joint into which the cadmium anode assembly could be inserted. Just below the standard taper joint there extended out from the cell a small bore overflow tube with a stop-cock. A glass electrode cup placed in the compartment would surround the cadmium anode and prevent mixing of the electrolysis products with the body of solutions in the remainder of the cell.

The cell was constructed so that solution in the anode compartment was led directly into the barrel of a large hollow bore stop-cock, the housing for which was sealed directly at the base of the anode compartment. At the open position of the stop-cock, the hole in the side of the barrel lead into a volume-calibrated measuring tube sealed immediately below the stop-cock housing. With following solution in the anode compartment, and leading solution in the measuring tube below, the opening of the stop-cock served to form the boundary between them.

The vertical measuring tube had marks etched on the outside surface at intervals along its length. The volumes between these marks were established by previous investigators who weighed samples of mercury delivered by the tube. At the lower end of the measuring tube was sealed a large bore tube which was bent in an arc to form the lower part of the U, and extended up to join the base of the cathode compartment on the other side of the cell. The cathode compartment was at the same level as the

anode compartment, and constructed similarly to it. The cathode compartment was fitted with a small-bore overflow tube, a removable electrode cup, and the standard taper ground glass joint at the top. The cell was mounted on a heavy brass stand.

The anode assembly consisted of a plug of C.P. cadmium into which a heavy copper wire had been frozen. This electrode was then affixed in a male standard taper ground glass joint with Pyseal wax so that the assembly was water-tight. The cathode was a cylinder of corrugated silver sheets, fashioned by the Klett Manufacturing Company for their electrophoresis equipment. By electrolyzing the silver cylinder in a 1 Normal hydrochloric acid solution, a silver-silver chloride electrode was obtained. The electrode was attached to the end of a small diameter hollow copper tube, which in turn was sealed in a male standard taper ground glass joint in similar fashion as the cadmium anode.

In order to take full advantage of the refractive index difference between solutions, the boundary to be observed should be illuminated from the side of the cell opposite the viewer, with the light source at the proper height with respect to the boundary. As the boundary progresses down the tube, the light source must be correspondingly lowered to keep the boundary in view. For this research an electric lamp was placed in a box with a slit in one side, and rigged like an elevator. A small electric motor, controlled by a double-pole toggle switch, moved the light source up and down. A telescope cathetometer was used to observe the boundary.

The electronic constant current controller was designed and constructed by A. A. Read and D. W. Hilker of the Electronic Shop in the Institute for Atomic Research. The unit consists of a high voltage

rectifier and filter section which is adjustable to provide up to 4000 volts output at 10 milliamperes, a regulated 400 volt power supply which provides power for the current regulator amplifier, and a series type current regulator. The controller provided current constant within 0.1% during a 45 minute experiment. A 100 ohm standard resistor, calibrated by the National Bureau of Standards, was placed in series with the cell and current regulator. The potential drop across this resistor was measured with a Rubicon Type B High Precision Potentiometer, so that the current through the cell could be calculated.

A large aquarium type constant temperature bath was used. It had glass sides so that objects were clearly visible through it when filled with distilled water. The temperature was maintained at 25.00°C., and held constant within 0.02° by the same type mercury-platinum thermo-regulator as was used on the bath for the conductance work.

Timing the movement of the boundary was made with two stop watches mounted side by side in a wooden frame. The frame had a hinged lid which rested on the crowns of the watches, so that by depressing the lid, one watch could be started while the other was stopped at the same instant. This afforded a method of making continuous individual time readings of the boundary's progress between marks on the measuring tube of the cell. The watches were checked on a Western Electric Time Rate Recorder, and found to be accurate within five seconds over a twenty-four hour period.

Sufficient quantities of the rare-earth nitrate solutions were prepared for both the conductance and transference number measurements. The method of preparation has already been described.

Solutions of lithium chloride were used as the indicator in the

moving boundary experiments, since they satisfy the requirements listed in the historical review section. The stock solution of LiCl was prepared by dissolving "Baker's Analyzed" lithium carbonate in slightly less than an equivalent amount of redistilled C. P. hydrochloric acid. Excess  $\text{Li}_2\text{CO}_3$  was filtered off, and the solution was boiled while a stream of nitrogen bubbled through it to remove carbon dioxide. The resulting pH of the solution was 6.6 . The stock solution was analyzed by using an infra-red lamp to evaporate aliquots to dryness with a slight excess of sulfuric acid. The samples were ignited at  $750^\circ\text{C}$ . and weighed as lithium sulfate. Solutions of desired concentrations were made from the stock LiCl solution by volume dilution with calibrated glassware.

The moving boundary cell was cleaned before use with hot  $\text{H}_2\text{SO}_4\text{-K}_2\text{Cr}_2\text{O}_7$  solution. It was then thoroughly rinsed and allowed to soak in conductivity water for several days. Just before use, the cell was given several additional rinses with conductivity water.

To prepare the cell for an experiment, the hollow bore stop-cock was taken from the cell and warmed gently in a gas flame, so that a very thin film of Dow-Corning silicone stop-cock grease could easily be applied. The housing for the stop-cock was carefully flamed out too, so that it might be dry and warm to assure an even coating of grease on the parts with an electrically tight seal when the stop-cock was twisted back into place. Then the entire cathode side of the cell, lower U-tube, calibrated measuring tube, the open stop-cock interior, cathode electrode cup, and the silver-silver chloride cathode were all rinsed three times with the rare-earth nitrate solution to be measured. The rinsed regions of the cell were then carefully filled with rare-earth nitrate solution so as to avoid

trapping bubbles anywhere, particularly in or near the open stop-cock. The filled stop-cock was then closed, the cathode electrode cup inserted, and the glass joint of the cathode assembly greased and twisted into place so that excess solution passed out the overflow tube. Even though the overflow stop-cock was then closed, the cathode side of the cell was still open to the atmosphere through the narrow bore copper tube leading up from the silver-silver chloride cylinder.

The excess rare-earth solution remaining in the lower part of the anode compartment from the previous operations was then poured out, and the compartment rinsed three times with conductivity water, and three times with lithium chloride solution of the concentration to be used. The anode electrode cup and the cadmium anode were rinsed with the lithium chloride solution at the same time. The anode compartment was then filled carefully to avoid bubbles, and the electrode cup inserted. Following these operations, the glass joint of the anode assembly was greased and twisted into place carefully to be sure that no bubbles remained in the compartment as excess solution passed out the overflow tube. The overflow stop-cock on this side of the cell was left open for expansion of the solution while the cell was coming to temperature equilibrium in the bath, but was closed before starting the current through the cell.

The outside of the cell was rinsed off in the sink with distilled water to remove spilled electrolytes, before it was placed in the constant temperature bath. In the bath the cell was carefully positioned so that the measuring tube was in proper alignment between the light source and the cathetometer. About half an hour was allowed for temperature equilibrium to take place. During this time the cell was tested for electrical

leaks through the bath water with a vacuum tube test meter. The positive lead from the current controller was connected to the cadmium anode, while the silver-silver chloride cathode was connected into the negative side of the circuit. After the anode overflow cock was closed, the hollow bore stop-cock was opened to form the boundary, and the current immediately turned on to start the electrolysis. The applied voltage was adjusted until the controller was operating properly to hold the current steady. The voltage was then increased about twenty-five percent to allow for the expected resistance increase through the cell as the experiment progressed. The final driving potential was generally around 1000 to 1200 volts, while the current through the cell was from 4 to 8 milliamperes depending on the concentrations of solutions used.

The boundary became visible in the measuring tube about 10 minutes after electrolysis was started. The progress of the boundary was observed by following it down the tube with the light source and the cathetometer. The hair line of the telescope was placed so that it appeared to be on the first mark on the calibrated tube, and the first stop-watch was started just as the leading edge of the boundary merged with the mark and the hair line. The lid of the watch holder was depressed whenever the boundary merged with each succeeding mark so that one watch was stopped while the other was started. While the boundary was passing between marks, time readings were recorded, and the potentiometer was read to obtain the potential drop across the standard resistor in series with the cell.

For the first concentration of a rare-earth nitrate, the proper concentration of the LiCl indicator solution to use was found by experiment. A series of four to six experiments was carried out using various concen-



trations of LiCl with the same concentration of R.E.(NO<sub>3</sub>)<sub>3</sub>. When the results were correlated by plotting the observed transference number  $T_{R.E.+++}$ , versus the concentration of LiCl used, the familiar plateau curves of MacInnes and Smith (84) were obtained. The point at the middle of the plateau was taken as the correct value of the LiCl concentration satisfying the Kohlrausch ratio. The correct  $T_+$ , at the normality of the rare-earth ion used, was given by the ordinate of the plateau.

Within a few percent, the ratio of normalities of the electrolytes in the cell was found to be essentially constant over the range of rare-earth nitrate concentrations used:

$$\frac{C_{LiCl}}{C_{R.E.(NO_3)_3}} \approx k .$$

The number "k" was evaluated from the results of the plateau curve for the first rare-earth concentration, and generally found to be in the neighborhood of 0.8 for the three salts studied. For experiments using the remaining solutions of a particular rare-earth, a first approximation for the proper lithium chloride concentration,  $C_{LiCl}$ , was calculated from the number "k". To verify that automatic adjustment of  $C_{LiCl}$  to fit the Kohlrausch ratio was taking place in the moving boundary cell, a second and a third experiment with slightly varying LiCl concentrations were carried out. If the  $T_+$ -values from these experiments did not agree within 0.1%, further trials were run to definitely establish the location of the Kohlrausch plateau. Ordinarily such additional experiments were not necessary, the first three being sufficient.

Experiments at five or six concentrations of each rare-earth nitrate were carried out in the range 0.01 to 0.1 Normal.

As a preliminary to the rare-earth nitrate measurements, a series of experiments were carried out with 0.1 Normal KCl, to check the reliability of the apparatus, and to perfect experimental technique. The average result for the best experiments of the series was  $T_{K^+} = 0.4900$ , compared with the accepted value of 0.4898 given by Harned and Owen (103).

## 2. Calculations and Results

For each individual experiment, the average current was computed from the series of voltage readings. The calibrated volumes of the measuring tube were grouped into sets, and the corresponding time in seconds for the boundary to pass through each set of volumes was calculated. An observed transference number was calculated for each set of calibrated volumes, and the final result for the experiment taken as the average over all the sets. The equation used to calculate the observed transference number for the cation was derived on page 72. A typical transference number experiment is shown in Table VIII.

As shown on page 75, the transference number, corrected for the volume and solvent-conductance effects is

$$T_+(\text{corrected}) = T_+(\text{observed}) - \frac{\Delta V C_n}{1000} + T_+(\text{observed}) \left[ \frac{L_{\text{solvent}}}{L_{\text{solution}}} \right] .$$

For these corrections the specific conductance  $L$ , were obtained directly from the experimental data given in the Electrolytic Conductance section. The volume change  $\Delta V$  has been shown on page 74 to be a function of the partial molal volumes:

$$\Delta V = -\frac{\bar{V}_{Cd}}{2} + \frac{\bar{V}_{CdCl_2}}{2} + \bar{V}_{LiNO_3} - \bar{V}_{LiCl} - \frac{T_+}{3} \bar{V}_{R.E.(NO_3)_3} .$$

Table VIII. A transference number experiment

Date: April 23      Salt:  $Hg(NO_3)_2$       Concentration: 0.047724 N.  
 Concentration Indicator Electrolyte: 0.04112 N LiCl

Marks	Time	Voltage	Marks	Volume	Time	$T_+$ (observed)
0-1	187.4	0.50852	0-7	0.7130	1413.8	0.4566
1-2	210.3	0.50853	0-8	0.8062	1598.2	0.4567
2-3	202.0	0.50855	0-9	0.9094	1803.2	0.4566
3-4	201.0	0.50857	0-10	1.0130	2008.5	0.4566
4-5	203.6	0.50859	1-8	0.7120	1410.8	0.4569
5-6	204.8	0.50864	1-9	0.8152	1615.8	0.4568
6-7	204.7	0.50866	1-10	0.9188	1821.1	0.4568
7-8	184.4	0.50867	1-11	1.0215	2025.6	0.4566
8-9	205.0	0.50868	2-9	0.7091	1405.5	0.4568
9-10	205.3	0.50872	2-10	0.8127	1610.8	0.4568
10-11	204.5	0.50873	2-11	0.9155	1815.3	0.4566
11-12	202.7	0.50874	2-12	1.0175	2018.0	0.4565
12-13	25.18	0.50876	3-10	0.7097	1408.8	0.4561
			3-11	0.8125	1613.3	0.4560
			3-12	0.9146	1816.0	0.4560
			3-13	1.0422	2067.8	0.4563
			4-11	0.7115	1412.3	0.4561
			4-12	0.8135	1615.0	0.4560
			4-13	0.9411	1866.8	0.4564
			5-12	0.7114	1411.4	0.4563
			5-13	0.8390	1663.2	0.4567
			6-13	0.7358	1458.4	0.4568

Average Voltage: 0.50864

Average  $T_+$ (observed): 0.4565

The partial molal volume of cadmium metal,  $\bar{V}_{\text{Cd}}$ , is its molar volume, calculated from the molecular weight and density of cadmium (104). The other partial molal volumes in the  $\Delta V$  equation are functions of the concentration of the electrolyte in solution. They were calculated from the apparent molal volumes, which in turn were calculated from density data for aqueous solutions of the particular salt. The apparent molal volume  $\phi_v$  is related to the molality  $m$ , and the density  $d$ , of a solution by

$$\phi_v = \frac{1000(d_0 - d)}{m d d_0} + \frac{M_2}{d},$$

where  $d_0$  is the density of the solvent and  $M_2$  is the molecular weight of the solute. From the International Critical Tables (104) pages 65, 77, and 78, density data were found for  $\text{CdCl}_2$ ,  $\text{LiCl}$ , and for  $\text{LiNO}_3$ . The densities of the rare-earth nitrate solutions were determined experimentally with a pycnometer. Although densities of erbium nitrate solutions have been measured with the magnetic float method by B. O. Ayers (36), data for samarium and holmium nitrate solutions have not heretofore been reported, and are therefore given in Table IX.

Values of the apparent molal volume  $\phi_v$  were calculated from the density data for each salt, and expressed in terms of a power series in the molality with the aid of least-squares treatment of the  $\phi_v$  data. The partial molal volumes,

$$\bar{V} = \phi_v + m \left( \frac{\partial \phi_v}{\partial m} \right),$$

Table IX. Densities of some rare-earth nitrate solutions

Salt	Normality	Molality	Density
Sm(NO <sub>3</sub> ) <sub>3</sub>	0.014772	0.0049396	0.99849
	0.036932	0.012355	1.0006
	0.051706	0.017301	1.0020
	0.11078	0.037106	1.0076
Ho(NO <sub>3</sub> ) <sub>3</sub>	0.0095440	0.0031912	0.99801
	0.019075	0.0063791	0.99897
	0.038197	0.012778	1.0009
	0.047724	0.015968	1.0018
	0.095454	0.031961	1.0067

could then be calculated easily from each of the power series formulas for  $\phi_v$ . The final expressions that were used in this research for the partial molal volumes are recorded in Table X.

Table X. Partial molal volumes of some electrolytes

CdCl <sub>2</sub> :	$\bar{V}_{\text{CdCl}_2} = 24.339 + 19.982 m - 26.196 m^2$
LiCl:	$\bar{V}_{\text{LiCl}} = 17.182 + 1.369 m^{\frac{1}{2}} + m - 0.357 m^{3/2}$
LiNO <sub>3</sub> :	$\bar{V}_{\text{LiNO}_3} = 29.150 - 0.4669 m^{\frac{1}{2}} + 1.963 m - 0.632 m^{3/2}$
Sm(NO <sub>3</sub> ) <sub>3</sub>	$\bar{V}_{\text{Sm(NO}_3)_3} = 46.479 + 676.3 m - 16,571 m^2$
Ho(NO <sub>3</sub> ) <sub>3</sub>	$\bar{V}_{\text{Ho(NO}_3)_3} = 57.56 - 1073.6 m + 24,379 m^2$
Er(NO <sub>3</sub> ) <sub>3</sub>	$\bar{V}_{\text{Er(NO}_3)_3} = 45.68 + 27.491 m^{\frac{1}{2}} - 5.206 m$ $- 104.82 m^{3/2} + 160.70 m^2$

The equation for  $\text{Er}(\text{NO}_3)_3$  was calculated by B. O. Ayers (36). The lack of extensive density data for samarium and holmium nitrates may make their partial molal volumes in Table X somewhat in error. However, the equations are perfectly adequate for application to transference number corrections, since the total volume correction,  $\Delta V C_n/1000$ , never amounted to more than 0.3% of the observed transference number. The molality of cadmium chloride used in the  $\bar{V}_{\text{CdCl}_2}$  equation was calculated on the basis of the total charge passed through the cell during an experiment. The molality of lithium nitrate for the  $\bar{V}_{\text{LiNO}_3}$  equation was assumed to be the same as that for the LiCl solution used for any particular experiment.

The cation transference numbers at 25.00°C. in the range 0.01 to 0.1 Normal for aqueous solutions of samarium nitrate, holmium nitrate, and erbium nitrate are given in Tables XI - XIII. The data are plotted in Figure 4. Data could not be obtained much below 0.01 Normal since the boundary was not visible for solutions of such dilution.

Table XI. Cation transference numbers for samarium nitrate

Normality	$T_+$ (observed)	Volume correction	Solvent correction	$T_+$ (corrected)
0.11078	0.4680	-0.0011	0.0000	0.4669
0.073898	0.4728	-0.0007	0.0000	0.4721
0.051706	0.4749	-0.0005	0.0001	0.4745
0.036932	0.4775	-0.0003	0.0001	0.4773
0.014772	0.4813	-0.0001	0.0002	0.4814

Least-squares Empirical Equation:  $T_+ = 0.4899 - 0.06759 \sqrt{C_n}$

Table XII. Cation transference numbers for holmium nitrate

Normality	$T_+$ (observed)	Volume correction	Solvent correction	$T_+$ (corrected)
0.095454	0.4485	-0.0009	0.0000	0.4476
0.066813	0.4533	-0.0007	0.0000	0.4526
0.047724	0.4567	-0.0005	0.0001	0.4563
0.038197	0.4597	-0.0004	0.0001	0.4594
0.019075	0.4636	-0.0002	0.0002	0.4636
0.009544	0.4680	-0.0001	0.0003	0.4682

Least-squares Empirical Equation:  $T_+ = 0.4775 - 0.09625 \sqrt{C_n}$

Table XIII. Cation transference numbers for erbium nitrate

Normality	$T_+$ (observed)	Volume correction	Solvent correction	$T_+$ (correction)
0.094717	0.4503	-0.0008	0.0000	0.4495
0.063106	0.4546	-0.0006	0.0001	0.4541
0.047327	0.4594	-0.0005	0.0001	0.4590
0.031559	0.4625	-0.0003	0.0001	0.4623
0.015766	0.4664	-0.0001	0.0002	0.4665

Least-squares Empirical Equation:  $T_+ = 0.4790 - 0.09611 \sqrt{C_n}$

By using the relations

$$\lambda_+ = \Lambda T_+$$

$$\lambda_- = \Lambda - \lambda_+$$

$$T_+^0 = \frac{\lambda_+^0}{\Lambda^0}$$

the individual ionic conductances at the experimental concentrations were

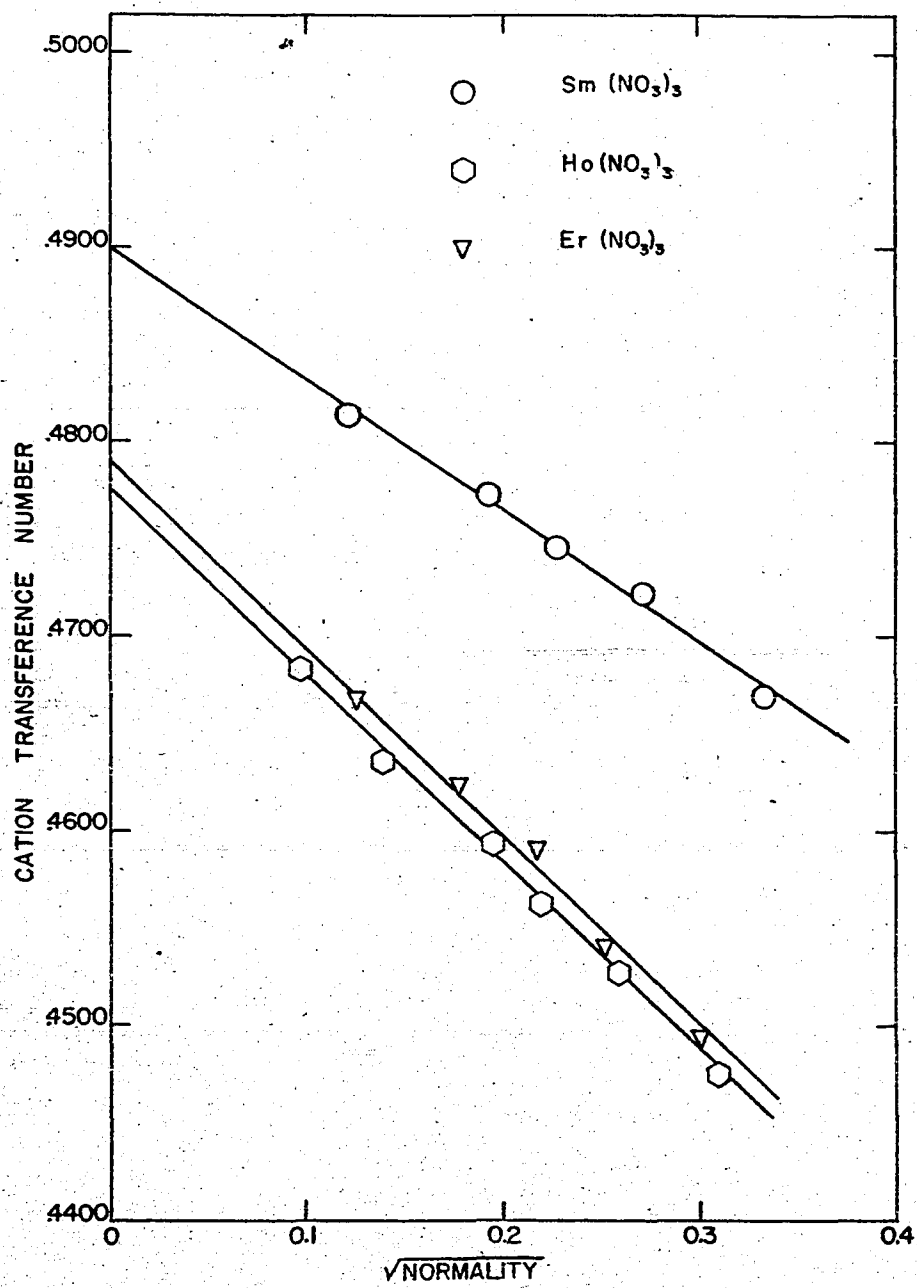


Figure 4. Transference numbers of samarium, holmium, and erbium nitrates at 25.00°C.



calculated, as was  $T_+^0$ , the cation transference number at infinite dilution. The results of these calculations are shown in Table XIV.

As with the conductance data, the discussion of the transference results will be reserved for the final section of the thesis.

Table XIV. Ionic equivalent conductances in some rare-earth nitrate solutions

Salt	Normality	$\lambda_+$	$\lambda_-$
$\text{Sm}(\text{NO}_3)_3$	0.11078	40.57	46.31
	0.073898	43.31	48.42
	0.051706	45.62	50.52
	0.036932	47.78	52.33
	0.014772	53.22	57.34
	Infinite Dilution	68.64	
		$T_+^0 = 68.64/140.06 = 0.4901$	
$\text{Ho}(\text{NO}_3)_3$	0.095454	41.49	51.21
	0.066813	43.63	52.76
	0.047724	45.52	54.25
	0.038197	46.79	55.07
	0.019075	50.49	58.43
	0.009544	53.85	61.15
Infinite Dilution	66.5		
		$T_+^0 = 66.5/137.92 = 0.4822$	
$\text{Er}(\text{NO}_3)_3$	0.094717	41.58	50.87
	0.063106	44.03	52.90
	0.047327	45.66	53.77
	0.031559	47.78	55.53
	0.015766	51.34	58.70
	Infinite Dilution	65.6	
		$T_+^0 = 65.6/137.0 = 0.4788$	

## V. ACTIVITY COEFFICIENTS

In thermodynamics the use of activity coefficients arises from the need of expressing the partial chemical potential of a component "i" in an actual solution as a valid function of its concentration. Ideally, were it not for the interactions between various kinds of particles in a solution, the partial chemical potential of component "i",  $\mu_i$ , would depend solely on a constant  $\mu_i^\circ$ , characteristic of the given solute and solvent at specified temperature and pressure, and on a function of the mole-fraction  $x_i$  in the form

$$\mu_i = \mu_i^\circ + RT \ln(x_i) \quad .$$

For actual solutions, which are not ideal in the sense of obeying the above equation, values of the partial chemical potentials at various concentrations can be obtained only by empirical measurement. Although there is no known theoretical connection of general validity relating the partial chemical potentials to the composition, it is especially convenient to express these thermodynamic quantities for real solutions in the same form as the ideal equation by employing functions of the respective components, called activities,  $a_i$ :

$$\mu_i = \mu_i^\circ + RT \ln(a_i) \quad .$$

The activity functions were first introduced by G. N. Lewis (105) in 1907. To make the partial chemical potentials functions of the mole-fraction of

the respective component "i", the activity becomes

$$a_i = f_i x_i ,$$

where  $f_i$  is the rational activity coefficient, and has the property

$$f_i \longrightarrow 1 \quad \text{as} \quad x_i \longrightarrow 0.$$

This property of  $f_i$  defines the standard state of the solution as one at infinite dilution of the component "i" for which the partial chemical potential  $\mu_i$  approaches the ideal dependence on  $x_i$  alone. If, instead of mole-fractions, the concentrations are expressed as molalities, the activity becomes

$$a_i = \delta_i m_i ,$$

where  $\delta_i$  is the molal activity coefficient, and has the property

$$\delta_i \longrightarrow 1 \quad \text{as} \quad m_i \longrightarrow 0.$$

For very dilute electrolytic solutions, the Debye-Hückel theory offers a method of calculating activity coefficients, which is based on the assumption that the deviation of the solution from ideality arises solely from the electrostatic interactions between the ions. A summary of the theory has already been presented in the section on General Theory.

In principle, activity coefficients may be quantitatively evaluated by determining the partial chemical potential for every desired concentration  $x_i$  or  $m_i$ . In practice, experimental measurements are made of various properties from which the partial chemical potentials may be

calculated. The most useful properties for such investigations have been the colligative properties, and the electromotive forces of galvanic cells.

The colligative properties have in common the establishment of equilibrium between the liquid solution and the pure solvent in some one of its phases. When the solution is in equilibrium with the vapor of the solvent (component "1") above it, then

$$\mu_1 = F_{1(g)}^{\circ} \quad ,$$

where  $F_{1(g)}^{\circ}$  is the molal Gibbs free energy of the pure solvent as a gas at the specified temperature  $T$ . Any pressure variation of these quantities, resulting from a small change in the composition of the solution, leads to the equation

$$(d\mu_1)_{T,P} = (V_{1(g)}^{\circ} - \bar{V}_1) dP \quad ,$$

in which  $V_{1(g)}^{\circ}$  is the molal volume of the gaseous pure solvent, and  $\bar{V}_1$  is the partial molal volume of the solvent in solution. The term  $(d\mu_1)_{T,P}$  represents the explicit change of  $\mu_1$  with the change in composition.

Therefore the activity  $a_1$  may be introduced to obtain

$$RT d \ln(a_1) = (V_{1(g)}^{\circ} - \bar{V}_1) dP,$$

an equation which forms the basis for the determination of activities, and therefore of activity coefficients, from measurements of the vapor pressure of the solvent above its solutions. If, on the other hand, a small change in concentration leads to a temperature variation when the pressure is

kept constant, the activity is derived from the equations

$$R \, d \ln(a_1) = d \left( \frac{\mu_1}{T} \right)_{T,P} = - \frac{H_{1(g)}^{\circ} - \bar{H}_1}{T^2} \, dT = - \frac{\bar{L}_1}{T^2} \, dT ,$$

in which  $H_{1(g)}^{\circ}$  is the molal enthalpy of the gaseous solvent,  $\bar{H}_1$  is the partial molal enthalpy of the solvent in the solution, and  $\bar{L}_1$  is the partial molal latent heat of vaporization of the solvent from the solution. If a particular constant pressure is chosen, conveniently one at unit atmosphere, then the temperatures to be measured, at equilibrium between the solution and the vapor, are those at the boiling point. Thus, determination of the boiling-point elevation of a solution is a second experimental method of obtaining activity coefficients.

The solution may be in equilibrium with the liquid phase of the solvent, a condition which exists in studies of the osmotic pressure. However, experimental application of this phenomena to the determination of activity coefficients is difficult, and has not been extensive.

When the solution is in equilibrium with the crystalline phase of the solvent, then

$$\mu_1 = F_{1(c)}^{\circ} ,$$

where  $F_{1(c)}^{\circ}$  is the molal Gibbs free energy of the pure solvent as a solid. The equations for the activity,  $a_1$ , are completely analogous to those for the boiling point method:

$$d \ln(a_1) = + \frac{(\bar{L}_{c1})_1}{RT^2} \, dT ,$$

in which  $(\bar{L}_{c1})_1$  is the partial molal latent heat of fusion for the

crystalline solvent into the solution. This equation is the basis for the method of measuring the freezing-point depressions of the solution to calculate activity coefficients.

The use of the colligative properties yields activities for the solvent directly. The activity coefficients for the solute may be calculated from the Gibbs-Duhem equation with the aid of graphical integrations.

The electromotive force of a thermodynamically reversible galvanic cell is related to the free-energy change for the cell process by the equation

$$-n \mathcal{F} E = \Delta F ,$$

in which  $\mathcal{F}$  is the faraday constant. For cells without liquid junction the free-energy change takes the form

$$\Delta F = \sum_i (\mu_i - F_i^{\circ}(\text{at the electrode})) ,$$

so that by measuring the electromotive force  $E$  of the cell, the partial chemical potentials, and therefore the activity coefficients, may in principle be obtained. A type of cell which has found wide application for activity coefficient measurements is the concentration cell with transference, for which the electromotive force is related to the activity,  $a$ , of the solute by an equation of the form

$$-E = n \frac{RT}{\mathcal{F}} \int_{C_1}^{C_2} T_+ d \ln(a)$$

This method can yield only relative values of the activity coefficients at two electrolyte concentrations,  $C_1$  and  $C_2$ .

Other more exotic methods for determining activity coefficients have been developed, such as the application of artificial gravitational fields with an ultracentrifuge, but these methods have found only limited use.

Instead of any of the direct methods mentioned above, a comparative technique was employed in this research to determine the activity coefficients of the nitrates of samarium, holmium, erbium, and ytterbium in aqueous solution. By comparing the concentrations of two solutions of different electrolytes, that have attained a common identical vapor pressure, the activity coefficient of the solute in one solution may be calculated with thermodynamic reasoning from a knowledge of the activity coefficient of the second solute in its solution. This is the essence of the Isopiestic Comparisons method. For this research solutions of the rare-earth nitrates were brought to vapor-pressure equilibrium in a closed chamber with solutions of potassium chloride, the reference electrolyte for which thermodynamic data were at hand throughout its entire concentration range. At equilibrium the partial chemical potentials of the solvent were equal in each of the three phases present: rare-earth nitrate solution, vapor phase, and KCl solution. Consequently with a common solvent activity in each solution, the Gibbs-Duhem equation could be applied to calculate the rare-earth nitrate activity coefficients from the equilibrium concentrations of each solution and from the known data for KCl.

Details of the procedure will be discussed in the sections that follow.

A. Theory of the Isopiestic Comparisons Method

The method of isopiestic comparisons rests on the attainment of thermodynamic equilibrium of a common solvent through the vapor phase above solutions of differing solutes. For equilibrium between solutions of rare-earth nitrates and potassium chloride, the partial chemical potentials of the solvent in each solution are equal:

$$(\mu_{\text{H}_2\text{O}})_{\text{R.E.}(\text{NO}_3)_3} = (\mu_{\text{H}_2\text{O}})_{\text{KCl}} .$$

Since the activity of the solvent,  $a_{\text{H}_2\text{O}}$ , is defined by

$$\mu_{\text{H}_2\text{O}} = F_{\text{H}_2\text{O}}^\circ + RT \ln(a_{\text{H}_2\text{O}})$$

the solvent activities in both solutions at equilibrium are also equal:

$$(a_{\text{H}_2\text{O}})_{\text{R.E.}(\text{NO}_3)_3} = (a_{\text{H}_2\text{O}})_{\text{KCl}} .$$

A new function, the Molal Osmotic Coefficient  $\phi$ , is now defined as a function of the partial chemical potential of the solvent:

$$\mu_{\text{H}_2\text{O}} = F_{\text{H}_2\text{O}}^\circ - \phi RT \frac{\nu m M_{\text{H}_2\text{O}}}{1000}$$

in which  $\nu$  is the number of moles of ions into which one mole of solute dissociates,  $m$  is the molality of the electrolyte in the solution, and  $M_{\text{H}_2\text{O}}$  is the molecular weight of water. From the definition of the activity in terms of the partial chemical potential, we have

$$\ln(a_{\text{H}_2\text{O}}) = -\phi \nu m M_{\text{H}_2\text{O}} / 1000 ,$$



so that the isopiestic equilibrium condition becomes

$$(\phi \nu^m)_{\text{R.E.}(\text{NO}_3)_3} = (\phi \nu^m)_{\text{KCl}},$$

or

$$\phi_{\text{R.E.}(\text{NO}_3)_3} = \frac{2m_{\text{KCl}}}{1m_{\text{R.E.}(\text{NO}_3)_3}} \phi_{\text{KCl}}. \quad (1)$$

The most general form of the Gibbs-Duhem equation is

$$SdT - VdP + \sum_i N_i d\mu_i = 0,$$

where  $N_i$  is the number of moles of component "i" in the phase. At fixed temperature and pressure for a binary aqueous solution, the Gibbs-Duhem equation reduces to

$$x_{\text{H}_2\text{O}} d \ln(a_{\text{H}_2\text{O}}) + x_{\text{solute}} d \ln(a_{\text{solute}}) = 0,$$

where  $x_i = N_i / \sum_i N_i$  is the mole-fraction. The conversions from mole-fractions to molalities are

$$x_{\text{H}_2\text{O}} = \frac{1000/M_{\text{H}_2\text{O}}}{1000/M_{\text{H}_2\text{O}} + m} \quad \text{and} \quad x_{\text{solute}} = \frac{m}{1000/M_{\text{H}_2\text{O}} + m}.$$

In terms of molalities, the Gibbs-Duhem equation consequently becomes

$$\frac{1000}{M_{\text{H}_2\text{O}}} d \ln(a_{\text{H}_2\text{O}}) + m d \ln(a_{\text{solute}}) = 0.$$

But  $a_{\text{H}_2\text{O}}$  may be expressed in terms of the molal osmotic coefficient,

so that

$$d(\phi/m) = \nu_m d \ln(m_{\pm} \gamma_{\pm})$$

in which  $a_{\text{solute}} = (a_{\pm})^{\nu} = (m_{\pm} \gamma_{\pm})^{\nu}$

where  $\gamma_{\pm}$  is the mean ionic molal activity coefficient.

To find the molal osmotic coefficient in terms of the molal activity coefficient, one proceeds as follows:

$$d(\phi/m) = \frac{m}{m_{\pm}} dm_{\pm} + m d \ln(\gamma_{\pm}),$$

in which  $m_{\pm} = m(\nu_+^{\nu_+} \cdot \nu_-^{\nu_-})^{1/\nu} = m \cdot \text{constant}.$

Then

$$\int_{\substack{\text{infinite} \\ \text{dilution} \\ \phi = 0}}^{\phi/m} d(\phi/m) = \int_{\substack{\text{infinite} \\ \text{dilution} \\ m = 0}}^m dm + \int_{\substack{\text{infinite} \\ \text{dilution} \\ \gamma_{\pm} = 1}}^{\ln(\gamma_{\pm})} m d \ln(\gamma_{\pm}).$$

Or

$$\phi = 1 + \frac{1}{m} \int_0^{\ln(\gamma_{\pm})} m d \ln(\gamma_{\pm}) \quad (\text{II})$$

The integral is determined graphically. From the known activity coefficient data for KCl, the osmotic coefficients for this electrolyte may be calculated from Equation II. Then from experimental equilibrium values of the molalities  $m_{\text{KCl}}$  and  $m_{\text{R.E.}(\text{NO}_3)_3}$ , the osmotic coefficients for the rare-earth nitrates may be calculated from Equation I.

To find the activity coefficients from the molal osmotic coefficients, one treats the derived Gibbs-Duhem Equation in the following manner:

$$d(\phi m) = m d \ln(m_{\pm} \gamma_{\pm}).$$

$$d\phi + \phi d \ln(m) = d \ln(m_{\pm}) + d \ln(\gamma_{\pm}).$$

Now the divergence function  $h$  is defined in the following way:

$$h = 1 - \phi$$

$$dh = -d\phi.$$

Then

$$d \ln(\gamma_{\pm}) = -dh + (1 - h)d \ln(m) - d \ln(m_{\pm}).$$

Or

$$\int_{\substack{\text{infinite} \\ \text{dilution} \\ \gamma_{\pm} = 1}}^{\ln(\gamma_{\pm})} d \ln(\gamma_{\pm}) = \int_{\substack{\text{infinite} \\ \text{dilution} \\ h = 0}}^h -dh - \int_{\substack{\text{infinite} \\ \text{dilution} \\ m = 0}}^{\ln(m)} h d \ln(m) + \int d \ln \frac{m}{m_{\pm}}$$

In order to take advantage of a function which approaches the  $m = 0$  axis more rapidly than does the logarithm function, the final result is written as follows:

$$\log(\gamma_{\pm}) = -\frac{h}{2.30258} - \frac{2}{2.30258} \int_0^{\sqrt{m}} \frac{h}{\sqrt{m}} d\sqrt{m} \quad (\text{III})$$

This equation with a graphical integration gives the mean molal activity coefficients from the experimental osmotic coefficients expressed in terms of the function  $h$ .

## B. Historical Review of the Isopiestic Method

Before reviewing the contributions of various experimentalists to the method of isopiestic comparisons, it would be well to consider the attributes of a suitable apparatus. The experimental apparatus and technique must perform the double service of bringing about a condition of true equilibrium of the solvent among its various solutions as efficiently as possible, and of allowing accurate analyses of the solutions to be made once equilibrium has been achieved. On the basis of these two objectives, several general principles for the apparatus and procedure may be listed.

1). Since evaporation and condensation of the solvent between solutions involve energy changes, the total system must be in complete thermal as well as isopiestic equilibrium at the thermodynamic equilibrium. For this reason it is necessary to provide good thermal contact between the solutions to reduce retardation of equilibration due to thermal resistance.

2). In addition to immersing the apparatus in a well controlled constant temperature bath, it must be shielded from temperature fluctuations within the bath. This has usually been accomplished with a thermal buffer in the form of a relatively large copper block in which the cups of solutions rest. If the fit between the cups and the block is tight, the block also provides the necessary thermal contact between solutions.

3). Two of the limiting factors in the attainment of equilibrium are the diffusion of the solute through the solutions of changing concentrations, and conduction of heat through the solutions themselves. Both of these processes can be accelerated by some kind of arrangement for moderately gentle stirring, not vigorous enough to cause local heating effects

or to splash solution out of the cups. Strips of platinum gauze, folded in the form of bellows, and placed in the equilibrating solutions will assist heat conduction. If the depth of the solutions in the cups is kept quite shallow, the distance of heat conduction through the solutions is minimized.

4). Another factor is adequate diffusion of water vapor in the gaseous phase. Complete removal of air is necessary in this regard, and is effected by evacuation of the equilibration chamber. Drops of water may be placed in recesses and corners in the chamber before evacuation, so that their evaporation may drive out the air from these places. The air must be evacuated slowly, in stages, to outgas the solutions and avoid splashing. Clean, dry air is slowly admitted to the apparatus at the conclusion of the experiment.

5). Analyses of the solutions depend only on noting the changes in water content before and after an experiment, if the initial concentrations are known. These changes are determined simply by weighing the solutions. Therefore an optimum sample size, small enough to minimize the amount of solvent which has to distill, and yet compatible with accuracy in weighing, must be found.

6). The dishes or cups must be chemically inert to the solutions used, must be arranged to be tightly capped during weighing, and yet should be so shaped that a maximum of surface area of solution may be exposed during an experimental run in the apparatus.

Bousefield and Bousefield (106, 107) in 1918 were the first to suggest the utility of an isopiestic comparisons technique as an indirect vapor pressure method for determining activity coefficients. They made some

preliminary experiments with the isopiestic method, but it was left for D. A. Sinclair (108) in 1933 to establish many of the principles of the method, outlined above, and to demonstrate how successful the technique could be. He emphasized the importance of preparing a good thermal connection between the solutions. In order that the isopiestic method be as accurate as direct vapor pressure measurements in which pressure differences of 0.001 mm can be observed, the thermal contact must be good enough to rapidly equilibrate the temperatures of two solutions originally differing in vapor pressure by 0.001 mm. Since the  $(dP/dT)_{250}$  for water is 1.4 mm per degree, the corresponding temperature difference which must be equalized while the solutions come to pressure equilibrium is 0.0007°C. Sinclair used silver-plated copper dishes,  $1\frac{1}{2}$  inches square by  $\frac{3}{4}$  inch deep, four of which were placed in square formation in a silver-plated copper block 1 inch thick. This was mounted in a desiccator evacuated to 15 mm Hg before being placed in a thermostat. For stirring, the desiccator was rocked back and forth at a 20° angle with a one-second period of oscillation. Dilute sodium hydroxide solution was used to fill in the cracks between the dishes to improve thermal contact. This procedure had the disadvantage, of course, that the outside of the dishes had to be washed free of alkali and dried before weighing. The sequence of operations was to pipette a two-cubic-centimeter sample of solution of known concentration into each dish. These were then weighed, placed in the desiccator for equilibration, and then reweighed as quickly as possible after being removed from the apparatus. Equilibration time varied from one to three days.

R. A. Robinson (109, 110) who has done the most work in the field,

and has contributed a huge mass of experimental data since 1934, used essentially the same technique as used by Sinclair. Robinson used gold-plated silver dishes, and in later work chromium-plated silver or stainless steel dishes, of approximately the same size as Sinclair's. Of eight square dishes held in the copper block, two contained solutions of the reference electrolyte, while the other six held the solutions under study. The dishes were fitted with flap-lids, held open during an experiment by a wire bridge attached to the exit tube of the desiccator, so arranged that at the conclusion of the experiment the lids were allowed to fall by rotating the exit tube through a small angle without opening the desiccator. The desiccator was rocked in the thermostat for from one to three days, as with Sinclair's work.

Provision for tightly fitting caps for use in weighing is described by Scatchard, Hamer, and Wood (111) in their paper of 1938. The top parts of cylindrical platinum cups, 3.5 centimeters high and 2.5 centimeters in diameter, were constricted to a smaller diameter so that the cups looked like milk cans. A nickel ring was silver-soldered to the outside of this constriction. The outside of the ring was carefully ground with a  $3^{\circ}$  taper to fit a nickel lid. The cups fitted snugly in cylindrical holes in a gold-plated copper block which in turn was mounted in a stainless steel vessel arranged for evacuation. The vessel sat on a table, in the thermostat, which rotated about an axis inclined at  $45^{\circ}$ . Samples of about one gram each were weighed into the cups, and the vessel was evacuated down to around 2 mm Hg. Up to six days equilibration time were allowed for the more dilute solutions.

C. M. Mason (112, 113, 114) who measured some trivalent metal

chlorides, used ordinary glass stoppered weighing bottles for his concentrated solutions, and gold-plated silver bottles in the dilute range. Platinum gauze was placed in the bottles to aid in the stirring and heat conduction through the solutions. His monel metal desiccator, fitted with a brass needle valve for evacuation, was rocked back and forth 45 times per minute in the thermostat. The precision of the experimental molalities of identical solutions in an equilibration was reported to be 0.1%. The average deviation of the experimental data from a smooth curve was 0.3% to 0.5%.

J. H. Jones (115) in 1943 used nickel cups for alkali chlorate, bromate, and perchlorate solutions in an all brass desiccator with a rocking device.

Whereas most investigators found that acceptable accuracy could not be obtained with solutions below 0.1 molal, A. R. Gordon (116) in 1943 tried to extend the range to 0.03 molal with some refinements in the apparatus. He neatly solved the problem of good thermal contact between solutions by placing a cup of one solution directly into a larger cup of the reference solution, both of which were made of gold-plated silver. This inner-and-outer cup arrangement fit snugly into a glass vacuum desiccator, 4.2 centimeters in diameter, which in turn fit into a copper box. The box went into a Dewar flask, packed tightly with glass wool, and the Dewar rested in a large glass vacuum desiccator, 25 centimeters in diameter. The large glass desiccator was affixed as usual to a rocking table in the constant temperature bath which was regulated to  $\pm 0.003^{\circ}\text{C}$ . A glass bead was previously placed in each cup to stir as the desiccator rocked. Gordon allowed an equilibration time of from 7 to 18 days. After the next of



Dewars and desiccators had been dismantled, dry air was slowly admitted to the small desiccator, and immediately upon opening the desiccator, ground glass stoppers were fit onto the cups. Both cups were weighed as a unit first, and then the outside of the smaller cup was rinsed and dried so that it could be weighed. Acceptable precision was obtained for solutions of NaCl and KCl below 0.1 molal. However, more than one pair of solutions cannot be equilibrated at a time, and the complexity of the apparatus makes it unhandy for an extended series of measurements.

Others who did experimental work in the field are Owen and Cooke (117) in 1937, Janis and Ferguson (118) in 1939, Phillips, Watson, and Felsing (119) in 1942, and Patterson and Tyree (20) in 1955, but their apparatuses were similar to ones already described.

### C. Experimental Investigation

#### 1. Apparatus and Procedure

The apparatus used to carry out the isopiestic equilibrations for this research included a set of twenty-four equilibration cups, three stainless steel equilibration chambers with a heavy copper block for each, a mechanism to rock the chambers, and a large constant temperature bath.

The gold-plated sterling silver equilibration cups were manufactured by the Randahl Silver Company of Skokie, Illinois. They were cylindrical in shape, 3.5 centimeters high, and 2.5 centimeters in diameter. A silver ring, tapered to form a seat for a gold-plated silver lid, was soldered around the outside of the opening of each cup. In preliminary work a thin film of silicone grease was used between the ring and the lid to avoid wear

of the metal parts, and to provide a vapor tight seal. However it was soon discovered that the film of grease remaining on the ring of the cup would absorb a noticeable amount of water vapor during an equilibration. Furthermore the amount of water vapor absorbed each time was not constant, and the grease would slowly release its absorbed water after removal from the saturated atmosphere of the equilibration chamber. Therefore use of the metal lids had to be abandoned, since they would not work well without a grease film. In their place a set of small polyethylene caps were obtained which were of such size as to just snap on over the soldered ring around the cup opening. These polyethylene caps were very satisfactory. They kept the weight of a cup filled with water constant within 0.2 mg over several hours, and avoided the use of grease and wear of any metal parts.

The flat bottom of each equilibration cup extended out beyond the walls to give a flange about 0.5 centimeter wide extending around the entire base of the cup. The purpose of the flange was to allow a collar to be dropped down over and around the cup so that it sat on the flange and held the cup securely in a receptacle prepared for it.

A block of solid copper was used as a thermal buffer and as the means of mounting the cups with a good thermal connection between them. A block was made for each of three equilibration chambers. Each block was about 25 centimeters long, 11 centimeters wide, and 3 centimeters high. In the block eight cylindrical wells, 1.6 centimeters deep, were drilled. They were of a diameter very slightly larger than the base of the cups, and served as the receptacles into which the cups were placed. The interior upper half of the wall of each well was threaded, so that a brass retaining ring could be screwed into each well of a block. By placing a cup in a

well, dropping a Bakelite collar down over the cup so that it sat on the flange of the cup, and screwing in a brass retaining ring over the collar, the cup could be held very tightly in contact with the copper block. The retaining ring always slid over the Bakelite collar as the ring was turned in the block, so that the cup remained stationary in the well without a chance of wear on any of its surfaces. This arrangement was essentially the same as that used by Mason (113). The interiors of the wells in the blocks were gold plated to avoid corrosion and to provide a gold-to-gold contact between cup and block. The remaining surface of each block was polished and heavily lacquered.

Each copper block fit into a stainless steel equilibration chamber. Around the top of each chamber was a flat flange which served as a seat for a heavy stainless steel cover. A Neoprene gasket provided a vacuum tight seal between cover and chamber. Twelve stud bolts with wing-nuts served to hold the cover tightly against the Neoprene gasket on the flange of the chamber. The cover of each chamber was fitted with a Hoke #RF-275 angle pattern stainless steel needle valve for evacuation. Whenever the chamber was immersed in the constant temperature bath, the hollow metal connector used to join the valve with the vacuum line was replaced with another connector which was solidly filled with solder to keep water out of the valve. No thermostat water ever leaked into a chamber either through the Neoprene gasket or through the valve between the spindle and packing nut.

A heavy steel rod about 10 centimeters long was firmly attached to the center of each end of a chamber so that each rod extended out in opposite directions from the chamber, in parallel with its long dimension. Then, when the ends of the two rods on a chamber were placed in brackets

mounted on opposite inside walls of the constant temperature bath, the chamber would be free to rock about an axis through the rods. Another heavy steel bar was attached to one end of a chamber, but this was bent to a vertical position so that it stuck out above the surface of the water when the chamber was mounted in the bath. Thus when the three chambers were mounted side by side with their rods in their respective brackets along the length of the inside walls of the bath, there were three steel bars emerging in a line from the surface of the water. The top end of each bar could be connected with a pin to a movable horizontal arm running along the length of the constant temperature tank at a level about 3 to 4 inches above its top. When this movable arm was driven back and forth by a wheel and crank mechanism, the equilibration chambers were rocked back and forth in the bath. The drive wheel for the mechanism was powered by an electric motor through a Graham variable speed transmission and reduction gear box, so that any frequency of oscillation could be attained from zero to 70 cycles per minute. In addition, the radius of crank could be adjusted, so that any amplitude of rock was available from  $10^{\circ}$  to  $60^{\circ}$  from the vertical. The entire apparatus was so arranged that any one or any two chambers could be removed from the bath to be opened, while the remaining chamber or chambers could continue rocking in the bath.

The constant temperature bath consisted of an inner and outer tank between which blown-mica was held for insulation. The inner stainless steel tank was 53 inches long, 20 inches wide, and 20 inches deep. Its walls were structurally reinforced to hold the brackets by which the equilibration chambers were suspended in the bath. A copper tube carrying cooling water passed through the bath water, and a battery of three infra-

red lamps distributed above the water surface were used for heating. The extra length of the bath allowed the lamps to be mounted so that they never showed directly on the chambers themselves as they rocked in the bath. Two thermoregulators at different points in the bath activated separate relays to which the lamps were connected in such an arrangement as to give the best temperature control. Two heavy Cenco centrifugal stirrers, catalogue number 18850, were mounted at the ends of the bath. Each of these pumped water at the rate of 100 gallons per minute, and kept the water moving quite vigorously throughout the bath. Two Emerson calorimetry thermometers, graduated in units of  $0.01^{\circ}\text{C}$ ., and calibrated by the National Bureau of Standards, were used to read the temperature of the thermostat water at any two different regions in the bath simultaneously. They always showed that the bath temperature was uniform throughout, and was constant at  $25.00^{\circ}\text{C}$ . within  $\pm 0.01^{\circ}$  over weeks at a time.

The constant temperature tank, the stainless steel chambers with their copper blocks, and the rocking mechanism were constructed by Mr. Harvey Meyer under the direction of Mr. E. R. Clark in the Metallurgy Fabrication Shop at the Institute for Atomic Research.

Evacuation of the chambers was made with a rotary, oil-seal vacuum pump in combination with a trichlorethylene-dry-ice trap to remove water vapor from the vacuum line. Weighings were made on an Ainsworth analytical balance.

The rare-earth nitrate solutions were prepared as described in the Conductance section of the thesis, except that larger quantities of the oxides were used to obtain stock solutions of around 2 molal. Two or three solutions of successively smaller concentrations were then prepared from the stock by weight dilution. Thus a set of three or four stock solutions

of widely differing concentrations was on hand for each rare-earth nitrate. From a set, one solution could be chosen from which a convenient weight might be taken for the desired concentration range in which a given experiment was to be carried out. Potassium chloride solutions were obtained by weighing out fused crystals of the C.P. salt and making weight dilutions with conductance water.

The laboratory procedure for an isopiestic comparisons experiment was as follows: The gold-plated sterling silver equilibration cups to be used were first cleaned of any stains or tranish by dipping them in "Quik-Dip" commercial silver cleaner. They were immediately rinsed under distilled water, and given a final rinsing with conductivity water. When the cups were clean they would drain free, with no drops of water adhering anywhere on the walls. The cups were then dried at 60°C. in the oven and allowed to cool in the atmosphere of the laboratory. Strips of platinum gauze folded in the form of bellows were cleaned and rinsed similarly and then ignited in the flame of a Bunsen burner to make them absolutely free from any dust or grease. A freshly ignited platinum gauze bellows was placed in the bottom of each equilibration cup. Empty weights of each cup with its platinum gauze and polyethylene cap could then be found.

Suitable volumes of rare-earth nitrate stock solution and KCl stock solution were pippered into their respective cups, and weighed. Then the required amount of conductance water to make a 2-gram sample of solution was added to each cup, and weighings were again taken so that initial concentrations could be calculated. Two cups were weighed out in this manner for each salt equilibrated in an experiment. The initial concentrations of the two solutions for each salt were made to be about 3% on

either side of the expected final concentration, so that the total initial concentration difference was generally around 6%. Often two different rare-earth nitrates could be equilibrated against the same KCl solutions in a single chamber, so that six cups were weighed out with solutions, instead of only four for a single rare-earth nitrate - KCl experiment. An equilibration was considered completed when the concentrations of both solutions of the identical salt came within 0.15% of the average for that salt, for each pair of identical salt solutions in the system. Usually, above concentrations of 0.2 molal, each member of a pair could be brought to within 0.1% of one another.

After the cups of solutions were weighed, they were affixed in the equilibration chamber, and their caps removed. These caps were carefully stored in a manner to assure their identity one from another when the time came to replace them on the cups. Several drops of water were placed in various recesses in the chamber, so that during the evacuation, their evaporation would drive out the air and replace solvent lost from the cups. No water was ever found remaining in the chamber outside the cups at the conclusion of an experiment.

Both sides of the Neoprene gasket were lightly coated with Apiezon "T" grease on the areas that would be squeezed between cover and chamber. After the gasket and cover were bolted into place, the chamber was evacuated to 30 mm Hg. The solutions in the chamber were allowed to outgas at this pressure while the chamber rocked for a day in the constant temperature bath. Then on the following day the chamber was temporarily removed from the thermostat for a few minutes so that the pressure could be reduced to 20 mm. There was no point in trying to reduce the pressure further since

the only result would be to remove too much solvent from the system. The chambers had to be evacuated with this two step process to avoid splashing the solutions.

The total rocking equilibration time for solutions in the high concentration range (above 0.7 molal) was four days. Solutions of intermediate concentrations required a week for equilibration, and solutions in the range below 0.2 molal had to be equilibrated as much as two weeks before two solutions of a pair would agree within 0.15% of their average.

At the conclusion of the required equilibration time, clean, dry air was slowly admitted to the chamber through traps of calcium chloride and glass wool. If the humid air of the laboratory were admitted to a chamber, the atmosphere in the chamber would become supersaturated with water vapor, and droplets would condense on everything inside. The polyethylene caps were quickly snapped onto the cups as soon as the cover to the chamber was removed, and then the cups were weighed. The time interval between removal of the cover from the chamber and capping the last cup was never more than 60 seconds. By experiment it was found that at most 0.2 mg of water would evaporate from an open cup during this 60-second period.

If the solutions were not at equilibrium at the end of the allotted time, the cups were returned to the chamber for re-evacuation and further rocking. Three experiments could be run concurrently in the three chambers of the apparatus.

All weights were reduced to values in vacuo. The final isopiestic concentrations were calculated from the initial concentrations with the relations

$$\text{Weight of solute} + \text{Weight of solvent} = \text{Weight of solution,}$$



and

$$\text{Molality} = \frac{\text{Weight of solute/Molecular-weight of solute}}{\text{Weight of solvent/1000}}$$

## 2. Selection of Standard Data for Potassium Chloride

To calculate the activity coefficients from the isopiestic data, one needs on hand a standard set of activity coefficient (or osmotic coefficient) data for the reference salt, potassium chloride. To obtain a set of activity data which would be representative of most of the work reported in the literature, papers on the thermodynamics of potassium chloride solutions by the following authors were reviewed, and the results of these researches were tabulated: H. S. Harned (120), E.M.F. of concentration cell of flowing amalgam type, 1929; Scatchard and Prentiss (121), freezing-point depressions, 1933; Harned and Cook (122), E.M.F. of concentration cells of flowing amalgam, 1937; Shedlovsky and MacInnes (123), E.M.F. of concentration cell with transference, 1937; R. A. Robinson (124), isopiestic comparisons with NaCl, 1939; T. Shedlovsky (125), E.M.F. of concentration cells, 1950; and Scatchard, Hamer and Wood (111), isopiestic comparisons with NaCl, 1938. Average values at round concentrations were calculated from the data in these papers by omitting data which would give a difference of more than 0.003 in the activity coefficient from the average if they were included. These average values of the activity coefficients for KCl were then used to calculate a set of osmotic coefficients from Equation II derived under "Theory of the Isopiestic Comparisons Method". The results of the computation agreed so well with the osmotic coefficients reported by Robinson and Stokes in a review paper (126) and by Scatchard,

Hamer, and Wood (111) from their isopiestic experiments, that the mean of the osmotic coefficients reported in these two papers was chosen as the standard set of reference data for potassium chloride. This agreement is shown in Table XV:

Table XV. Osmotic coefficients for potassium chloride

Molality	KCl Osmotic Coefficient		
	Calculated from literature ( $\bar{\gamma}_{\pm}$ ) Average	Robinson & Stokes (126)	Scatchard, Hamer, & Wood (111)
0.10	0.9273	0.927	0.9264
0.20	0.9137	0.913	0.9131
0.30	0.9059	0.906	0.9063
0.40	0.9010	0.902	0.9023
0.50	0.9004	0.899	0.9000
0.60	0.8978	0.898	0.8987
0.70	0.8981	0.897	0.8980
0.80	0.8970	0.897	0.8980
0.90	0.8962	0.897	0.8982
1.0	0.8972	0.897	0.8985
1.2	0.8996	0.899	0.8996
1.4	0.9014	0.901	0.9008
1.6	0.9034	0.904	0.9024
1.8	0.9067	0.908	0.9048
2.0	0.9105	0.912	0.9081
2.5	0.9247	0.924	0.9194
3.0	0.9379	0.937	0.9330
3.5	0.9481	0.950	0.9478
4.0	0.9568	0.965	0.9635

The averages of the osmotic coefficients reported by Robinson and Stokes and by Scatchard, Hamer, and Wood, were condensed into the form of two equations, calculated by the method of least squares, which reproduce the data to better than 0.10%. These equations are

$$(\phi_m)_{\text{KCl}} = 0.00290125 + 0.90140558 m - 0.0227841 m^2 + 0.016382 m^3$$

in the range  $m = 0.1$  to  $1.14$ ;

$$(\phi_m)_{\text{KCl}} = 0.04729877 + 0.81982168 m + 0.03318215 m^2$$

in the range  $m = 1.14$  to  $4.5$ .

In these equations,  $\phi_m$  is the product of the molal osmotic coefficient and the molality. These equations were used to calculate the standard KCl osmotic coefficients at each experimental isopiestic concentration. Equation I from "Theory of the Isopiestic Comparisons Method" could then be directly applied to obtain the osmotic coefficients for the rare-earth salts.

### 3. Redetermination of Activity Coefficients for Lanthanum Chloride

A preliminary investigation of the activity coefficients of lanthanum chloride in solutions of concentrations above 0.1 molal was undertaken to compare data obtainable with the apparatus and techniques of this research with the results of isopiestic comparisons carried out by Robinson (127, 128) and by Mason (113, 114). Work with lanthanum chloride also provided an opportunity to survey the various methods of treating the experimental data that were used by these authors.

The lanthanum oxide for the solutions was produced by ion-exchange

techniques at the Iowa State College Institute for Atomic Research. Spectrographic analysis showed the presence of 0.06% of calcium in the sample, and although the elements cerium, praseodymium, neodymium, gadolinium, samarium, yttrium, and iron were spectrographically investigated in the sample, they were not detected. The calcium was removed by reprecipitating the  $\text{La}_2\text{O}_3$  with oxalic acid as described under "Preparation of Solutions" in the Conductance section. The purified lanthanum oxide was then dissolved in redistilled hydrochloric acid, and evaporated to a highly concentrated solution on a hot plate. To make absolutely certain of the purity of the  $\text{LaCl}_3$ , a double recrystallization with hydrogen chloride gas was carried out at  $0^\circ\text{C}$ . The filtered lanthanum chloride crystals were freed from adsorbed hydrogen chloride gas by drying them in a tube at  $60^\circ\text{C}$ . in a stream of air. No HCl odor was detected after 24 hours' exposure in the drying tube. The crystals were then dissolved in conductance water, and a titration with 0.05 N HCl was made on an aliquot to find the stoichiometric pH, as with the nitrates. The pH of the bulk of the  $\text{LaCl}_3$  solution could then be adjusted properly. Both oxalate analyses for the cation, and AgCl analyses for the anion were carried out. Results of the two analytical methods were in agreement by 0.15%. Lower concentration stock solutions were prepared by weight dilution from the original  $\text{LaCl}_3$  stock.

The experimental isopiestic comparisons were carried out as described under "Apparatus and Procedure."

Osmotic coefficients of lanthanum chloride solutions at the experimental isopiestic molalities were calculated from the isopiestic equilibrium condition,

$$\phi_{\text{LaCl}_3} = \frac{m_{\text{KCl}}}{2 m_{\text{LaCl}_3}} \phi_{\text{KCl}},$$

in which the  $\phi_{\text{KCl}}$ 's were computed with the equations given in Section 2.

Results are given in Table XVI. Figure 5 shows a graph of  $\phi_{\text{LaCl}_3}$  plotted versus  $m_{\text{LaCl}_3}$  from the data in Table XVI. On the same graph are the points obtained by Mason (113) in 1938. A comparison of the two sets of data at round concentrations is given in Table XVII.

Table XVI. Isopiestic molalities and osmotic coefficients for  $\text{LaCl}_3$  and  $\text{KCl}$

$m_{\text{LaCl}_3}$	$m_{\text{KCl}}$	$\phi_{\text{KCl}}$	$\phi_{\text{LaCl}_3}$
0.11313	0.19261	0.9137	0.7778
0.11604	0.19600	0.9135	0.7715
0.17565	0.30485	0.9060	0.7862
0.18433	0.32291	0.9051	0.7928
0.18812	0.32965	0.9047	0.7927
0.19930	0.35126	0.9039	0.7965
0.23123	0.41190	0.9018	0.8091
0.25847	0.46737	0.9005	0.8141
0.27699	0.50245	0.8999	0.8162
0.30316	0.55929	0.8990	0.8293
0.43513	0.85066	0.8973	0.8771
0.44867	0.88298	0.8973	0.8829
0.51722	1.0514	0.8987	0.9134
0.55968	1.1594	0.8991	0.9313
0.63200	1.3514	0.8997	0.9619
0.63766	1.3686	0.8998	0.9656
0.71392	1.5814	0.9022	0.9992
0.80228	1.8501	0.9068	1.0456
1.0188	2.5584	0.9232	1.1592
1.1095	2.8813	0.9318	1.2099

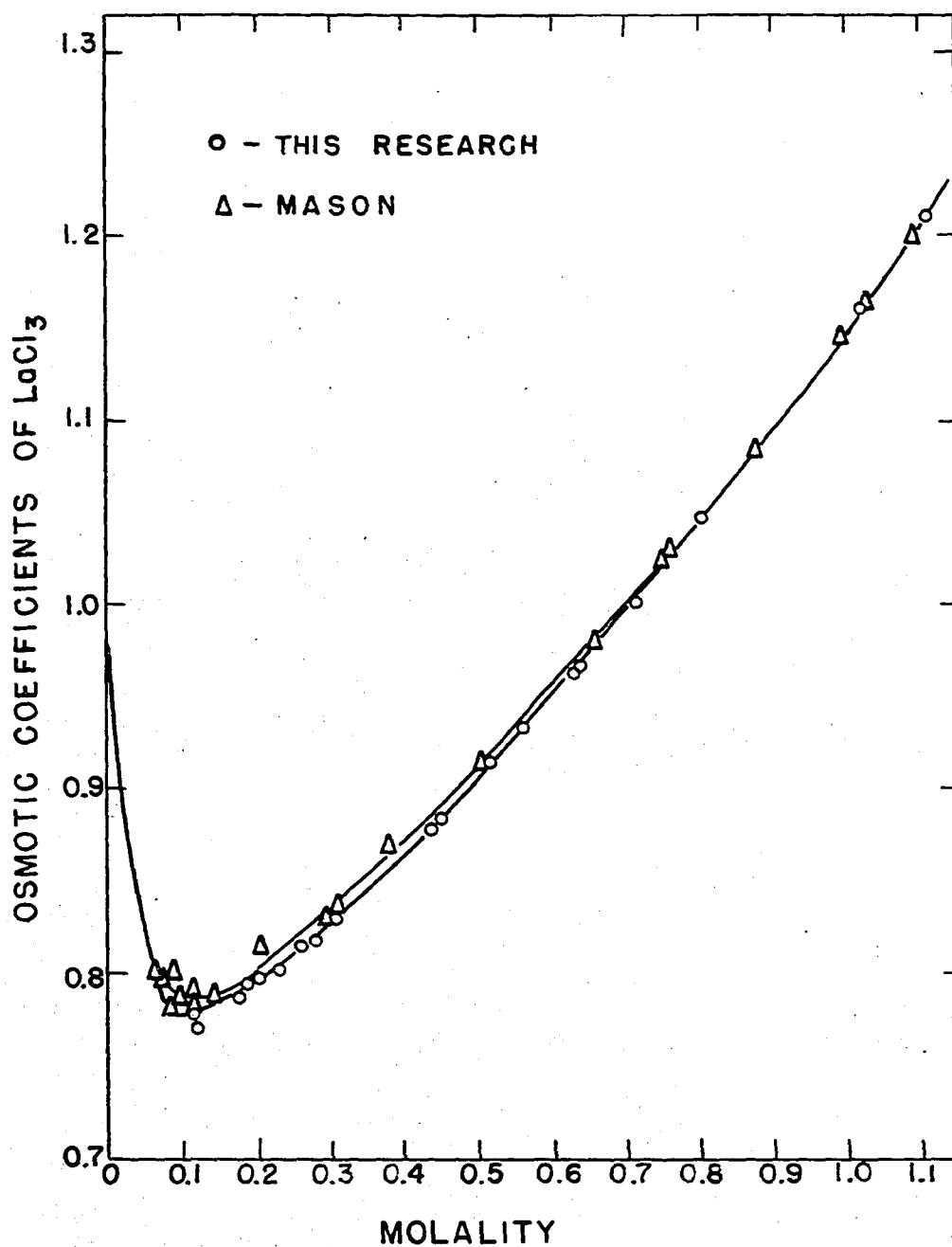


Figure 5. Molal osmotic coefficients of  $\text{LaCl}_3$  at  $25.00^\circ\text{C}$ .

Table XVII. Comparison of  $\text{LaCl}_3$  osmotic coefficients

Molality	Osmotic coefficient	
	Mason (Ref. 113)	This research
1.1	1.205	1.205
1.0	1.150	1.149
0.8	1.046	1.046
0.6	0.952	0.948
0.5	0.910	0.905
0.4	0.869	0.863
0.3	0.831	0.826
0.2	0.801	0.797
0.1	0.788	0.778

In order to use Equation III, derived in the section on isopiestic theory, the curve of  $h/\sqrt{m}$  vs.  $\sqrt{m}$  must be plotted, with which the graphical integration can be made. The limits of the integration are from zero to  $\sqrt{m}$ . However the isopiestic method does not yield data with any precision below 0.1 molal. On the other hand, the nature of the  $h/\sqrt{m}$  vs.  $\sqrt{m}$  curve makes any extrapolation to zero concentration very uncertain without the assistance of points below 0.1 molal. Robinson (128) adopted the electromotive force of cells data of Shedlovsky and MacInnes (129) to calculate points below 0.1 molal for his extrapolation, but this procedure cannot be used with other salts, such as the nitrates. Mason (113, 114) developed several extrapolation methods based on the Debye-Hückel theory for activity coefficients, all of them giving different results. For this research three different methods of applying Equation III, to calculate  $\text{LaCl}_3$

activity coefficients, were undertaken for comparative purposes.

Method A: In order to continue comparing the results of this research with those of Mason, one of his extrapolation procedures was used for the data in Table XVI, so that treatment of the experimental data could be the same. Mason estimated the intercept on the  $h/\sqrt{m}$  axis by assuming the geometry of the curve to be of some such form as

$$\frac{h}{\sqrt{m}} = a + b\sqrt{m} + c m$$

where the constant "a" would be the intercept on the  $h/\sqrt{m}$  axis. The integral term in Equation III would then become

$$\int_0^{\sqrt{m}} \frac{h}{\sqrt{m}} d\sqrt{m} = a\sqrt{m} + \frac{1}{2}bm + \frac{1}{3}cm^{3/2}$$

Since  $\log(\delta_{\pm})_{\text{LaCl}_3}$  can be found from the Debye-Hückel theory, Equation III reduces to

$$(\log \delta_{\pm})_{\text{LaCl}_3}^{\text{Debye-Hückel}} = \frac{-h - 2(a\sqrt{m} - \frac{1}{2}bm - \frac{1}{3}cm^{3/2})}{2.30258}$$

By substituting three values of  $m$  in the above equation, the constants  $a$ ,  $b$ , and  $c$  could be evaluated. Using some such method as this, Mason calculated an intercept of 2.844 on the  $h/\sqrt{m}$  axis. By extrapolating the  $h/\sqrt{m}$  vs.  $\sqrt{m}$  curve of the data in Table XVI to Mason's intercept, and measuring the areas under the curve on large graph paper with a Keuffel and Esser compensating polar planimeter, the  $\text{LaCl}_3$  activity coefficients were calculated



from Equation III. Results appear in Table XVIII:

Table XVIII. Calculation of activity coefficients of  $\text{LaCl}_3$  (A)  
(Extrapolation to 2.844)

m	$\int_0^{\sqrt{m}} h/\sqrt{m} d\sqrt{m}$	$\delta_{\pm} \text{LaCl}_3$	$\delta_{\pm}$ of Mason (113)
0.1	0.44361	0.3280	0.333
0.2	0.51953	0.2887	0.292
0.3	0.55785	0.2758	0.297
0.4	0.58045	0.2733	0.277
0.5	0.59339	0.2775	0.282
0.6	0.60021	0.2862	0.290
0.7	0.60243	0.2982	0.303
0.8	0.60125	0.3139	0.318
0.9	0.59725	0.3330	0.338
1.0	0.59089	0.3560	0.360
1.1	0.41737	0.3825	0.388

Method B: If only areas under the curve from 0.1 molal and up are measured, there need be no geometric assumption for the extrapolation of the curve below this lower limit of the isopiestic data. Such a procedure would yield differences in logs of the activity coefficient at  $m = 0.1$  and  $m = m$ . For this method, the value at  $m = 0.1$  was calculated directly from the Debye-Hückel equation for activity coefficients. The rational activity coefficient, given by the Debye-Hückel equation on page 21, is related to

the molal activity coefficient by the relation

$$\log(\gamma_{\pm}) = \log(f_{\pm}) - \log(1 + \nu m M_1 / 1000)$$

in which  $\nu$  is the number of moles of ions into which one mole of solute dissociates, and  $M_1$  is the molecular weight of the solvent. The Ionic Strength  $S$ , in terms of which the equation on page 21 is written, is related to the molarity  $C$  by

$$S = \frac{1}{2} C (\nu_+ z_+^2 + \nu_- z_-^2),$$

and the molarity is calculated from the molality by

$$C = 1000 m d / (1000 + m M_2),$$

in which  $d$  is the density, and  $M_2$  is the molecular weight of the solute. Values of the fundamental physical constants needed for the Debye-Hückel equation have been given on page 57. Spedding, Porter, and Wright (31) give 5.75 Angstroms as the value of the  $a$  parameter for lanthanum chloride. With all these substitutions, the Debye-Hückel equation used to calculate activity coefficients for dilute solutions of  $\text{LaCl}_3$  was

$$\log(\gamma_{\pm})_{\text{LaCl}_3} = \frac{-3.7419 \sqrt{\frac{1000 m d}{1000 + m M_2}}}{1 + 4.6290 \sqrt{\frac{1000 m d}{1000 + m M_2}}} - \log(1 + 0.07206 m)$$

From this equation, at  $m = 0.1$ ,  $\gamma_{\pm} = 0.3289$ .

To obtain the logarithm differences for the activity coefficients, Equation III was applied as follows:

$$\log(\delta_m) = \frac{-h \int_0^{0.31623} \frac{h}{\sqrt{m}} d\sqrt{m} - 2 \int_{0.31623}^{\sqrt{m}} \frac{h}{\sqrt{m}} d\sqrt{m}}{2.30258}$$

$$\log(\delta_{0.1}) = \frac{-(h)_{0.1} - 2 \int_0^{0.31623} \frac{h}{\sqrt{m}} d\sqrt{m}}{2.30258}$$

$$\left[ \log(\delta_{0.1}) - \log(\delta_m) \right] = \frac{-(h)_{0.1} + h + 2 \int_{0.31623}^{\sqrt{m}} \frac{h}{\sqrt{m}} d\sqrt{m}}{2.30258} \quad (\text{IV})$$

Then the activity coefficient at molality  $m$ , relative to the calculated Debye-Hückel value at 0.1 molal, is

$$\log(\delta_{\pm})_m = -\left[ \log(\delta_{0.1}) - \log(\delta_m) \right] + \left[ \log(\delta_{0.1})_{\text{Debye-Hückel}} \right].$$

The results of these calculations appear in Table XIX.

Method C: This method also makes use of the difference in logs of the activity coefficients at two concentrations, but the reference concentration was taken to be 0.03119 at which Spedding, Porter, and Wright (31) give  $\delta_{\pm} = 0.4319$ . The  $h/\sqrt{m}$  vs.  $\sqrt{m}$  curve could be extrapolated fairly

Table XIX. Calculation of Activity Coefficients of  $\text{LaCl}_3$  (B)  
 $(\gamma_{0.1}) = 0.3289$

$m$	$\int_{0.31623}^{\sqrt{m}} \frac{h}{\sqrt{m}} d\sqrt{m}$	$[\log(\gamma_{0.1}) - \log(\gamma_m)]$	$\gamma_{\pm\text{LaCl}_3}$
0.1	0.0	0.0	0.3289
0.2	0.07592	0.05539	0.2896
0.3	0.11424	0.07521	0.2766
0.4	0.13684	0.07925	0.2741
0.5	0.14978	0.07251	0.2784
0.6	0.15660	0.05915	0.2871
0.7	0.15882	0.04128	0.2991
0.8	0.15764	0.01906	0.3148
0.9	0.15364	-0.00661	0.3340
1.0	0.14728	-0.03563	0.3571
1.1	0.13880	-0.06679	0.3836

easily to this concentration, from which the reference value of  $h$  was found to be  $(h)_{0.03119} = 0.2045$ . Therefore, for this method, Equation IV became

$$[\log(\gamma_{0.03119}) - \log(\gamma_m)] = \frac{-0.2045 + h + 2 \int_{0.1766}^{\sqrt{m}} \frac{h}{\sqrt{m}} d\sqrt{m}}{2.30258}$$

The results of the calculations by Method C are given in Table XX.

Table XX. Calculation of activity coefficients of  $\text{LaCl}_3$  (C)  
 $(\gamma_{0.03119}) = 0.4319$

$m$	$\int_{0.1766}^{\sqrt{m}} h/\sqrt{m} d\sqrt{m}$	$[\log(\gamma_{0.03119}) - \log(\gamma_m)]$	$\gamma_{\pm \text{LaCl}_3}$
0.03119	0.0	0.0	0.4319
0.1	0.12817	0.12136	0.3266
0.2	0.20409	0.17675	0.2875
0.3	0.24241	0.19657	0.2747
0.4	0.26501	0.20061	0.2721
0.5	0.27795	0.19387	0.2764
0.6	0.28477	0.18051	0.2850
0.7	0.28699	0.16263	0.2970
0.8	0.28581	0.14042	0.3126
0.9	0.28181	0.11475	0.3316
1.0	0.27545	0.08573	0.3545
1.1	0.26697	0.05456	0.3809

A final comparison of all the lanthanum chloride activity coefficient data is shown in Table XXI. Included in this table are the results reported by Robinson (127,128) in 1937 and 1939, and by Mason (113,114) in 1938 and 1941. Results of the three methods of calculation used in this research are summarized in the last three columns of the table.

#### 4. Calculations and Results for the Rare-earth Nitrates

Osmotic coefficients were calculated from the experimental data by using the isopiestic equilibrium condition, Equation I, discussed previously.

Table XXI. Comparison of activity coefficients for  $\text{LaCl}_3$

m	Robinson (127)	Robinson (128)	Mason (113)	Mason (114)	Method A	This Research Method B	Method C
0.1	0.325	0.383	0.333	0.356	0.328	0.329	0.327
0.2	0.279	0.337	0.292	0.312	0.289	0.290	0.288
0.3	0.265	0.323	0.297	0.298	0.276	0.277	0.275
0.4	0.264	0.322	0.277	0.295	0.273	0.274	0.272
0.5	0.269	0.328	0.282	0.303	0.278	0.278	0.276
0.6	0.278	0.338	0.290	0.312	0.286	0.287	0.285
0.7	0.292	0.354	0.303	0.324	0.298	0.299	0.297
0.8	0.317	0.373	0.318	0.340	0.314	0.315	0.313
0.9	0.336	0.396	0.338	0.362	0.333	0.334	0.332
1.0	0.358	0.424	0.360	0.387	0.356	0.357	0.355
1.1	0.385	0.456	0.388	0.416	0.382	0.384	0.381

Robinson's second set of results (128) should be lowered by 0.061 to bring the data into accord with Shedlovsky's (125)  $\text{LaCl}_3$  corrected data published subsequently to Robinson's work.

Mason's second set of activity coefficients (114) were calculated by a semi-empirical method, entirely different from that used in this research.

As with Method B used for  $\text{LaCl}_3$ , the graphical integrations necessary in Equation III were made from a reference concentration, at which the Debye-Hückel theory may be applied, up to the experimental molality. The reference concentration chosen for the nitrate calculations was 0.04 molal, since this is more in the range where the Debye-Hückel theory might be applicable, than the concentration 0.1 molal at the lower limit of the isopiestic data. By calculating a few Debye-Hückel points in the range below 0.04 molal, and plotting them on an  $h/\sqrt{m}$  vs.  $\sqrt{m}$  curve, the experimental  $h/\sqrt{m}$  vs.  $\sqrt{m}$  curve could very easily be extrapolated to 0.04 molal with a slope coinciding with the Debye-Hückel curve coming in to 0.04 molal from the opposite direction. (The single exception to this procedure was the curve for holmium nitrate, which will be discussed later. The integration plot of  $\frac{h}{\sqrt{m}}$  vs.  $\sqrt{m}$  for ytterbium nitrate, typical also for samarium and erbium nitrates, is shown in Figure 6. The integration curve for holmium nitrate is illustrated in Figure 7.

In order to use the Debye-Hückel equation for activity coefficients, some evaluation of the distance-of-closest-approach parameters,  $\overset{\circ}{a}$ , had to be made for the rare-earth nitrates. The method used was that of Jaffe (35) who employed the electrophoretic conductance equations of Dye (8) to estimate values of the  $\overset{\circ}{a}$ -parameter from experimental conductance data for the required salt. Dye's expressions for the electrophoretic contribution to the conductance, given on pages 29 and 30, depend on the same identical  $\overset{\circ}{a}$ -parameter that appears in the Debye-Hückel theory, so that values of  $\overset{\circ}{a}$  giving the best fit for the conductance data may be used to calculate  $\sigma_{\pm}$ .

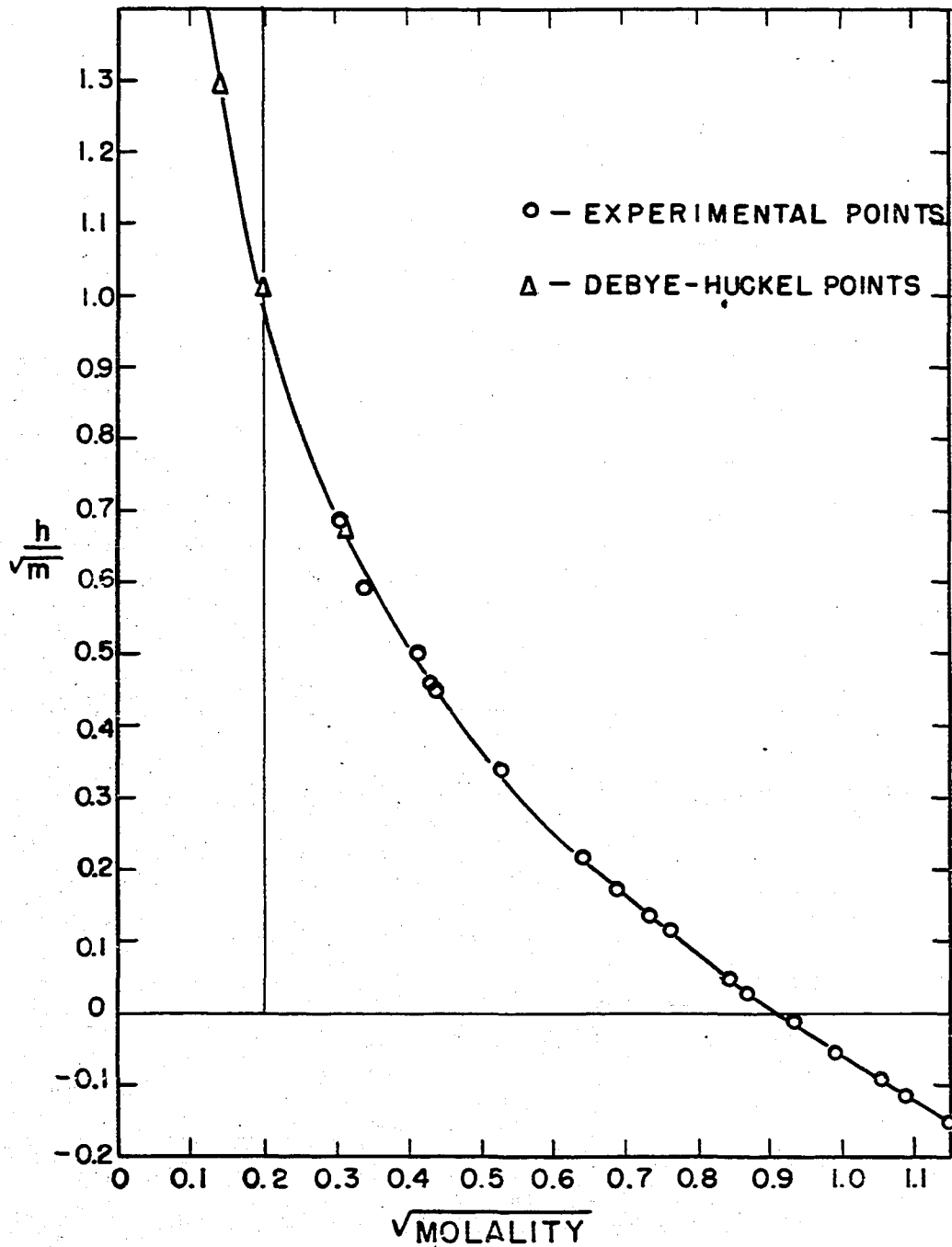


Figure 6. Graphical integration of  $\text{Yb}(\text{NO}_3)_3$  isopiestic data for calculation of activity coefficients.



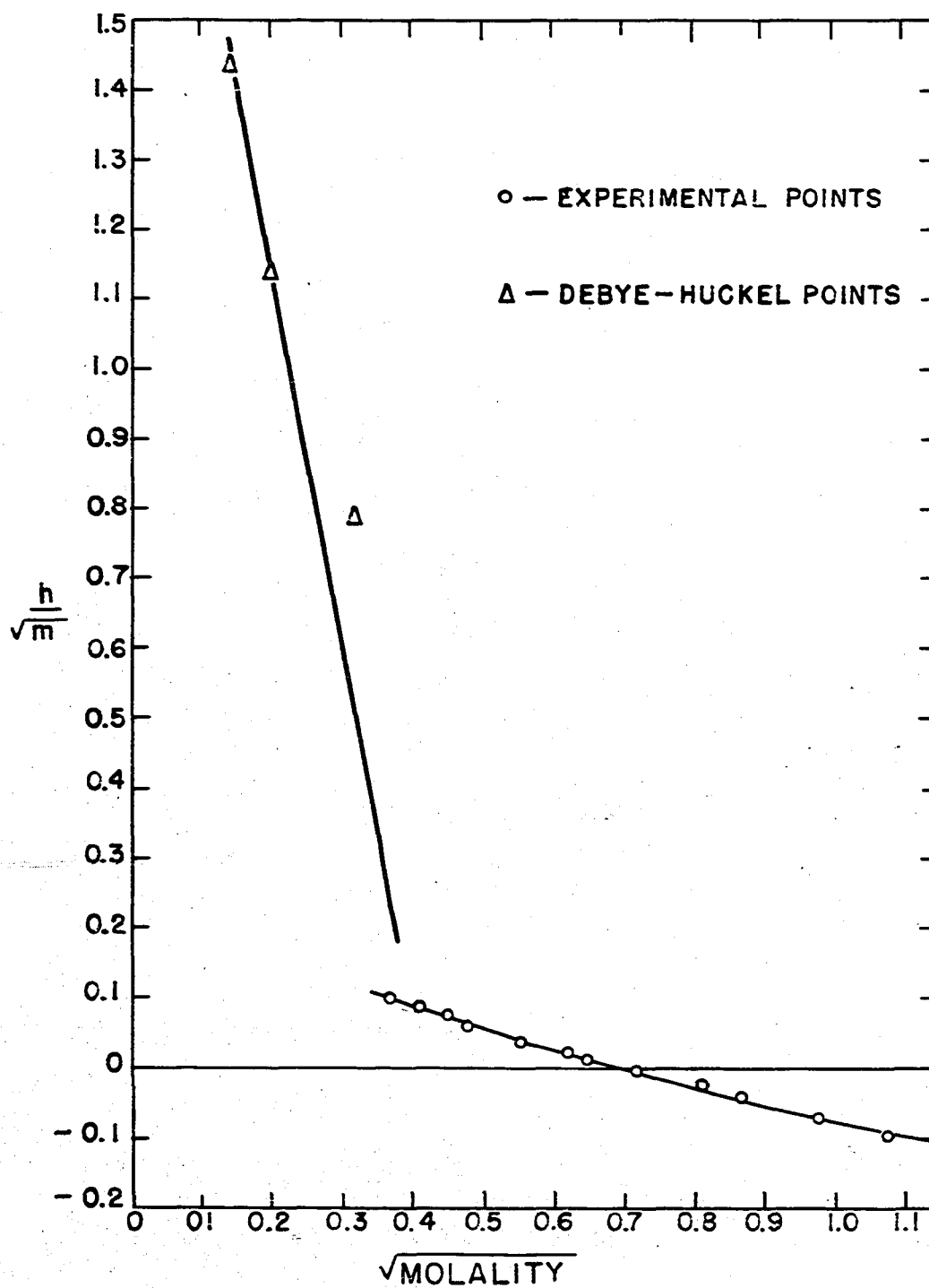


Figure 7. Graphical integration of  $\text{Ho}(\text{NO}_3)_3$  isopiestic data for calculation of activity coefficients.

The form of the Onsager law given on page 57 was rearranged in the following way:

$$\Lambda_0 = (\Lambda + \Delta\Lambda_{\text{Electrophoretic}}) + \frac{2.48719 \Lambda_0^2 c_n}{(\Lambda_0 + 142.84) \left( 1 + \sqrt{\frac{0.75}{\Lambda_0 + 142.84}} \right)}$$

For a particular selected value of  $\overset{\circ}{a}$ , values of  $\Lambda_0$  were calculated from the above equation in the concentration range 0 to 0.01 Normal for the given rare-earth nitrate. The value of  $\overset{\circ}{a}$  giving a set of constant values for  $\Lambda_0$  through the widest concentration range, i.e., a flat curve for  $\Lambda_0$  vs.  $\sqrt{C_n}$ , was selected as the correct value of the parameter for that salt. Results of these calculations are given in Table XXII.

Table XXII. Values of  $\overset{\circ}{a}$  in ångstroms from conductance data

Salt	$\overset{\circ}{a}$
Sm(NO <sub>3</sub> ) <sub>3</sub>	4.4
Ho(NO <sub>3</sub> ) <sub>3</sub>	5.1
Er(NO <sub>3</sub> ) <sub>3</sub>	5.6
Yb(NO <sub>3</sub> ) <sub>3</sub>	6.05

From these values of  $\bar{a}$ , activity coefficients were calculated from the Debye-Hückel equation

$$\log(\gamma_{\pm})_{\text{R.E.}(\text{NO}_3)_3} = \frac{-3.7419 \sqrt{\frac{1000m}{1000 + mM_2}}}{1 + 0.80505 \bar{a} \sqrt{\frac{1000m}{1000 + mM_2}}} - \log(1 + 0.07206km)$$

and molal osmotic coefficients were calculated from Equation II in the isopiestic theory section. Results are given in Table XXIII.

Table XXIII. Debye-Hückel activity coefficients for rare-earth nitrates

Salt	Molality	$\gamma_{\pm}$	$\phi$
$\text{Sm}(\text{NO}_3)_3$	0.005	0.6144	0.8425
	0.01	0.5293	0.8130
	0.02	0.4439	0.7778
	0.04	0.3642	0.7450
$\text{Ho}(\text{NO}_3)_3$	0.005	0.6238	0.8563
	0.01	0.5429	0.8250
	0.02	0.4624	0.7967
	0.04	0.3877	0.7717
$\text{Er}(\text{NO}_3)_3$	0.005	0.6301	0.8680
	0.01	0.5522	0.8372
	0.02	0.4749	0.8080
	0.04	0.4034	0.7853
$\text{Yb}(\text{NO}_3)_3$	0.005	0.6357	0.8720
	0.01	0.5602	0.8425
	0.02	0.4857	0.8172
	0.04	0.4170	0.7984

Experimental isopiestic molalities and osmotic coefficients for the nitrates of samarium, holmium, erbium, and ytterbium are presented in Tables XXIV - XXVII on the following pages. In Tables XXVIII - XXX appear values of  $\phi$  at round concentrations, read from the  $h/\sqrt{m}$  vs.  $\sqrt{m}$  curves; measured values of the areas under the integration curves; and the log differences for the activity coefficients, calculated from the relation

$$\frac{[\log(\gamma_{0.04}) - \log(\gamma_m)]}{2.30258} = \frac{-(h)_{0.04} + h_m + 2 \int_{0.2}^{\sqrt{m}} h/\sqrt{m} d\sqrt{m}}{2.30258}$$

The final columns in Tables XXVIII - XXX show the mean molal activity coefficient,  $\gamma_{\pm}$ , calculated from

$$\log(\gamma_{\pm})_m = - [\log(\gamma_{0.04}) - \log(\gamma_m)] + [\log(\gamma_{0.04})]_{\text{Debye-Hückel}}$$

in which  $[\log(\gamma_{0.04})]_{\text{Debye-Hückel}}$  was obtained from Table XXIII.

The values of  $\gamma_{\pm}$  for  $\text{Ho}(\text{NO}_3)_3$  were calculated from an arbitrary reference point, taken at  $(\gamma_{\pm})_{0.1 \text{ molal}} = 0.326$ , the value for  $\text{La}(\text{NO}_3)_3$  given by Lewis and Randall in Thermodynamics (130), p. 362. The results of this computation from round values of the osmotic coefficients appear in Table XXXI.

Osmotic coefficients for the four nitrates are plotted in Figure 8. The activity coefficients calculated as shown in Tables XXVIII - XXX are plotted in Figure 9. The final graph, Figure 10, shows the activity coefficient curve for  $\text{Ho}(\text{NO}_3)_3$  based on an arbitrary reference point, from the data in Table XXXI.

Table XXIV. Isopiestic molalities and osmotic coefficients for  $\text{Sm}(\text{NO}_3)_3$  and  $\text{KCl}$

$m_{\text{Sm}(\text{NO}_3)_3}$	$m_{\text{KCl}}$	$\phi_{\text{KCl}}$	$\phi_{\text{Sm}(\text{NO}_3)_3}$
0.10535	0.17129	0.9157	0.7444
0.12698	0.20677	0.9125	0.7430
0.18739	0.30427	0.9061	0.7356
0.34584	0.58286	0.8987	0.7573
0.38155	0.64808	0.8980	0.7626
0.44286	0.76530	0.8974	0.7754
0.51918	0.91412	0.8974	0.7901
0.73144	1.3532	0.9027	0.8350
0.85701	1.6342	0.9037	0.8616
0.89592	1.7250	0.9051	0.8713
0.90566	1.7477	0.9055	0.8737
0.93758	1.8214	0.9067	0.8807
1.0285	2.0392	0.9109	0.9030
1.2387	2.5584	0.9232	0.9534
1.3633	2.8813	0.9318	0.9847
1.5230	3.3179	0.9442	1.0285

Table XXV. Isopiestic molalities and osmotic coefficients for  $\text{Ho}(\text{NO}_3)_3$  and  $\text{KCl}$ 

$m_{\text{Ho}(\text{NO}_3)_3}$	$m_{\text{KCl}}$	$\phi_{\text{KCl}}$	$\phi_{\text{Ho}(\text{NO}_3)_3}$
0.11794	0.25084	0.9093	0.9670
0.13453	0.28575	0.9070	0.9633
0.16555	0.35322	0.9038	0.9642
0.20196	0.43217	0.9013	0.9644
0.22338	0.48145	0.9003	0.9702
0.30453	0.66223	0.8979	0.9763
0.38470	0.84624	0.8973	0.9869
0.41328	0.91224	0.8974	0.9905
0.51551	1.1499	0.8993	1.0029
0.65698	1.4841	0.9017	1.0185
0.75176	1.7154	0.9049	1.0325
0.95120	2.2239	0.9149	1.0696
1.1570	2.7460	0.9282	1.1014
1.3248	3.1694	0.9399	1.1243
1.5828	3.8576	0.9601	1.1700
1.6656	4.0712	0.9665	1.1812
1.8744	4.6361	0.9839	1.2167

Table XXVI. Isopiestic molalities and osmotic coefficients for  $\text{Er}(\text{NO}_3)_3$  and  $\text{KCl}$ 

$m_{\text{Er}(\text{NO}_3)_3}$	$m_{\text{KCl}}$	$\phi_{\text{KCl}}$	$\phi_{\text{Er}(\text{NO}_3)_3}$
0.10503	0.18224	0.9146	0.7935
0.15990	0.27912	0.9074	0.7920
0.18431	0.32583	0.9050	0.7999
0.29414	0.53592	0.8993	0.8193
0.30083	0.55137	0.8991	0.8239
0.45518	0.88398	0.8973	0.8713
0.56778	1.1305	0.8992	0.8951
0.63485	1.2898	0.9000	0.9142
0.70508	1.4630	0.9015	0.9353
0.89175	1.9438	0.9089	0.9906
1.0128	2.2735	0.9161	1.0282
1.1847	2.7655	0.9281	1.0832
1.2686	3.0095	0.9354	1.1095
1.3632	3.2943	0.9435	1.1400
1.4074	3.4298	0.9474	1.1544
1.4950	3.6887	0.9550	1.1782
1.5390	3.8240	0.9591	1.1915
1.6878	4.2926	0.9733	1.2377
1.7502	4.4847	0.9792	1.2545

Table XXVII. Isopiestic molalities and osmotic coefficients for  $\text{Yb}(\text{NO}_3)_3$  and  $\text{KCl}$ 

$m_{\text{Yb}(\text{NO}_3)_3}$	$m_{\text{KCl}}$	$\phi_{\text{KCl}}$	$\phi_{\text{Yb}(\text{NO}_3)_3}$
0.096766	0.16656	0.9161	0.7884
0.11694	0.20454	0.9127	0.7982
0.17197	0.30087	0.9062	0.7927
0.18735	0.33182	0.9047	0.8011
0.19055	0.33734	0.9045	0.8006
0.28176	0.51359	0.8997	0.8200
0.41478	0.79542	0.8973	0.8604
0.47774	0.93786	0.8975	0.8810
0.54254	1.0869	0.8987	0.9002
0.58344	1.1859	0.8992	0.9139
0.70930	1.5069	0.9020	0.9581
0.75748	1.6338	0.9037	0.9746
0.87302	1.9438	0.9089	1.0119
0.98905	2.2735	0.9161	1.0529
1.1148	2.6464	0.9255	1.0985
1.1892	2.8722	0.9316	1.1250
1.3225	3.2943	0.9435	1.1751
1.3658	3.4298	0.9474	1.1896
1.5017	3.8679	0.9604	1.2368
1.6302	4.2926	0.9733	1.2814
1.6870	4.4847	0.9792	1.3015



Table XXVIII. Osmotic and activity coefficients for  $\text{Sm}(\text{NO}_3)_3$  at round concentrations

$m$	$\phi$	$\int_{0.2}^{\sqrt{m}} h/\sqrt{m} d\sqrt{m}$	$[\log(\gamma_{0.04}) - \log(\gamma_m)]$	$\gamma_{\pm\text{Sm}(\text{NO}_3)_3}$
0.04	0.7450	0.0	0.0	0.3642
0.1	0.7447	0.11800	0.10262	0.2876
0.2	0.7356	0.20802	0.18477	0.2380
0.3	0.7472	0.26061	0.22541	0.2167
0.4	0.7672	0.29577	0.24726	0.2061
0.5	0.7870	0.32063	0.26026	0.2000
0.6	0.8067	0.33927	0.26789	0.1965
0.7	0.8273	0.35345	0.27126	0.1950
0.8	0.8491	0.36421	0.27114	0.1951
0.9	0.8721	0.37249	0.26834	0.1963
1.0	0.8958	0.37857	0.26333	0.1986
1.1	0.9203	0.38301	0.25655	0.2018
1.2	0.9440	0.38597	0.24883	0.2054
1.3	0.9692	0.38771	0.23939	0.2099
1.4	0.9947	0.38842	0.22893	0.2150
1.5	1.0216	0.38816	0.21703	0.2210
1.6	1.0496	0.38702	0.20388	0.2278

Table XXIX. Osmotic and activity coefficients for  $\text{Er}(\text{NO}_3)_3$  at round concentrations

$m$	$\phi$	$\int_{0.2}^{\sqrt{m}} h/\sqrt{m} d\sqrt{m}$	$[\log(\phi_{0.04}) - \log(\gamma_m)]$	$\gamma_{\pm} \text{Er}(\text{NO}_3)_3$
0.04	0.7853	0.0	0.0	0.4034
0.1	0.7933	0.09620	0.08008	0.3354
0.2	0.8026	0.16746	0.13794	0.2936
0.3	0.8225	0.20576	0.16257	0.2774
0.4	0.8547	0.22938	0.16910	0.2733
0.5	0.8797	0.24404	0.17097	0.2721
0.6	0.9046	0.25396	0.16878	0.2735
0.7	0.9341	0.26020	0.16138	0.2782
0.8	0.9639	0.26368	0.15146	0.2846
0.9	0.9931	0.26497	0.13990	0.2923
1.0	1.0238	0.26455	0.12621	0.3016
1.1	1.0553	0.26268	0.11090	0.3125
1.2	1.0876	0.25963	0.09422	0.3247
1.3	1.1195	0.25549	0.07677	0.3380
1.4	1.1506	0.25047	0.05891	0.3522
1.5	1.1803	0.24471	0.04101	0.3670
1.6	1.2098	0.23857	0.02286	0.3827
1.7	1.2396	0.23171	0.00396	0.3997
1.8	1.2710	0.22441	-0.01602	0.4185

Table XXX. Osmotic and activity coefficients for  $\text{Yb}(\text{NO}_3)_3$  at round concentrations

$m$	$\phi$	$\int_{0.2}^{\sqrt{m}} h/\sqrt{m} d\sqrt{m}$	$[\log(\gamma_{0.04}) - \log(\gamma_m)]$	$\gamma_{\pm \text{Yb}(\text{NO}_3)_3}$
0.04	0.7984	0.0	0.0	0.4170
0.1	0.7883	0.09542	0.08727	0.3411
0.2	0.8026	0.16662	0.14286	0.3001
0.3	0.8246	0.20480	0.16651	0.2842
0.4	0.8561	0.22806	0.17303	0.2800
0.5	0.8876	0.24258	0.17196	0.2806
0.6	0.9196	0.25132	0.16566	0.2847
0.7	0.9547	0.25616	0.15462	0.2921
0.8	0.9886	0.25812	0.14160	0.2991
0.9	1.0206	0.25788	0.12749	0.3109
1.0	1.0550	0.25593	0.11086	0.3230
1.1	1.0927	0.25238	0.09140	0.3378
1.2	1.1295	0.24762	0.07129	0.3538
1.3	1.1667	0.24160	0.04990	0.3717
1.4	1.2021	0.23482	0.02864	0.3904
1.5	1.2365	0.22718	0.00706	0.4102
1.6	1.2718	0.21884	-0.01551	0.4321
1.7	1.3067	0.21024	-0.03814	0.4552

Table XXXI. Osmotic coefficients and activity coefficients of  $\text{Ho}(\text{NO}_3)_3$  based on  $(\gamma_{\pm})_{0.1} = 0.326$

m	$\phi$	$[\log(\gamma_{0.1}) - \log(\gamma_m)]$	$\gamma_{\pm} \text{Ho}(\text{NO}_3)_3$
0.1	0.9647	0.0	0.326
0.2	0.9673	0.009366	0.319
0.3	0.9757	0.01083	0.318
0.4	0.9869	0.008370	0.320
0.5	0.9996	0.003533	0.323
0.6	1.0134	-0.002953	0.328
0.7	1.0280	-0.01066	0.334
0.8	1.0431	-0.01928	0.341
0.9	1.0585	-0.02855	0.348
1.0	1.0743	-0.03844	0.356
1.1	1.0902	-0.04875	0.365
1.2	1.1063	-0.05946	0.374
1.3	1.1226	-0.07049	0.383
1.4	1.1388	-0.08174	0.393
1.5	1.1552	-0.09327	0.404
1.6	1.1716	-0.10496	0.415
1.7	1.1879	-0.11678	0.427
1.8	1.2043	-0.12877	0.438
1.9	1.2207	-0.14087	0.451

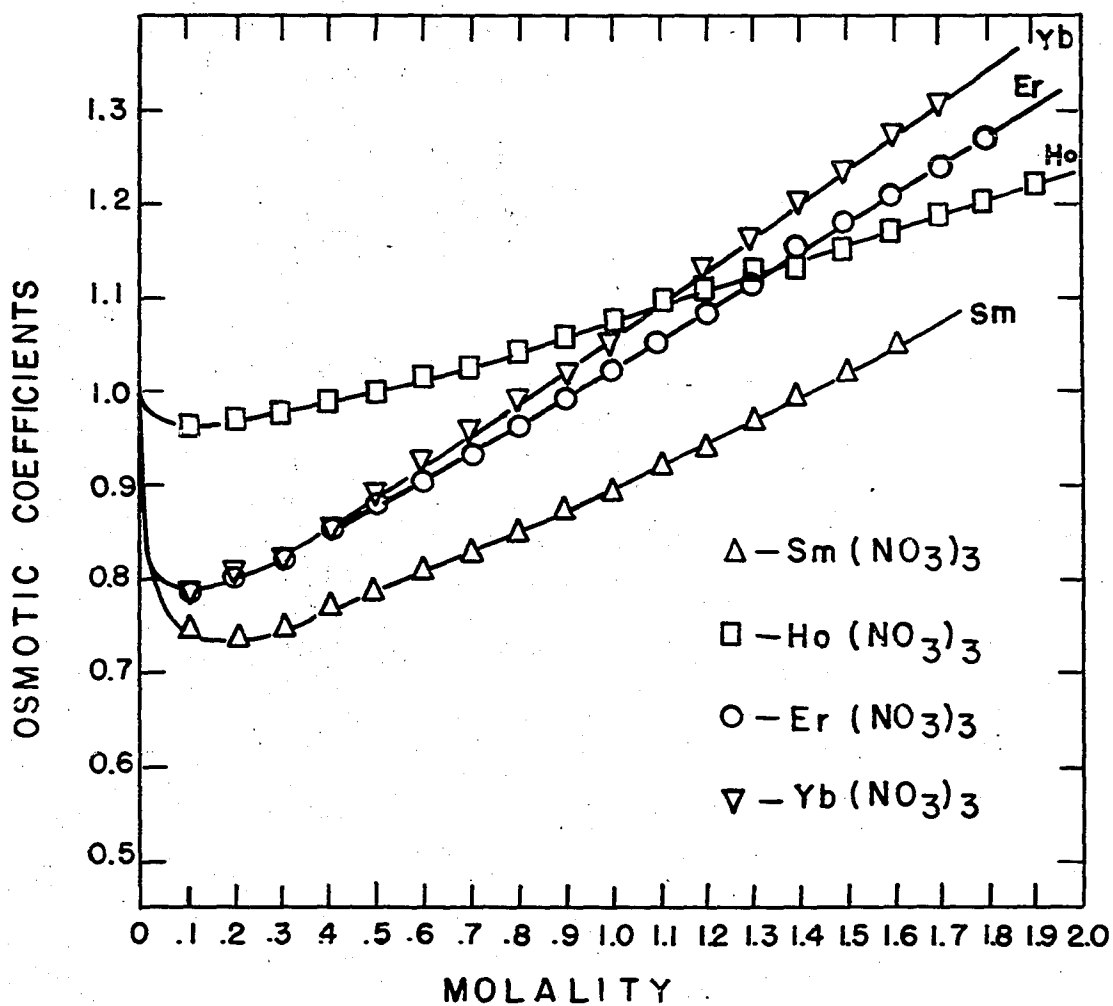


Figure 8. Molal osmotic coefficients of rare-earth nitrates at 25.00°C.

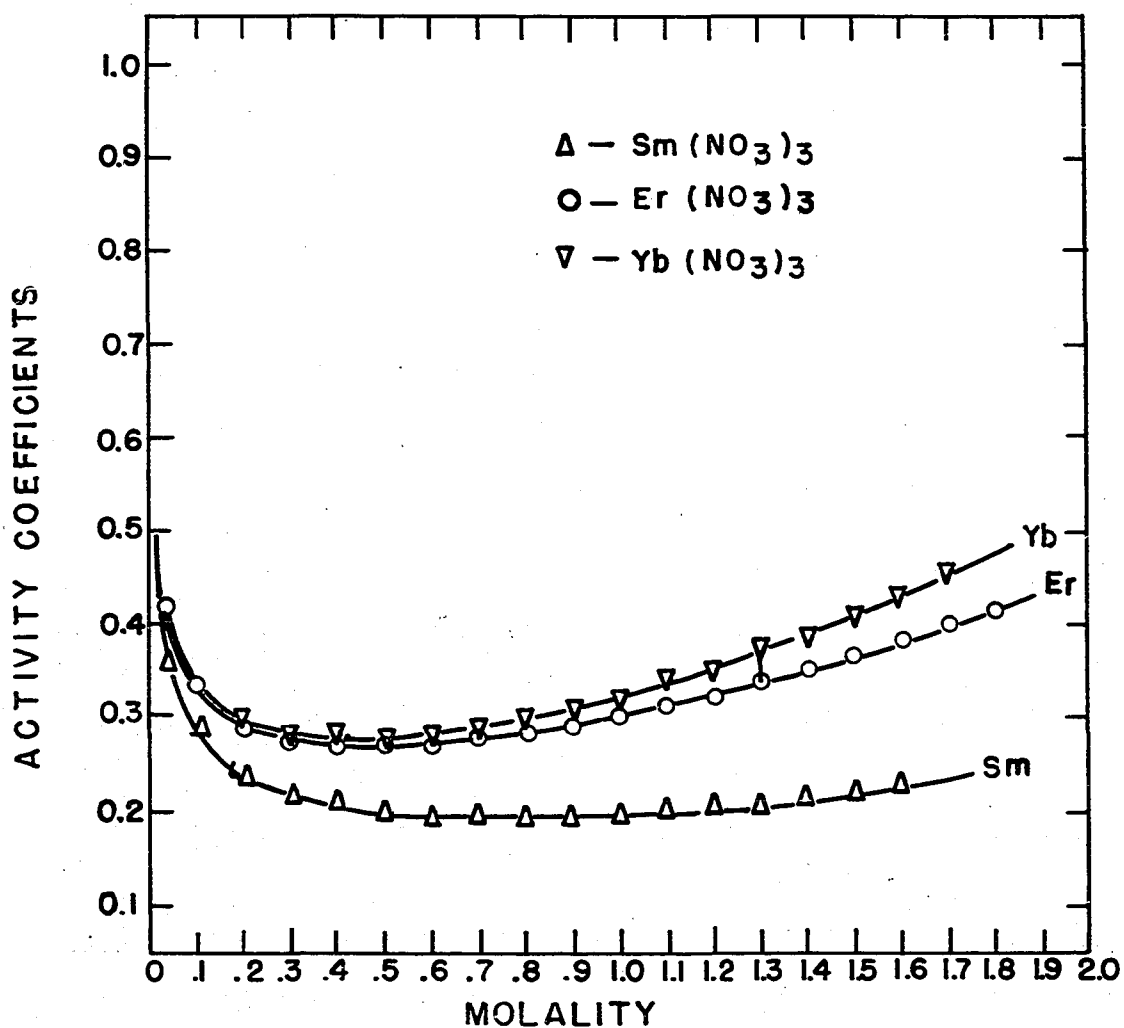


Figure 9. Molal activity coefficients of rare-earth nitrates, based on Debye-Hückel values at 0.04 m.

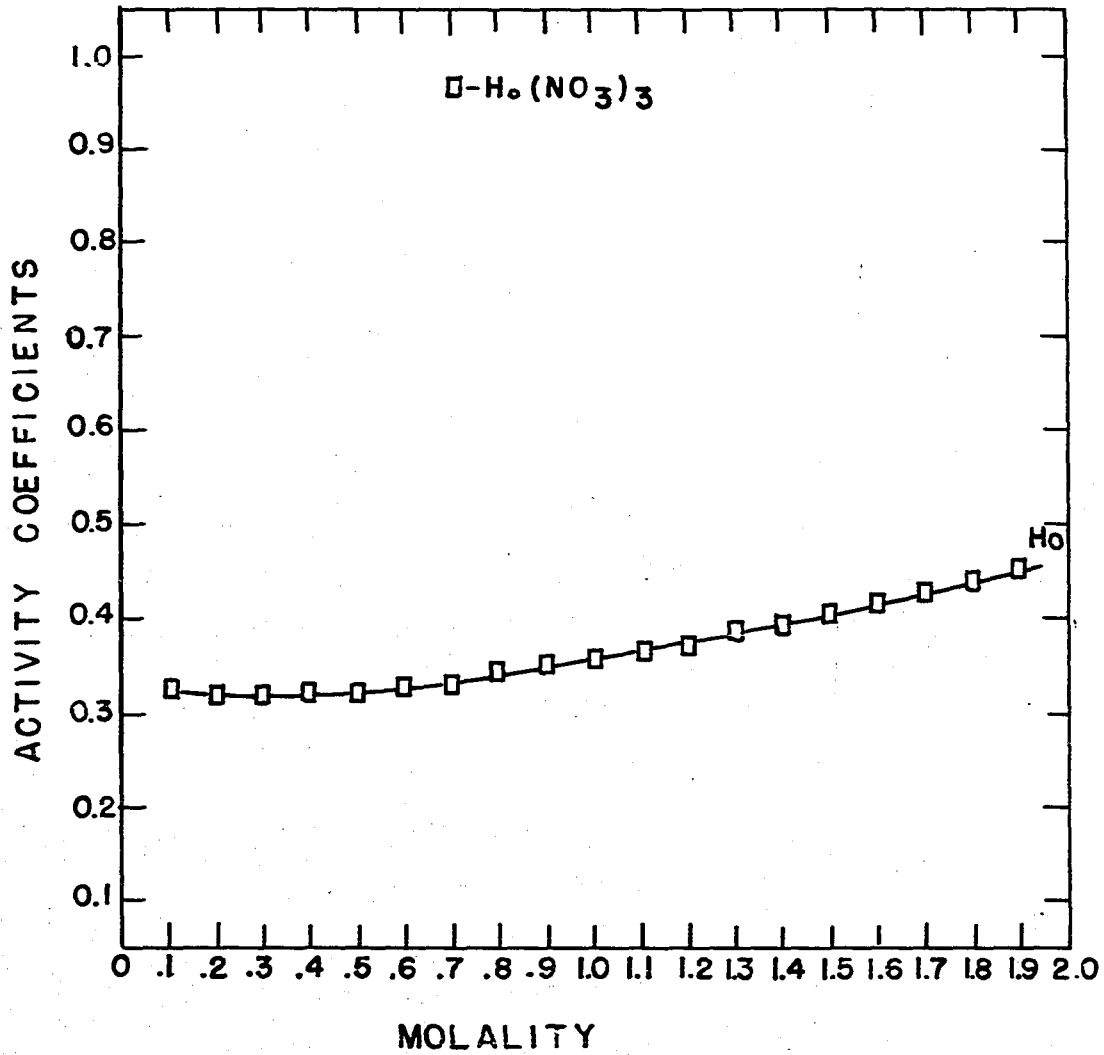


Figure 10. Molal activity coefficients of Ho(NO<sub>3</sub>)<sub>3</sub>, based on arbitrary reference value at 0.1 m.

## VI. GENERAL DISCUSSION AND CONCLUSIONS

The reliability of the data reported in this research is governed, in part, by the accuracy with which the solution concentrations are known. The average-deviations from the mean concentrations for sets of triplicate oxalate analyses of rare-earth nitrate solutions fell in the range  $\pm 0.06\%$  to  $\pm 0.006\%$ . Most of the analytical sets had average-deviations of better than  $\pm 0.04\%$ . In the case of activity coefficients, for which stock solutions of widely differing concentrations were used, analyses were made on each stock solution. For a set of solutions of any given rare-earth nitrate, the analyses were self-consistent by  $\pm 0.03\%$ ; that is, an analysis of a solution agreed with the concentration calculated from its weight dilution with this precision. For the volume dilutions used in the conductance and transference numbers work, samples of liquid could be delivered by a calibrated 20 ml. pipette with a reproducibility of 0.03%, and better for larger pipettes.

The reliability of the data also depends on the accuracy and precision with which the experimental measurements could be made. The null point on the Jones conductivity bridge could very easily be found with the following precisions: 20,000  $\pm 1$  ohm, 10,000.0  $\pm 0.2$  ohm, and 2,000.00  $\pm 0.04$  ohm. These are precisions of from 0.005% to 0.002%. The effect of the solvent correction

$$L_{\text{R.E.}(\text{NO}_3)_3} = L_{\text{measured}} - L_{\text{H}_2\text{O}},$$

is greatest for the most dilute solutions, and becomes smaller for in-



creasing concentrations. As an example one might consider 0.00036890 N  $\text{Sm}(\text{NO}_3)_3$ , for which the average  $L_{\text{measured}}$  was  $5.0477(10)^{-5}$ . The value for  $L_{\text{H}_2\text{O}}$  could easily be measured to three significant figures, which for this case was  $0.0742(10)^{-5}$ , and yields  $4.9735(10)^{-5} \text{ ohm}^{-1}\text{cm}^{-1}$  for  $L_{\text{Sm}(\text{NO}_3)_3}$ . Even if  $L_{\text{H}_2\text{O}}$  were in error by 1 in the second significant figure, the resultant error in the specific conductance of the  $\text{Sm}(\text{NO}_3)_3$  would be only 0.02%. As indicated under "Apparatus and Procedure" for the conductance work, each rare-earth nitrate solution was measured in two or three different conductance cells, and at least two samples of the same solution were measured in a given cell. The average-deviations of the experimental measurements from the reported average-values were never more than 0.1% in any case. Most generally the average-deviations were better than this; they extended to 0.01% for the more concentrated solutions. Throughout the concentration range studied for the four rare-earth nitrates, the mean of the average-deviations was 0.05%. Since the direct errors in the experimental measurements were less than this, the specific conductances reported in Tables III-VI have a precision of 0.05%. Their accuracy, on the other hand, depends directly on the calibration of the conductance cells. This aspect of the work has already been discussed on pages 51-53.

The precision of a derived result may be calculated from the relations

$$P_i = \frac{\partial D}{\partial i} E_i$$

$$P = \sqrt{\sum_i P_i^2}$$

in which  $E_i$  is the precision measure of the factor  $i$ , and  $P$  is the

precision of the calculated result, D. For the equivalent conductance,

$$\Lambda = \frac{1000 I_{R.E.(\text{NO}_3)_3}}{C_n}$$

the precision can be found for a particular example. From Table III the specific conductance of 0.0014764 N  $\text{Sm}(\text{NO}_3)_3$  is  $1.9098(10)^{-4} \text{ ohm}^{-1}\text{cm}^{-1}$ .

Therefore

$$P_L = \frac{\partial \Lambda}{\partial L} E_L = \frac{1000 E_L}{C_n} = \frac{1000 (1.9098(10)^{-4} \cdot 0.05\%)}{0.0014764} = 0.065 \quad ,$$

and

$$P_{C_n} = \frac{\partial \Lambda}{\partial C_n} E_{C_n} = \frac{-1000 I_{\text{Sm}(\text{NO}_3)_3}}{(C_n)^2} E_{C_n}$$

$$= \frac{1000 \cdot 1.9098(10)^{-4}}{(0.0014764)^2} (0.0014764 \cdot 0.04\%) = 0.052 \quad ,$$

so that

$$P = \sqrt{(0.065)^2 + (0.052)^2} = 0.083$$

The equivalent conductance and associated precision for 0.0014764 N  $\text{Sm}(\text{NO}_3)_3$  is consequently  $129.35 \pm 0.08 \text{ ohm}^{-1}\text{eq}^{-1}\text{cm}^2$ .

Errors in the measurement of transference numbers by the moving boundary method depend on the precision with which the time, voltage, and volume calibration of the measuring tube can be known. The time interval required by the boundary to travel between two adjacent marks on the tube was of

the order of 200 seconds. This could be measured on the stop-watch to 0.2 second, or 0.1%. As seen from the transference number experiment recorded in Table VIII, the average voltage across the standard resistor in series with the cell, was always within 0.02% of any of the experimental readings taken during the electrolysis. The volume calibrations were probably precise to 0.05%. Using the same procedure to find the precision of a derived result that was employed for the equivalent conductance, one can find the precision of the calculated transference number from the data in Table VIII to be  $T_{\pm} = 0.4565 \pm 0.0005$ .

The accuracy and precision of the experimental isopiestic molalities for the determination of activity coefficients depend on how precise the concentrations of the stock solutions were known, and how well identical solutions in an equilibration chamber could be made to agree. As stated previously the molalities of the stock solutions were known to  $\pm 0.04\%$ . An equilibration was considered completed when the concentrations of both solutions of the identical salt came within 0.1% of the average for that salt. There were some experiments below 0.2 molal, reported in the tables, for which the precision fell between  $\pm 0.10\%$  and  $\pm 0.15\%$ . Consequently the precision of the osmotic coefficient data can be computed to be  $\pm 0.2\%$  at the worst for isopiestic molalities of  $\pm 0.15\%$  precision, but becomes  $\pm 0.1\%$  for concentrations above 0.2 molal.

The reliability of the  $[\log(\gamma_{\text{ref.}}) - \log(\gamma_m)]$  data depends on the quality of the osmotic coefficient values used to plot the  $h/\sqrt{m}$  vs.  $\sqrt{m}$  curve, and on the accuracy with which the areas under the curve could be measured. The first of these factors has already been considered. The areas under the curve were measured with a Keuffel and Esser compensating

polar planimeter, accurate to  $0.1 \text{ cm}^2$  on a  $100 \text{ cm}^2$  standard circle or square. The planimeter could be manipulated with a reproducibility of  $\pm 0.2 \text{ cm}^2$  on an irregular figure. The integration curves were plotted on graph paper of such size that an error of  $5.5 \text{ cm}^2$  in the area measurement would produce a change of only 0.001 in the final activity coefficient. Although the activity coefficient data in the tables are reported to as many places as the area measurement provide, the final values will have a precision of around  $\pm 0.2\%$ , exclusive of the reliability of any reference value chosen.

The isopiestic behavior of holmium nitrate was very strange compared with that for the other three rare-earth nitrates. The precisions of the initial and final concentrations were every bit as good as with the other nitrates, but the osmotic coefficients for  $\text{Ho}(\text{NO}_3)_3$  are abnormally high, as shown in Tables XXV and XXXI and Figure 8. As illustrated in Figure 7, it was impossible to extrapolate the integration curve to coincide with the Debye-Hückel curve in the very dilute range, so activity coefficients based on the 0.04 molal Debye-Hückel reference value could not be obtained.

The conductance curves for the nitrates of holmium, erbium, and ytterbium are very similar. The samarium nitrate conductance curve has a slightly greater slope. The transference number data are very similar again for holmium and erbium nitrates, while the curve for samarium nitrate has higher  $T_+$ -values, but a smaller slope. The osmotic and activity coefficient curves again show the marked similarity between erbium and ytterbium. These observations are to be expected since holmium and erbium are adjacent in the series of increasing atomic numbers, and only one element, thulium, separates erbium from ytterbium in the series. Compared

to these elements, the quantitative values for the electrochemical properties are somewhat different for the nitrate of samarium which is 5 atomic numbers removed from the three "heavy" rare-earths.

Since the data for the four nitrates in this research form a continuation of the studies by Jaffe (35) who started the nitrate series with work on lanthanum, neodymium, and gadolinium, the electrochemical behavior of the rare-earth nitrates throughout the series may now be pictured. In Figure 11 are shown the equivalent conductances at infinite dilution plotted versus the atomic numbers of the elements. The general trend is a decrease in equivalent conductance with increasing atomic number. However there is a pronounced maximum in the curve at neodymium, and another smaller peak at holmium. This same behavior is observed for the transference numbers at infinite dilution, plotted in Figure 12. The peaks at neodymium and holmium are evident for  $T_{+}^{\circ}$  calculated from the ratio  $\lambda_{+}^{\circ}/\Lambda_{\circ}$ . It is interesting that the equivalent conductances at infinite dilution obtained by Jaffe for the rare-earth perchlorates are also higher at neodymium and holmium than the general downward trend of the curve across the series would predict. Another noteworthy feature of the data is the comparison of the two  $T_{+}^{\circ}$ -values for each salt, one obtained by the extrapolation of the empirical least-squares line for the experimental data, and the other from the limiting conductance ratio  $\lambda_{+}^{\circ}/\Lambda_{\circ}$ . The two methods of determining  $T_{+}^{\circ}$  agree very well for the nitrates of gadolinium, samarium, and erbium; not so well for lanthanum and neodymium nitrates; and worst of all for holmium nitrate. A remarkably similar behavior is noticed for the transference number data of the rare-earth perchlorates determined by Jaffe. The least squares intercept and the ratio  $\lambda_{+}^{\circ}/\Lambda_{\circ}$  agree well for the

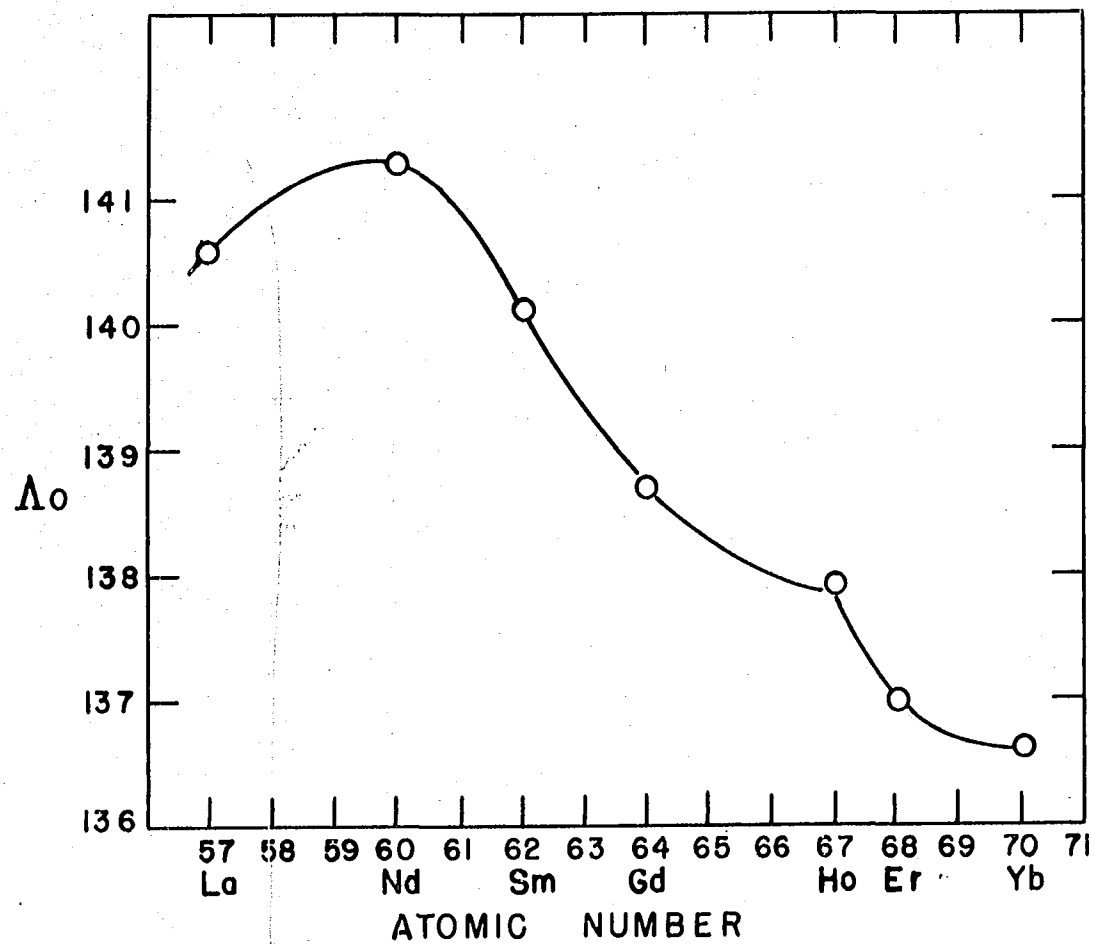


Figure 11. Equivalent conductances at infinite dilution of certain rare-earth nitrates.

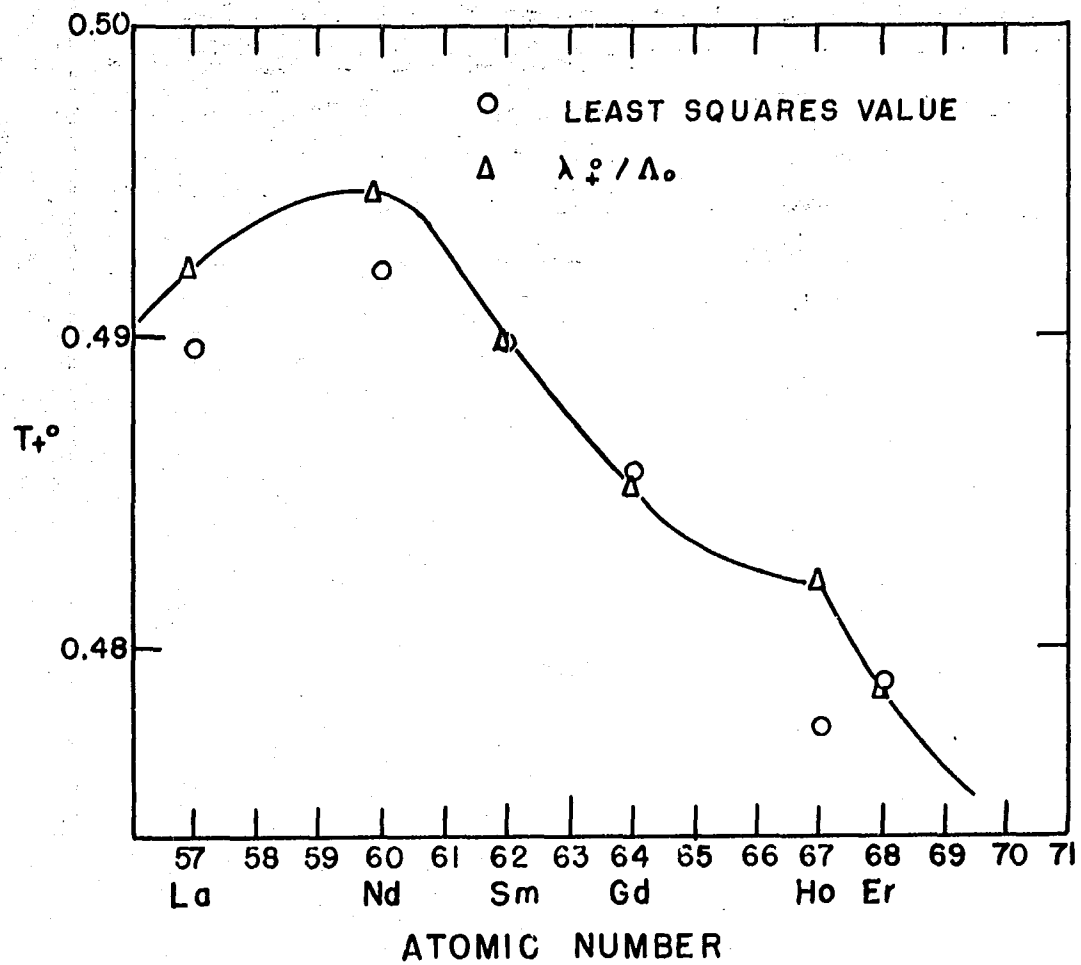


Figure 12. Cation transference numbers at infinite dilution of certain rare-earth nitrates.

perchlorates of praseodymium, gadolinium, and erbium,; but of the whole series, the agreement is worst for holmium perchlorate. Thus, although the experimental transference numbers plot as a straight line in the concentration range 0.01 to 0.1 Normal, there must be quite a pronounced curvature in the very dilute range of the holmium salts to bring the  $T_{+}^{\circ}$  vs.  $\sqrt{C_N}$  plot up to the value of  $\lambda_{+}^{\circ}/\Lambda_0$  at the ordinate. On the other hand for the salts of such elements as gadolinium and erbium, the  $T_{+}^{\circ}$  vs.  $\sqrt{C_N}$  plot must remain fairly straight back to zero concentration.

Another property which indicates the strange behavior of the holmium salts is the partial molal volume. Values of this property were obtained for three of the rare-earth nitrates incidental to the transference numbers work, and are reported in Table X on page 97. Partial molal volumes for the rare-earth perchlorates are given by Jaffe. The limiting values of some of these partial molal volumes are summarized in Table XXXII.

Table XXXII. Partial molal volumes of some rare-earth salts

Nitrate	$\bar{V}^{\circ}$	Perchlorate	$\bar{V}^{\circ}$
$\text{Sm}(\text{NO}_3)_3$	46.5	$\text{Sm}(\text{ClO}_4)_3$	84.8
		$\text{Gd}(\text{ClO}_4)_3$	83.6
$\text{Ho}(\text{NO}_3)_3$	57.6	$\text{Ho}(\text{ClO}_4)_3$	94.4
$\text{Er}(\text{NO}_3)_3$	45.7	$\text{Er}(\text{ClO}_4)_3$	84.2



For each anion in Table XXXII the partial molal volume of the holmium salt seems abnormally high. On the basis of these observations from the conductance, transference numbers, and partial molal volume data, we might expect holmium nitrate to exhibit some out-of-the-ordinary behavior when considered from the viewpoint of its osmotic and activity coefficients.

The osmotic coefficient curves, shown in Figure 8, are very similar in shape for the nitrates of samarium, erbium, and ytterbium. The curve for the first of these salts is somewhat removed from those of the latter two, as might be expected from the relative positions of these elements in the rare-earth series. The osmotic coefficient curve for holmium nitrate is quite different in both shape and slope. As shown in Table XXV the osmotic coefficients for this salt in the range 0.1 to 1.8 molal are very unexpectedly close to unity, and deviate from unity to a much smaller extent with change in concentration, than do the other nitrates. Because of this small slope of the osmotic coefficients for  $\text{Ho}(\text{NO}_3)_3$  it was impossible to extrapolate its integration curve to coincide cleanly with the Debye-Hückel curve in the very dilute range. Consequently activity coefficients based on the 0.04 molal Debye-Hückel reference value could not be obtained for this particular salt. For the other nitrates, the activity coefficient curves in Figure 9 are typical of electrolytic solutions. They drop steeply from unity at zero concentration, pass through a minimum, and then rise slowly again at high concentrations.

The linear Onsager limiting law for conductances in the form

$$\Lambda = \Lambda_0 - B\sqrt{C_n}$$

will predict the experimental data of the rare-earth nitrates up to

0.001 Normal concentration. The Dye extension, in which the electrophoretic contribution retains dependence on the  $\bar{a}$ -parameter, brings the theory into accord with experiment up to about 0.006 Normal for the four rare-earth nitrates studied. The Onsager limiting law for transference numbers, stated on page 71, may be given the form

$$T_+ = T_+^0 + \frac{T_+^0 B' \sqrt{C_n}}{\Lambda'}$$

for any particular salt. By solving this equation for  $T_+^0$ , assigning the symbol  $(T_+^0)'$  to values of  $T_+^0$  calculated from the equation at experimental concentrations, plotting  $(T_+^0)'$  versus  $\sqrt{C_n}$ , and extrapolating to zero concentration,  $T_+^0$  may be found in a manner perfectly analogous to that used for the conductances described on page 55. This procedure gave  $T_+^0$ -values in very good agreement with those calculated from the ratio  $\lambda_+^0/\Lambda_0$ . However the theoretical slopes were not in agreement with experiment, since the available data were beyond the range of applicability of the theory. The Debye-Hückel theory for activity coefficients has been shown to be valid for rare-earth salts up to 0.1 Normal (31, 35). As such, values calculated from the theory have been used as reference points with which activity coefficients were computed from the isopiestic data as described above. Beyond 0.1 Normal, in the range of the experimental isopiestic data, the Debye-Hückel theory, of course, has no validity.

Although the ionic size of the rare-earth elements decreases with increasing atomic number, a trend which should give the heavier rare-earth ions a larger mobility and larger equivalent conductance than the lighter ones, the exactly opposite case is in fact true, as shown in Figure 11.

However, smaller ions are known to be more tightly bound to a hydration shell than are larger ones, so that the hydration sphere about an ion plays an increasingly larger role in hindering the ion's progress in an electric field as its atomic number is raised across the rare-earth series. This interpretation is in accord with the decrease in equivalent conductance with increasing atomic number. The anomalies to this trend, at neodymium and holmium, might be attributed to ionic association, or to some change in the character of the hydration sphere about these ions compared with their neighboring rare-earths.

The behavior of holmium, as shown in both the work with nitrates, and in Jaffe's work with perchlorates, is certainly very strange. The special features of the conductance, transference numbers, partial molal volume, and osmotic and activity coefficient data with regard to holmium have already been discussed. Certainly further investigations with this element are warranted, and probably the determination of the osmotic coefficients should be repeated by another observer. Nevertheless, this author feels that the isopiestic data obtained for holmium nitrate are valid even though the resulting osmotic coefficients are surprising. When the isopiestic molalities of potassium chloride were plotted versus the corresponding equilibrium molalities of holmium nitrate on large scale graph paper, no point had a deviation of more than 0.2% from the smooth curve through the data. The experiments were brought to equilibrium with the same precision as the other rare-earth nitrates. The only possibility for error would be in the concentrations of the stock solutions themselves. The cross-check on the analyses of the three stock solutions used, as described in the first paragraph of this section (page 156) showed no discrepancy in the

concentrations, thus obviating even this error possibility. The abnormal thermodynamic behavior of holmium nitrate may be due to a slowly forming complex, or to some unique feature in the hydration of the dissolved ions.

This research has provided conductance data for four rare-earth nitrates. The ionic equivalent conductances at infinite dilution listed in Table VII are in relatively good agreement with those of other investigators. Transference numbers were given in the range 0.01 to 0.1 Normal for three rare-earth nitrates, along with the incidental partial molal volume data. Osmotic and activity coefficients have been calculated from experimental isopiestic data for  $\text{LaCl}_3$ ,  $\text{Sm}(\text{NO}_3)_3$ ,  $\text{Ho}(\text{NO}_3)_3$ ,  $\text{Er}(\text{NO}_3)_3$ , and  $\text{Yb}(\text{NO}_3)_3$ . Various methods of calculating the activity coefficients of  $\text{LaCl}_3$  were carried out, and these results appear in Table XXI, along with the values obtained by other investigators, so that comparisons may be made. Values of the distance-of-closest-approach parameter have been estimated from conductance data for the four rare-earth nitrates. These values, appearing in Table XXII, are probably accurate to  $\pm 0.2$  Angstrom. These parameters were used to calculate Debye-Hückel activity coefficients for very dilute solutions. From the  $[\log(\gamma_{\text{ref.}}) - \log(\gamma_m)]$  data, sets of activity coefficients for the rare-earth nitrates were obtained.

These data extend the knowledge of the electrochemical properties of the rare-earth nitrates to additional members of this series of salts which had been begun by an earlier investigator. The activity coefficients describe the thermodynamic properties of these rare-earth nitrates in concentrated solutions. The  $\bar{a}$ -parameters and individual ionic equivalent conductances provide means of cross-checking results of other related researches. Finally, variations with respect to the element holmium have

been described, which show that phenomena involving the rare-earth elements can be quite complex.

## VII. BIBLIOGRAPHY

1. Debye, P., and Hückel, E., Physik. Z. 24, 185-206, 305-325 (1923)
2. Onsager, L., Physik. Z. 28, 277-298 (1927); Trans. Faraday Soc. 23, 341-349 (1927)
3. Bjerrum, N., Kgl. Danske Vidensk. Selskab. Math.-fys. Medd. 7, No. 9, 1-48 (1926)
4. Guggenheim, E. A., Philosophical Magazine 19, 588 (1935)
5. Muller, H., Physik. Z. 28, 324 (1927); ibid., 29, 78 (1928)
6. Gronwall, T. H., LaMer, V. K., and Sandved, K., Physik. Z. 29, 358-393 (1928)
7. LaMer, V. K., Gronwall, T. H., and Greiff, L. J., J. Phys. Chem. 35, 2245-2288 (1931)
8. Dye, J. L., and Spedding, F. H., J. Am. Chem. Soc. 76, 888 (1954)
9. Robinson, R. A., and Stokes, R. H., Electrolyte Solutions, Butterworth's Scientific Publications, London, England (1955)
10. Fairbrother, F., and Scott, N., J. Chem. Soc. London 1955, 452-455
11. Evans, G. G., Gibb, T. R. P., Kennedy, J. K., and DelGreco, F. P., J. Am. Chem. Soc. 76, 4861-4862 (1954)
12. Van Dyke, R. E., J. Am. Chem. Soc. 72, 2823-2829 (1950)
13. Nachtrieb, N. H., and Fryxell, R. E., J. Am. Chem. Soc. 74, 897-901 (1952)
14. Dawson, L. R., and Belcher, R. L., Trans. Kentucky Acad. Sci. 13, 129-136 (1951)
15. Davies, C. W., J. Am. Chem. Soc. 59, 1760-1761 (1937)
16. Swift, E., J. Am. Chem. Soc. 60, 728-729 (1938)
17. Hartley, G. S., and Donaldson, G. W., Trans. Faraday Soc. 33, 457-469 (1937)
18. Pearce, J. N., and Blackman, L. E., J. Am. Chem. Soc. 57, 24-27 (1935)
19. Robinson, R. A., and Lavien, B. J., Trans. Proc. Roy. Soc. New Zealand 76, 295-299 (1947)

20. Patterson, C. S., Tyree, S. Y., and Knox, K., J. Am. Chem. Soc. 77, 2195-2197 (1955)
21. Davies, C. W., and James, J. C., Proc. Roy. Soc. London A195, 116-123 (1948)
22. James, J. C., J. Chem. Soc. London 1950, 1094-1098
23. Jenkins, I. L., and Monk, C. B., J. Am. Chem. Soc. 72, 2695-2698 (1950)
24. Oholm, L. W., Soc. Sci. Fennica Commentationes Phys.-Math. 9, No. 2, 2-14 (1936)
25. Robinson, R. A., Trans. Faraday Soc. 35, 1229-1233 (1939)
26. Mason, C. M., and Ernst, G. L., J. Am. Chem. Soc. 58, 2032 (1936)
27. \_\_\_\_\_, J. Am. Chem. Soc. 60, 1638-1647 (1938)
28. \_\_\_\_\_, J. Am. Chem. Soc. 63, 220 (1942)
29. Spedding, F. H., Porter, P. E., and Wright, J. M., J. Am. Chem. Soc. 74, 2055 (1952)
30. \_\_\_\_\_, \_\_\_\_\_, and \_\_\_\_\_ J. Am. Chem. Soc. 74, 2778 (1952)
31. \_\_\_\_\_, \_\_\_\_\_, and \_\_\_\_\_ J. Am. Chem. Soc. 74, 2781 (1952)
32. \_\_\_\_\_ and Yaffe, I. S., J. Am. Chem. Soc. 74, 4751 (1952)
33. \_\_\_\_\_ and Dye, J. L., J. Am. Chem. Soc. 76, 879 (1954)
34. \_\_\_\_\_ and Jaffe, S., J. Am. Chem. Soc. 76, 882 (1954)
35. \_\_\_\_\_ and \_\_\_\_\_ J. Am. Chem. Soc. 76, 884 (1954)
36. Ayers, B. O., "Apparent and Partial Molal Volumes of Some Rare-Earth Salts in Aqueous Solutions", Unpublished Ph.D. Thesis, Iowa State College Library, Ames, Iowa (1954)
37. Atkinson, G., "Compressibilities of Some Rare-Earth Nitrates and Chlorides in Aqueous Solution", Unpublished Ph.D. Thesis, Iowa State College Library, Ames, Iowa (1956)
38. Spedding, F. H., and Miller, C. F., J. Am. Chem. Soc. 74, 3158 (1952)
39. \_\_\_\_\_ and \_\_\_\_\_ J. Am. Chem. Soc. 74, 4195 (1952)
40. \_\_\_\_\_ and Flynn, J. P., J. Am. Chem. Soc. 76, 1474 (1954)

41. Spedding, F. H., and Flynn, J. P., J. Am. Chem. Soc. 76, 1477 (1954)
42. Naumann, A. W., "Heats of Dilution and Related Thermodynamic Properties of Aqueous Neodymium Chloride and Erbium Chloride Solutions", Unpublished Ph.D. Thesis, Iowa State College Library, Ames, Iowa (1956)
43. Eberts, R. E., "Relative Apparent Molal Heat Contents of Some Rare-Earth Chlorides and Nitrates in Aqueous Solutions", Unpublished Ph.D. Thesis, Iowa State College Library, Ames, Iowa (1957)
44. Bjerrum, N., Proc. Seventh Int. Cong. Pure and Applied Chem. Section 10, 1, London (1909)
45. Milner, S. R., Phil. Mag. 23, 551-578 (1912); ibid., 25, 742-751 (1913)
46. Kramers, H. A., Proc. Sect. Sci. Amsterdam 30, 145 (1927)
47. Fowler, R. H., Trans. Faraday Soc. 23, 434 (1927)
48. \_\_\_\_\_ and Guggenheim, E. A., Statistical Thermodynamics, The University Press, Cambridge, England (1952)
49. Onsager, L., Physik. Z. 28, 277-298 (1927); Chem. Rev. 13, 73-89 (1933)
50. Kirkwood, J. G., J. Chem. Phys. 2, 767 (1934)
51. Halpern, O., J. Chem. Phys. 2, 85-93 (1934)
52. G<sup>u</sup>ntelberg, E., Z. Physik. Chem. 123, 199 (1926)
53. Kohlrausch, F., and Nippoldt, W. A., Ann. Physik. 138, 280-298, 370-390 (1869)
54. Debye, P., Trans. Faraday Soc. 23, 334 (1927)
55. Washburn, E. W., and Bell, J. E., J. Am. Chem. Soc. 35, 117-184 (1913)
56. Taylor, W. A., and Acree, S. F., J. Am. Chem. Soc. 38, 2396-2430 (1916)
57. Hall, R. E., and Adams, L. H. J. Am. Chem. Soc. 41, 1515-1525 (1919)
58. Jones, G., and Josephs, R. C., J. Am. Chem. Soc. 50, 1049-1092 (1928)
59. Shedlovsky, T., J. Am. Chem. Soc. 52, 1793-1805 (1930)
60. Dike, P. H., Review of Scientific Instruments 2, 379-395 (1931)



61. Jones, G., and Bollinger, G. M., J. Am. Chem. Soc. 51, 2407-2416 (1929)
62. Washburn, E. W., and Parker, K., J. Am. Chem. Soc. 39, 235-245 (1917)
63. \_\_\_\_\_, J. Am. Chem. Soc. 38, 2431-2460 (1916)
64. Parker, H. G., J. Am. Chem. Soc. 45, 1366-1379 (1923)
65. Randall, M., and Scott, G. N., J. Am. Chem. Soc. 49, 636-647 (1927)
66. Smith, F. A., J. Am. Chem. Soc. 49, 2167-2171 (1927)
67. Shedlovsky, T., J. Am. Chem. Soc. 52, 1806-1811 (1930)
68. Jones, G., and Bollinger, G. M., J. Am. Chem. Soc. 53, 411-451 (1931)
69. \_\_\_\_\_ and Christian, S. M., J. Am. Chem. Soc. 57, 272-280 (1935)
70. \_\_\_\_\_ and Bollinger, D. M., J. Am. Chem. Soc. 57, 280-284 (1935)
71. Kendall, J., J. Am. Chem. Soc. 38, 2464-2465 (1916)
72. Shedlovsky, T., J. Am. Chem. Soc. 54, 1411-1428 (1932)
73. \_\_\_\_\_, J. Am. Chem. Soc. 54, 1405-1411 (1932)
74. Rossini, F. D., Gucker, F. T., Johnston, H. L., Pauling, L., and Vinal, G. W., J. Am. Chem. Soc. 74, 2699-2701 (1952)
75. Wyman, J., Phys. Review 35, 623 (1930)
76. International Critical Tables 5, McGraw-Hill Book Company, New York, New York, the United States of America (1929)
77. MacInnes, D. A., Shedlovsky, T., and Longworth, L. G., J. Am. Chem. Soc. 54, 2758 (1932)
78. Hittorf, W., Poggendorff's Ann. Physik. 89, 117-211 (1853); ibid., 98, 1-33 (1856); ibid., 103, 1-56 (1858); ibid., 106, 337-411 (1859)
79. Longworth, L. G., J. Am. Chem. Soc. 54, 2741-2758 (1932)
80. Lodge, O., Brit. Assn. Advancement Sci. Rep., pp. 389-413 (1886)
81. Steele, B. D., J. Chem. Soc. London 79, 414-429 (1901)
82. Franklin, E. C., and Cady, H. P., J. Am. Chem. Soc. 26, 499-530 (1904)
83. Denison, R. B., and Steele, B. D., J. Chem. Soc. London 89, 999-1013 (1906)

84. MacInnes, D. A., and Smith, E. R., J. Am. Chem. Soc. 45, 2246-2255 (1923)
85. \_\_\_\_\_ and Brighton, T. B., J. Am. Chem. Soc. 47, 994-999 (1925)
86. Allgood, R. W., LeRoy, D. J., and Gordon, A. R., J. Chem. Phys. 8, 418-422 (1940)
87. Longworth, L. G., and MacInnes, D. A., J. Opt. Soc. Am. and Rev. Sci. Instruments 19, 50-56 (1929)
88. LeRoy, D. J., and Gordon, A. R., J. Chem. Phys. 6, 398-402 (1938)
89. Bender, P., and Lewis, D. R., J. Chem. Education 24, 454-456 (1947)
90. MacInnes, D. A., Cowperthwaite, I. A., and Huang, T. C., J. Am. Chem. Soc. 49, 1710-1717 (1927)
91. Smith, E. R., J. Am. Chem. Soc. 50, 1904-1906 (1928)
92. Kohlrausch, F., Ann. Physik. 62, 209 (1897)
93. Smith, E. R., and MacInnes, D. A., J. Am. Chem. Soc. 46, 1398-1403 (1924)
94. \_\_\_\_\_ and \_\_\_\_\_ J. Am. Chem. Soc. 47, 1009-1015 (1925)
95. MacInnes, D. A., and Cowperthwaite, I. A., Proceedings of the National Academy of Sciences of the U.S.A. 15, 18-21 (1929)
96. Cady, H. P., and Longworth, L. G., J. Am. Chem. Soc. 51, 1656-1664 (1929)
97. Longworth, L. G., J. Am. Chem. Soc. 52, 1897-1910 (1930)
98. MacInnes, D. A., and Longworth, L. G., Chemical Reviews 11, 171-230 (1932)
99. Miller, W. L., Z. Physik. Chem. 69, 436-441 (1909)
100. Lewis, G. N., J. Am. Chem. Soc. 32, 862-869 (1910)
101. MacInnes, D. A., and Dole, M., J. Am. Chem. Soc. 53, 1357-1364 (1931)
102. Smith, E. R., Bureau Standards J. Research 8, 457-461 (1932)
103. Harned, H. S., and Owen, B. B., The Physical Chemistry of Electrolytic Solutions, Second Edition, Reinhold Publishing Corporation, New York, New York, The United States of America (1950)

104. International Critical Tables 3, McGraw-Hill Book Company, New York, New York, The United States of America (1928)
105. Lewis, G. N., Proc. Am. Acad. Arts Sci. 43, 259-293 (1907)
106. Bousefield, W. R., Trans. Faraday Soc. 13, 401 (1918)
107. \_\_\_\_\_ and Bousefield, G. E., Proc. Roy. Soc. London A103 429 (1923)
108. Sinclair, D. A., J. Phys. Chem. 37, 495 (1933)
109. Robinson, E. A., and Sinclair, D. A., J. Am. Chem. Soc. 56, 1830 (1934)
110. \_\_\_\_\_, J. Am. Chem. Soc. 57, 1161 (1935)
111. Scatchard, G., Hamer, W. J., and Wood, S. E., J. Am. Chem. Soc. 60, 3061 (1938)
112. Mason, C. M., and Ernst, G. L., J. Am. Chem. Soc. 58, 3032 (1936)
113. \_\_\_\_\_, J. Am. Chem. Soc. 60, 1638 (1938)
114. \_\_\_\_\_, J. Am. Chem. Soc. 63, 220 (1941)
115. Jones, J. H., J. Am. Chem. Soc. 65, 1353 (1943)
116. Gordon, A. R., J. Am. Chem. Soc. 65, 221 (1943)
117. Owen, B. B., and Cooke, T. F., J. Am. Chem. Soc. 59, 2273 (1937)
118. Janis, A. A., and Ferguson, J. B., Canadian Journal of Research 17B, 215 (1939)
119. Phillips, B. A., Watson, G. M., and Felsing, W. A., J. Am. Chem. Soc. 64, 244 (1942)
120. Harned, H. S., J. Am. Chem. Soc. 51, 416 (1929)
121. Scatchard, G., and Prentiss, S. S., J. Am. Chem. Soc. 55, 4355 (1933)
122. Harned, H. S., and Cook, M. A., J. Am. Chem. Soc. 59, 1290 (1937)
123. Shedlovsky, T., and MacInnes, D. A., J. Am. Chem. Soc. 59, 503 (1937)
124. Robinson, R. A., Trans. Faraday Soc. 35, 1217 (1939)
125. Shedlovsky, T., J. Am. Chem. Soc. 72, 3680 (1950)

126. Robinson, R. A., and Stokes, R. H., Trans. Faraday Soc. 45, 612-624 (1949)
127. \_\_\_\_\_, J. Am. Chem. Soc. 59, 84 (1937)
128. \_\_\_\_\_, Trans. Faraday Soc. 35, 1229 (1939)
129. Shedlovsky, T., and MacInnes, D. A., J. Am. Chem. Soc. 61, 200 (1939)
130. Lewis, G. N., and Randall, M., Thermodynamics, McGraw-Hill Book Company, New York, New York, The United States of America (1923)

relation

$$\Lambda_0 = \lambda_+^0 + \lambda_-^0$$

From the values found for  $\Lambda_0$ , and from  $\lambda_{\text{NO}_3^-}^0 = 71.42$ , the equivalent conductances at infinite dilution for the cation,  $\lambda_{\text{R.E.}^{+++}}^0$  were calculated for the three salts studied.

In Tables III-VI on the following pages are the conductance data for aqueous solutions of samarium nitrate, holmium nitrate, erbium nitrate, and ytterbium nitrate at 25.00°C.

Table III. Conductances of samarium nitrate

Normality	Specific conductance	Equivalent conductance	Calculated $\Lambda_0$
0.14783	0.012330	83.407	
0.11078	0.0096249	86.883	
0.073898	0.0067786	91.729	
0.051706	0.0049709	96.138	
0.036932	0.0036973	100.11	
0.014772	0.0016332	110.56	144.91
0.0073873	0.00086897	117.63	141.62
0.0059073	0.00070616	119.54	140.93
0.0036911	0.00045542	123.38	140.25
0.0014764	0.00019098	129.35	140.01
0.00073830	0.000097823	132.50	140.04
0.00059039	0.000078700	133.30	140.04
0.00036890	0.000049735	134.82	140.15
0.0		140.06	